PETROGRAPHY AND GEOCHEMISTRY OF THE MASOKE IRON FORMATION AND ITS ASSOCIATED FERRUGINOUS COUNTERPARTS, KANYE BASIN BOTSWANA

A Thesis submitted to Rhodes University in partial Fulfillment of the Requirements for the Degree of

MASTER OF SCIENCE

(EXPLORATION GEOLOGY)

By Ndifelani Oriel Nkabelane (G14N4064)

Supervisor Prof. Harilaos Tsikos

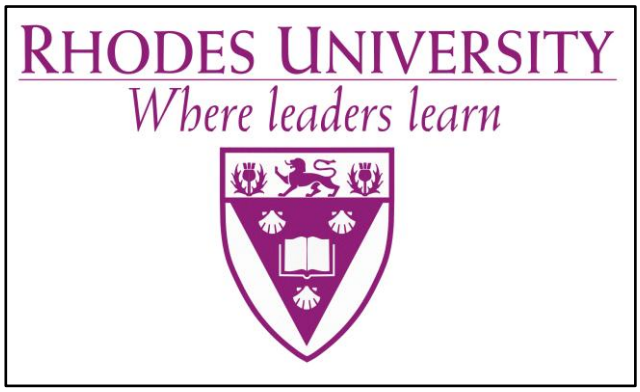

MSc Exploration Geology Programme 2018

Geology Department

Rhodes University

P.O. Box 94

Grahamstown 6140

South Africa

Abstract

A sequence of Transvaal Supergroup sediments extends into southern Botswana beneath Kalahari cover as the Kanye basin, these are known to host billions of tons @ 60>Fe. Masoke Iron Formation (Kanye Basin) which is stratigraphic correlative of The Ghaap Group and Chuniespoort Group of the Griqualand West basin and Transvaal basin, respectively. The Palaeoproterozoic Transvaal Supergroup in the Northern Cape Province of South Africa hosts high grade (>60%Fe) hematitic and specularitic iron and manganese mineralisation. It is therefore important to study and record the petrographic, mineralogy and geochemistry of Masoke Iron Formation, compare the results to the much known Kuruman and Griquatown Iron Formations.

This study systematically investigate and record the petrography, mineralogy and geochemistry of all Masoke Iron Formation of Taupone Group in the Kanye Basin, which is stratigraphic correlative of The Ghaap Group and Chuniespoort Group of the Griqualand West basin and Transvaal basin, respectively. The further objective is to compare Masoke Iron Formation to the equivalent units in the Transvaal basin and Griqualand basin.

In contrast to both Transvaal and Griqualand West Basin the Masoke iron Formation (Kanye Basin) has not been the subject of systematic scientific investigations. The study covers three main areas in the Kanye Basin: Keng Pan Area, Ukwi/Moretlwa hill and Janeng Hill Area. The mineralogy and geochemistry of these areas are presented in this study.

Kanye Basin has a potential to host a large iron ore deposit, the geological setting in this area incorporates many of the elements necessary for iron ore formation. These include: banded iron formation (BIF), major unconformities with prolonged periods of weathering, carbonate sequences etc. In addition, several large deposits and mines are known from this area. This area can potentially have both hypogene and supergene enrichment of BIF. In this model, prospectively for new deposits is a function of the following: presence of iron formation units, proximity of mapped Asbestos Hills and Voëlwater BIF, thrust faulting (as indicated by the aero-magnetic interpretation), duplication of the ore horizon by folding, intersection of the BIF by major extensional fault, proximity of Olifantshoek/Waterberg outcrop, Gamagara unconformity, presence of carbonates (dolomites) and thin Kalahari sand cover.

Major BIF units in the area of study include: the Masoke Iron Formation, equivalent to Kuruman Formation of the Asbestos Hills Subgroup, the Rooinekke iron formation of the Koegas Subgroup and the Hotazel Formation of the Voëlwater Subgroup. Supergene enrichment of these BIFs may occur wherever they are overlain by a major regional unconformity. The base of the Waterberg and the OlifantshoekSupergroups represent major unconformities in this regional target area. Potential for hypogene deposits is indicated by faulting (preferably extensional) proximal to BIF

Acknowledgements

I would like to sincerely thank Rio Tinto Mining and Exploration for all the technical, logistical and financial support; without this support my participation on the program would not have been possible. I would especially like to thank Mr Kevin Fox (Exploration Manager – AfricaEurope region), Nevan Pillay, Maxwell Matongo and Ulf Westhof ; the whole Rio Tinto staff for their most valuable assistance and support.

My greatest appreciation to my supervisor Professor Tsikos for all the guidance, critical discussions, motivation and academic support during the study. This study would have not been possible without your contribution and support. You have shown keen interest and support since the inception of this project.

Maxwell Matongo thanks for your support, motivation, critical discussions and eye for detail. This study would not have been possible without your guidance and assistance. It is through constant communication and discussions with you that I was able to achieve this milestone.

The program director Professor Jock Harmer, I like to thank you for your academic contributions in making the program relevant and meaningful to industry. To the staff at Rhodes University, the administrator of the MSc program, Mrs Ashley Goddard deserves a massive thank you for the unnoticed hard work to ensure that the program runs smoothly, Xolane Mhlanga for all the assistance during processing and analysis of results.

Furthermore, I would also like to acknowledge my family; my three beautiful girls, my wife and parents. My outmost and heartfelt thanks to my late brother Mr Papi Nkabelane; a brother who stood by me all the time and celebrated my success as his own. He taught me nothing but love and respect. To almighty be the glory.

Declaration

I, Ndifelani Oriel Nkabelane declare this dissertation, with exception to what has been acknowledged, to be my own work. It is submitted in fulfillment of the Degree of Master of Science at the Rhodes University. It has not been submitted before for any degree or examination in any other University or tertiary institution.

Signature (Candidate):…….

Date:……..……..…..

LIST OF PLATES

LIST OF TABLES

LIST OF PHOTOMICROGRAPHS

Chapter 1 INTRODUCTION

1.1 Abstract

A sequence of Transvaal Supergroup sediments extends into southern Botswana beneath Kalahari cover as the Kanye basin. These are known to host billions of tons of iron ore at >60wt% Fe. The Masoke Iron Formation (Kanye Basin), the best candidate stratigraphic host for Fe ore, is likely stratigraphic correlative of the Ghaap Group and Chuniespoort Group of the Griqualand West and Transvaal basins, respectively. Major BIF units in the area of study include the Masoke Iron Formation. This is a likely stratigraphic equivalent to the Kuruman Formation of the Asbestos Hills Subgroup, the Rooinekke iron formation of the Koegas Subgroup and the Hotazel Formation of the Voëlwater Subgroup.

Molopo Farms Complex (MFC) is an immense composite basic and ultrbasic intrusion, emplaced into strata of the Transvaal Supergroup within a fold basin structure (the geology of Botswana, J N Carney, T D Aldiss and N P Lock). Rio Tinto iron ore prospecting areas in the Molopo-Kanye structural basin hosting strata of late Neoarchean to late Paleoproterozoic Transvaal - Waterberg succession in south-eastern Botswana. In this area prospective Transvaal Supergroup rocks are inferred to persist under cover northwards from the Postmasburg-Sishen karst- hosted high-grade hematite iron ore district in the Griqualand West area. The main exploration target is thus for ancient supergene karst-hosted high-grade hematite iron ore deposits of the Sishen-type (Van Schalkwyk and Beukes, 1986; Beukes et al., 2003; Dalstra and Rosiere, 2008; Van Deventer, 2009).

Supergene enrichment of these BIFs may occur wherever they are overlain by a major regional unconformity. The base of the Waterberg and Olifantshoek Supergroups represent major unconformities in this regional target area. Potential for hypogene deposits is also indicated by faulting (preferably extensional) proximal to BIF. On either side of the Molopo River, along the border between South Africa and Botswana, a number of these factors coincide to produce potential iron ore deposits beneath thin Kalahari Sand cover. There is, however, very little known about the petrographic, geochemical and mineralogical composition of Masoke Iron Formation. The reason for this lack in information is due to the absence of outcrops and fresh material for analysis. This study details petrography, mineralogy and geochemistry of

the ferruginous sedimentary rocks of the Masoke Iron Formation of the Taupone Group, which is an apparent stratigraphic correlative of The Ghaap Group and Chuniespoort Group of the Griqualand West basin and Transvaal basin, respectively. This Iron Formation will be compared to the equivalent units in the Transvaal basin and Griqualand basin, the stratigraphic succession in the study area will be elucidated as possible, with a view to aiding further exploration work. The BIF in MFC is referred to as Masoke Iron Formation. This study will however; deal with these rocks as they do not belong to the Masoke Iron Formation. The study addresses these lithologies as they belong to the broad South Africa BIF families that are Kuruman Iron formation in the Griquatown Basin and Penge of the Transvaal in the east of the Kaapvaal Craton.

1.2 Iron markets

Iron ores consumed in the steel industry typically require iron content greater than 58 percent before being considered commercially usable. Iron ores that are not commercially usable must undergo beneficiation to raise the iron content. Approximately 98 percent of the world's usable iron ore production is consumed in blast furnaces to make pig iron, which is further processed to make steel (Association for Iron and Steel Technology, 1999, The making, shaping, and treating of steel, 11th Edition).

Global iron ore production grew 5% year-on-year in 2016, to a total of 2,106 Mt; figure 1.1. This was primarily driven by an additional 30 Mt of direct shipping ore from Australia, which was the major source of new fine-products entering the Chinese market. Lump production increased 26 Mt to constitute 15% of global production, but concentrate output was broadly flat at one quarter of world production. The latter total was despite a net reduction of 10 Mt in China (when measured as a 62% Fe equivalent material); China Steel: Yearbook Board, 2015.

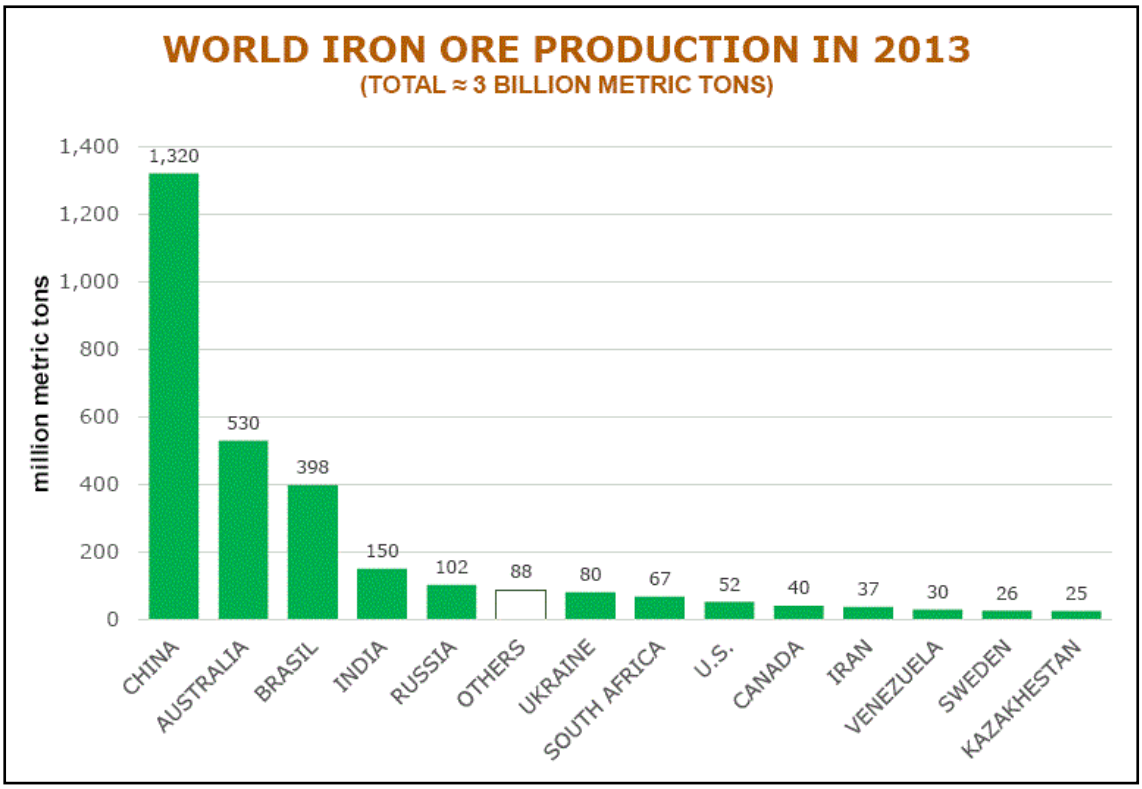

Figure 1.1: World iron ore production by country in 2013, USGS February 2014. China is still the biggest producer followed by Australia and Brasil respectively.

The iron ore market is driven by demand for steel, which in turn is linked to developments in the global economy and its growth. China accounts for more than 50% of the seaborne iron ore imports and almost half of the world steel production. Global iron ore demand is expected to remain low. Demand from china, who is the top importer of iron ore, is expected to decline (figure 1.2). The global steel production has been fluctuating in a narrow range from 65%-70% (average, 67% according to Wood Mackenzie, World Steel Association, Samruk-Kazyna, Mining industry and Trends – March 2017).

Iron ore prices have rallied in 2016 as consumption in China proved resilient and Mr. Trump's win boosted speculation about the outlook for demand. Iron ore prices improved markedly in the second half of 2016, having reached a low in mid-January last year when 62% Fe prices fell below US$40 per tonne CFR for only the second time since the inception of the S&P Global Platts' index in 2008 (the other instance was in December 2015). Prices reached a peak of US$84 per tonne in early

December 2016, averaging US$58 per tonne for the year, but lump premiums were at historic lows by year end.

Iron ore exports exceeded 1,513 Mt in 2016, compared with less than 1,439 Mt in 2015, and the seaborne market was more or less balanced for 62% Fe material. Technically, there was a small deficit in iron units due to relatively low inventories in the final two quarters, but any price effect was dwarfed by coking coal components. This tightness in the 62% Fe market, compounded by other pricing factors and financial speculation, contributed to considerable price volatility. The net increase in global trade was led by Australia, which contributed 44 Mt of incremental seaborne supply. The predominant products that entered the market were increases to Pilbara blend tonnages and Carajas fines.

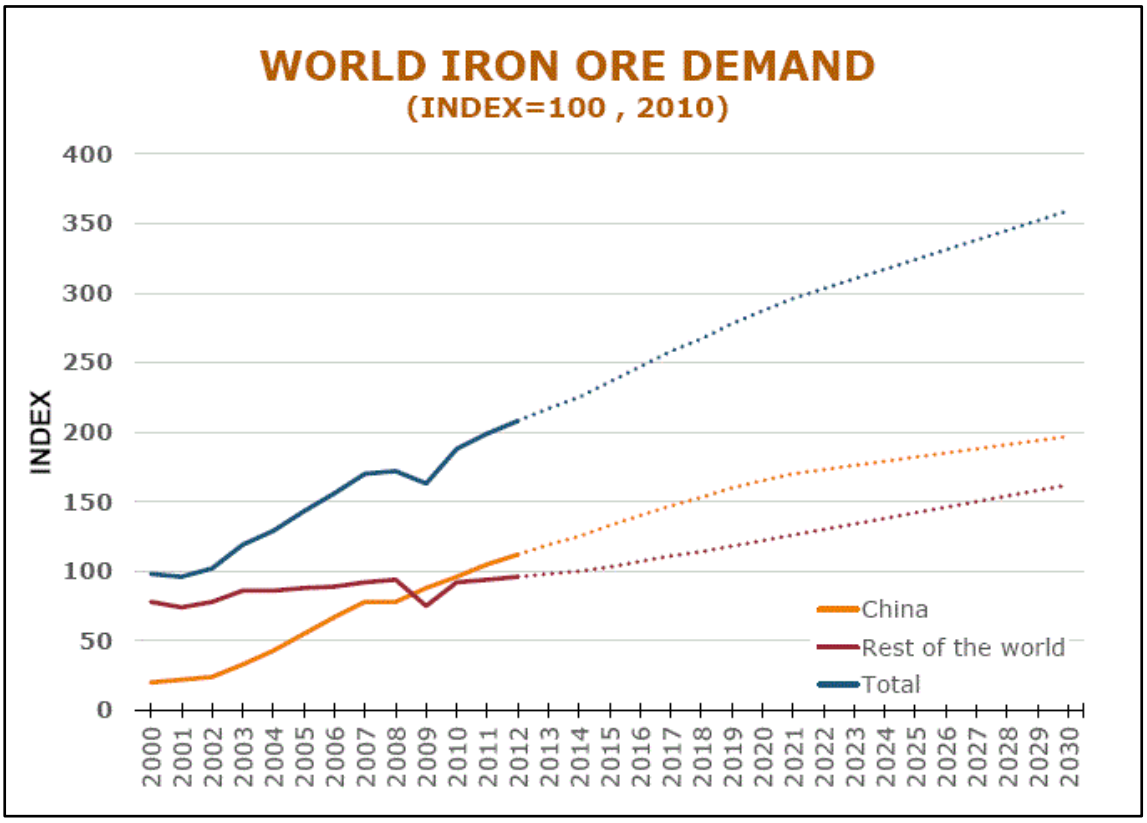

Figure 1.2: Total iron ore demand in the world from 2000 - 2013, the trends show an upward trajectory. There was a downturn between 2008 and 2009 because of the global financial crisis (GFC), USGS report February 2014

Iron ore exploration budgets fell in 2016 for the fourth consecutive year, with the estimated US$685 million expenditure representing a decline of US$460 million from 2015. Most of the fall can be attributed to Australia and China, which together

accounted for almost half of the global decline. The annual exploration budget for iron ore is now down 83% from the peak of US$3.98 billion in 2012. Overall, about 91 Mt per annum of new global iron ore production was added in 2016. The lower iron ore prices led to some site- specific cut-backs, but permanent closures were led by the 10 Mt (62% Fe production equivalent) shut in China, with very little elsewhere.

South African iron ore resources, an estimated nearly 5,370Mt, are ranked the 9th largest in the world (refer to figure 1.1). If the Bushveld Complex's lower-grade potential resources are included, the resource base increases by 26,400Mt, which would then rank South Africa's iron ore resources as the 6th largest in the world. In terms of export of iron ore, South Africa is ranked number 6th in the world. The principal deposits of iron ore of South Africa are the Superior-type BIFs of the Transvaal Supergroup in the Northern Cape Province, which can be traced as a prominent, arcuate range of hills for some 400km from Pomfret in the north to Prieska in the south. The most significant deposits occur in the vicinity of Postmasburg and Sishen, where high-grade hematite concentrations have been preserved in the narrow north-south trending belt of the iron- and manganese-bearing lithologies of the Asbestos Hills Subgroup (~2,670Mt at Beeshoek Mine, Sishen Mine and Welgevonden deposit – Astrup et al., 1998).

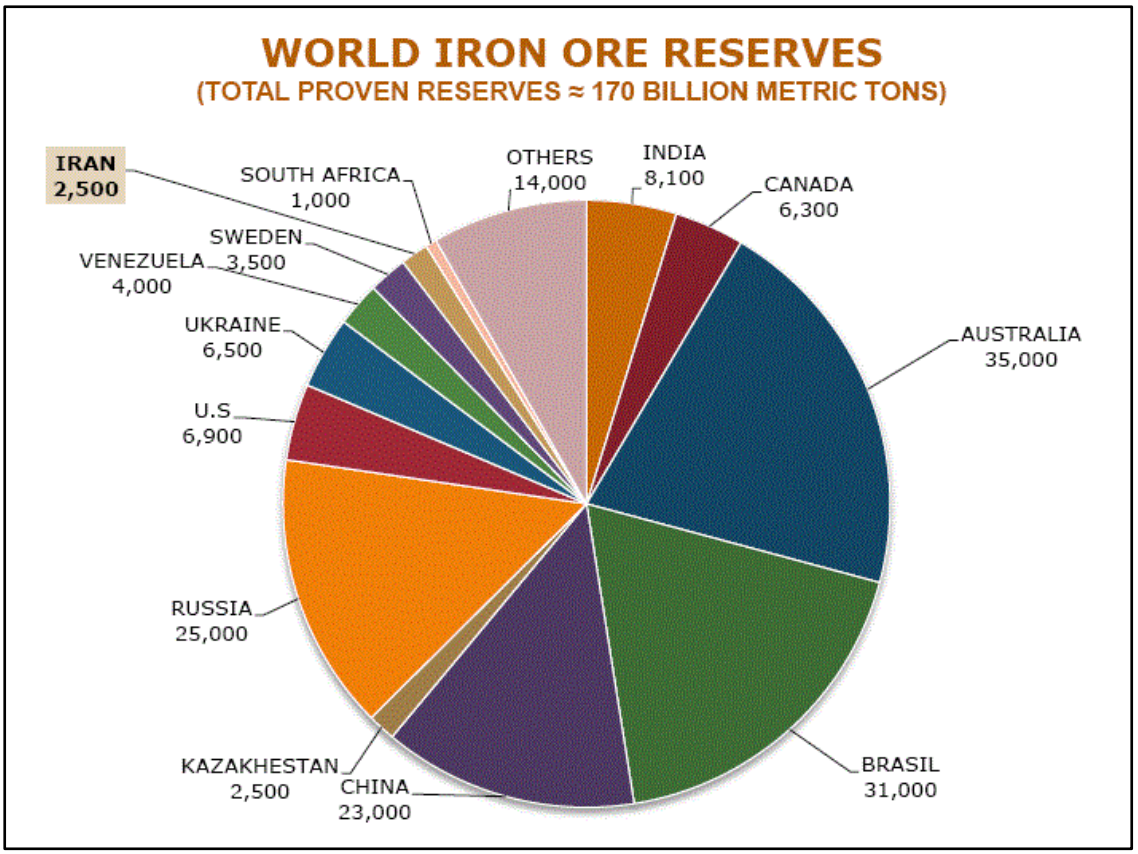

Figure1.3: Iron ore reserves by country, South Africa is in the top ten producing nations in the world, USGS report February 2014.

1.3 Overview of the study area

Rio Tinto iron ore prospecting areas in the Molopo-Kanye structural basin hosting strata of late Neoarchean to late Paleoproterozoic Transvaal and Waterberg succession in south-eastern Botswana. In this area prospective Transvaal Supergroup rocks are inferred to persist under cover northwards from the Postmasburg-Sishen karst- hosted high-grade hematite iron ore district in the Griqualand West area. The main exploration target is thus for ancient supergene karst-hosted high-grade hematite iron ore deposits of the Sishen-type (Van Schalkwyk and Beukes, 1986; Beukes et al., 2003; Dalstra and Rosiere, 2008; Van Deventer, 2009).

The rocks in the prospecting area comprise Archaean basement rocks, Neoarchaean to early Proterozoic sequences of the Transvaal Supergroup that include thick BIFs (BIF), overlain by Proterozoic clastic sequences of the

Olifantshoek and Waterberg Groups. Younger glacial, clastic and volcanic sequences of the Karoo Group cover much of the Proterozoic and Archaean rocks in the western and northern part of the area. Intrusive into the sedimentary sequences is a layered mafic ultramafic complex known as the ‘Molopo Farms Complex’, which is correlated with the Bushveld Intrusive Complex.

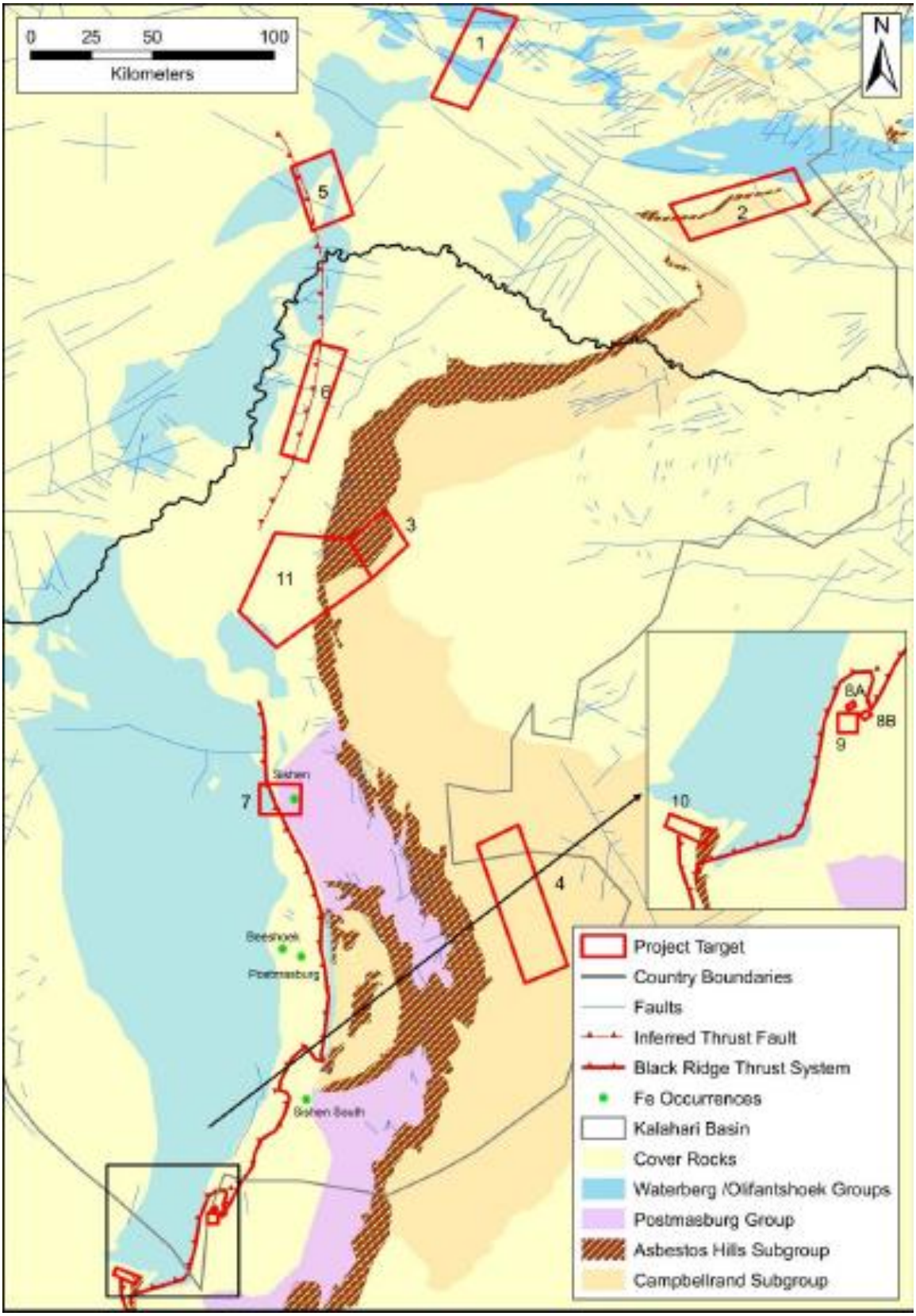

Figure 1.4: Regional geology of Molopo Farms Complex showing the South African equivalent Asbestos Hills Subgroup (modified after SADC map, 2009). The project is marked by polygon 1, 2 and 5.

1.4 Project location

The project is located 430km west of Gaborone in the Kgalagadi District of Botswana. It lies approximately 300km north of supergene-type Sishen deposits and 500km west of hydrothermal-type Thabazimbi deposits. The target horizon is the so-called Masoke Iron Formation (Kanye Basin) which is tentatively, albeit not conclusively, correlated with the Asbestos Hill (Griqualand West Basin) and Penge (Transvaal Basin) iron-formations.

Figure 1.5: Project location map showing parts Southern Botswana and the Northern Cape of South Africa, project location marked by the three red polygons Maokane, Khakhea and Janeng Hill.

The Transvaal equivalent strata have been mapped in southern Botswana as far west as the Kalahari Suture Zone in the area of Mabuasehube Pan, west of Kokong, and at Kokong. The Kokong Transvaal was based on borehole intersections alone. The northern boundary of Transvaal Group appears to be about the latitude of Jwaneng, extending just south of and parallel to the east-west trending Palala Shear Zone-Zoetfontein Fault (Figure 1.6).

The Kanye Basin was mapped by Crockett (1969, 1972) as the northern salient of the Northern Cape Basin and contains the Botswana equivalent of the Northern Cape Basin's Griqualand West Sequence (Carney, Aldiss, and Locke, 1994). Tombale (1986) and Mapeo (1990) mapped the more westerly and southern sections of the Kanye Basin as being the "Taupone Group Dolomite" a correlative of the Chuniespoort Dolomite in South Africa, with the Masoke Formation BIF and Kgwakgwe Chert formations being equivalent to the Penge Iron formation of the Chuniespoort Group. Further east in the Kanye Basin, Tombale'sSegwagwa Group correlates with the Pretoria Group of the Transvaal Supergroup. It's also noted that it's probably Segwagwa Group rocks inferred for the extreme far west of the Kanye Basin at Mabuasehube Pan, as upper Transvaal Pretoria group rocks were mapped there.

The Masoke Formation of the Taupone Group is probably the closest Botswana equivalent to economic RSA iron formations and is up to 400m thick (Carney, Aldiss, and Locke, 1994). Uplift and erosion of Transvaal equivalent sediments over the Lobatse Arch is thought to have reduced the value of Botswana iron formations relative to their South African equivalents, but the Kalahari covered Taupone Group north of the Knapdaar occurrence is thought to be most prospective for economic iron occurrences (Carney, Aldiss, and Locke, 1994). This generally north-south trending band of Taupone Group would also appear to include the exposed BIF outcrop at Motsoye Hill as a strike-slip fault of 25-30 kms. The offset appears to have moved the Taupone group strata to the west-northwest of the Knapdaar occurrence, in the vicinity of the Motsoye Hill BIF occurrence.

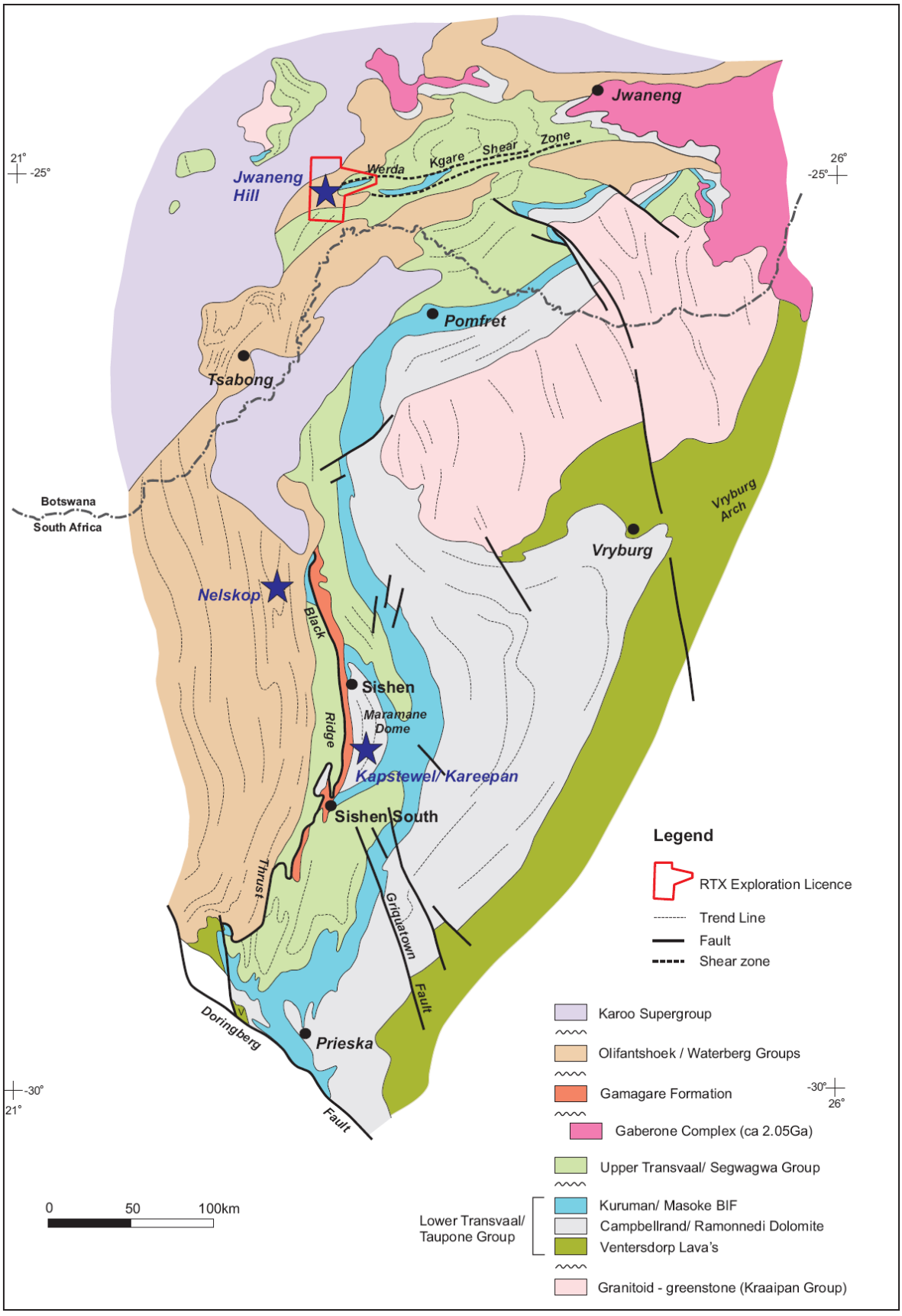

Figure 1.6: Solid geology map of the western Kaapvaal Province with field locations at Jwaneng Hill, Nelskop and Kapstewel/ Kareepan indicated by stars.

1.5 Aims and objectives

The project aims to study the Iron Formation of the Taupone Group and associated ferruginous sedimentary rocks, in the Molopo-Kanye structural basin in the Kgalagadi and Southern Districts of Botswana. Previous studies by the Department of Geological Survey (1975), particularly those published by Key, Tombale and Carney are brief and only concerned with the economic potential of this area. Thus, the Masoke iron Formation has not been the subject of thorough scientific investigations to date. Through this study, three main areas will be investigated, namely Keng Pan Area, Ukwi/Moretlwa hill and Janeng Hill Area. The studied iron formation in the above areas will be compared with the Kuruman; Griquatown and Hotazel iron Formations as they have been well documented both through petrographic and geochemical studies (Beukes 1978, 1984; Klein & Beukes 1992; Beukes and Gutzmer 2008).

The overarching objective of this study is therefore:

> *To systematically investigate and record the petrography, mineralogy and geochemistry of the ferruginous sedimentary rocks of the Iron Formation of the Taupone Group, which is an apparent stratigraphic correlative of The Ghaap Group and Chuniespoort Group of the Griqualand West basin and Transvaal basin, respectively. These iron formations will then be compared to the known BIFS units in the Transvaal basin and Griqualand basin, the stratigraphic succession in the study area will be elucidated as possible, with a view to aiding further exploration work. It is however, very important to remember that this Iron Formation of the Taupone Group will be studied as separate BIF units that belong to the broad South Africa BIF families that are Kuruman Iron formation in the Griquatown Basin and Penge of the Transvaal in the east of the Kaapvaal Craton.*

1.6 Thesis outline

There are six chapters that form the framework of this thesis. The first chapter presented introductory aspects of the research such as an abstract, exploration history, overview, aim and objectives of the study; and the methodology. Chapter 2 presents introduction to BIF and the geology and stratigraphy of the Transvaal Supergroup. This chapter is followed by geology of the study area; this is outlines

project specific geology and it also covers the different lithologies identified including their basic characterisation. The fourth chapter details the petrography and mineralogy of the identified lithologies. The chapter provides a detailed account of the mineralogy of each rock unit with particular emphasis placed on textures. The petrographic information obtained and sample groups derived in this chapter provide a key framework for the presentation and evaluation of the geochemical data presented later. It also summarise the methodologies employed to study these rocks. The 5th chapter of the thesis presents the whole-rock geochemistry of the BIF and underlying chert breccia. The 6th chapter provides a detailed discussion of the results presented in the previous chapters. The different BIF exposures are also compared geochemically and texturally and the implications that this study may have on further exploration work.

1.7 Methodology

In order to achieve the aims and objectives of the study, an investigation integrating field work, petrographic, mineralogical and geochemical studies will be carried out. Field mapping of outcrops will be conducted and drill holes will be logged and systematically sampled. The samples will be collected from both core and outcrops from the study area. The collected samples will be studied with the aid of reflected and transmitted light microscopy, followed by scanning electron microscopy (SEM), X-ray powder diffraction(XRD) and electron microprobe analysis (EPMA) on selected samples. Major and trace element analysis will be performed using standard X-ray fluorescence (XRF) instrumentation. The samples were prepared using a backloading preparation method. They were analysed with a PANalytical Empyrean diffractometer with PIXcel detector and fixed slits with Fe filtered Co-Kα radiation. The phases were identified using X'Pert Highscore plus software. The relative phase amounts were estimated using the Rietveld method.

1.7.1 Core logging

In addition to geological field mapping and geophysical data interpretation, the selected drill holes were logged. These drill holes were logged at project site,

Geological Survey core facility and Daheng warehouse in Gaborone. In total, seven drill holes were logged; detail logs will be presented in Chapter 3.

1.7.2 Mapping

Large part of the study area is covered by recent Kalahari sediments. The few outcrops in the area include Moretlwa Hill, Ukwi Hill and Tshitsane Hill. A mapping exercise was undertaken on Tshitsane, Ukwi and Moretlwa Hills to map the extent of exposed BIFs, chert and dolomites. The main aim of mapping was to map structures, identify contacts, take structural measurements of the exposures and determine whether these Hills were possibly karst feature. A geological was obtained from The Geological of Botswana that includes recent digital interpretations from Leigh Rankin and Nick Lockett. The Locket interpretation appears to be the most locally detailed for iron formations, with the maps providing geology using the local stratigraphic nomenclature. The Rankin maps provide excellent regional structural interpretations.

Geophysical sub-set containing the final high-resolution central Kalahari aeromagnetic data grids, the 2002 and 2004 Falcon data sets, and the southern Botswana and larger southern African ground gravity datasets; this was obtained to aid mapping iron formation beneath the Kalahari cover. Where it is available the Falcon data appears to well map the dense BIFS as gravity positive signatures, and would be appear to be the mapping and prospecting tool to use for the identification of both BIF outcrop and BIF covered beneath Kalahari cover in southern Botswana.

1.7.3 Sampling

A total of twenty-six samples were selected for this purpose; the greatest majority of which come from the selected drill cores. Twenty-four come from drill cores, three from outcrop samples while one represents drill chips from water-well drilling. The samples comprised BIF (twenty-one samples), chert breccia (one sample), shale (three samples) and ultra-mafic rock (one sample).

1.7.4 Sample preparation

All selected half-core samples were quartered using a diamond blade-cutter at the Department of Geology, Rhodes University; the one quarter of core was kept while the rest was crushed and pulverised for analysis. A ring-mill made of chrome and carbon body steel and rings was used to pulverise the selected samples. BIF samples were pulverised for five minutes each, whiles shale were pulverised for about two minutes each. During preparation it was essential to keep the equipment and the area clean to avoid contamination. Quartzite, paper towel, acetone and compressed air were used to clean the equipment, mainly to remove the fine particles and thus minimise contamination.

1.7.5 Petrography

Twenty-six polished thin-sections were prepared and studied under reflected light microscopy using a Leica microscope. All thin-sections were cut and polished at the laboratories of the Rhodes Department of Geology.

1.7.6 Data availability

Data and geology maps were obtained from the Botswana Geological Survey, Water Affairs and Private Mining and Mineral Exploration Companies. Extensive exploration surveys and drilling in the past was mainly focussed on diamonds, gold, PGM and other base metals by companies such as Rio Tinto, De Beers, Molopo Farms Company and Anglo American. This included heavy mineral sampling, airborne magnetic and gravity surveys, ground gravity and magnetic surveys and some drilling to delineate Kimberlite pipes and test PGM's in Molopo Farms Complex.

The data used for the compilation of the maps came mainly from the Central Kalahari Project (CKP) in the form of: borehole data, geological maps, geological reports, journal papers and geophysical data. Thousands of boreholes have been drilled in this area and are all kept in the Geological Survey and Water Affairs. Both the Geological Surveys and Daheng Exploration were visited for logging and sampling purposes. On request the core and chips can be made available by the

Geological Surveys of Botswana. Consultations can be made with private mining and exploration companies to view their core and log some of their core.

1.8 Problem statement

High-grade iron ore resources in Southern Africa, although large, are limited and continued exploration for these resources is essential to meet world demands and support sustainable economic growth locally and regionally. Most importantly for exploration purposes, especially in respect of possible “greenfield” target areas outside the Maremane Dome in the Northern Cape of South Africa, it is necessary to be able to correctly and determine the lateral extent of palaeo-erosional surfaces and associated lateritic palaeo-weathering profile, with which high-grade iron ores are apparently associated (Beukes & Gutzmer, 2008a).

This is particularly important for the study area in Botswana, because in this area prospective Transvaal Supergroup rocks are inferred to persist under Kalahari cover northwards from the iron ore-rich Griqualand West region. The main exploration target is thus for ancient supergene karst-hosted high-grade hematite iron ore deposits of the Sishen-type (Van Schalkwyk and Beukes, 1986; Beukes etal., 2003; Dalstra and Rosiere, 2008; Van Deventer, 2009). In the supergene model of Beukes et. al (2003), high grade iron ores are only developed where the Gamagara unconformity transects BIF whereby three successions are involved: the Asbestos Hills succession of the Maremane Dome, the Rooinekke Iron Formation of the Koegas Subgroup ssouth of the Dome, and the manganese ore-hosting Hotazel Iron Formation overlying basaltic andesites of the Ongeluk Formation north of the Dome. However, correct identification and correlation of the unconformity is not always a simple task. In the prospecting for ancient supergene BIF-hosted high-grade hematite ore in the Neoarchean to Early Paleoproterozoic Transvaal Supergroup it is important to consider that:

- Large expanses in the study area are covered by recent Kalahari sediments and often it is only the more resistant quartzites of the Elim/Olifantshoek red bed successions that outcrop. However, these quartzites have rather similar appearance in outcrop that causes uncertainties in correlation.

- The Intrusive Molopo Farms Complex that tends to replace the Transvaal sequence in places. A major problem in the Molopo Farms area remains to establish with more concrete certainty the relative ages and correlation of quartzites outcropping in the area and intersected in drill cores.

1.9 Rationale of the study

A sequence of Transvaal Supergroup sediments extends into southern Botswana beneath Kalahari cover as the Kanye basin. These are known to host billions of tons of iron ore at >60wt% Fe. The Masoke Iron Formation (Kanye Basin), the best candidate stratigraphic host for Fe ore, is likely stratigraphic correlative of the Ghaap Group and Chuniespoort Group of the Griqualand West basin and Transvaal basin, respectively. The Palaeoproterozoic Transvaal Supergroup in the Northern Cape Province of South Africa hosts high grade (>60%Fe) hematitic and specularitic iron and manganese mineralisation. It is therefore important to study and record the petrographic, mineralogy and geochemistry of Masoke Iron Formation.

The area of study has a potential to host and produce large iron ore deposits, as the geological setting in this area incorporates many of the elements necessary for iron ore formation. These include the occurrence of (Masoke) BIF and major unconformities registering potentially prolonged periods of palaeo-weathering. This area can therefore potentially have both hypogene and supergene enrichment of BIF leading to Fe ore formation. Prospecting for new deposits is likely a function of a combination of the following parameters, namely the presence of iron formation units; proximity of other mapped BIFs of the Asbestos Hills and Voëlwater Subgroups; thrust faulting as indicated by the aero-magnetic interpretation; duplication of putative ore-bearing horizons by folding; intersection of BIF by major faults; proximity of outcrops of siliciclastic strata of the Olifantshoek/Elim Supergroups containing the Gamagara unconformity;and the presence of underlying carbonates (dolomites) and thin overlying Kalahari sand cover.

Major BIF units in the area of study include the Masoke Iron Formation. This is a likely stratigraphic equivalent to the Kuruman Formation of the Asbestos Hills Subgroup, the Rooinekke iron formation of the Koegas Subgroup and the Hotazel

Formation of the Voëlwater Subgroup. Supergene enrichment of these BIFs may occur wherever they are overlain by a major regional unconformity. The base of the Waterberg and Olifantshoek Supergroups represent major unconformities in this regional target area. Potential for hypogene deposits is also indicated by faulting (preferably extensional) proximal to BIF. On either side of the Molopo River, along the border between South Africa and Botswana, a number of these factors coincide to produce potential iron ore deposits beneath thin Kalahari Sand cover. There is, however, very little known about the petrographic, geochemical and mineralogical composition of Masoke Iron Formation. The reason for this lack in information is due to the lack of outcrops and fresh material for analysis. This project will provide fresh sample for petrographic, geochemical and mineralogical analysis.

1.10 Selected drill holes

There is a number of drill holes drilled in the area of study including some historical drilling for diamonds, PGM and iron ore by a Chinese-owned company called “Daheng”. Seven drill holes were selected to meet the aims and objectives of the study. All selected intersected Transvaal-like lithologies, mainly BIFs, ferruginous chert, breccia, shales and ultra-mafic rocks of the Molopo Farms Complex. The drill hole selection was mainly based on the lithologies intersected during drilling. The primary aim was to identify and characterise various types of un-oxidised iron formation, oxidised iron formation, mineralised iron formations and non-mineralised iron formations. The selected drill holes are: GAST5, KP17, KKTA001, KKTA006 and KKTA013.

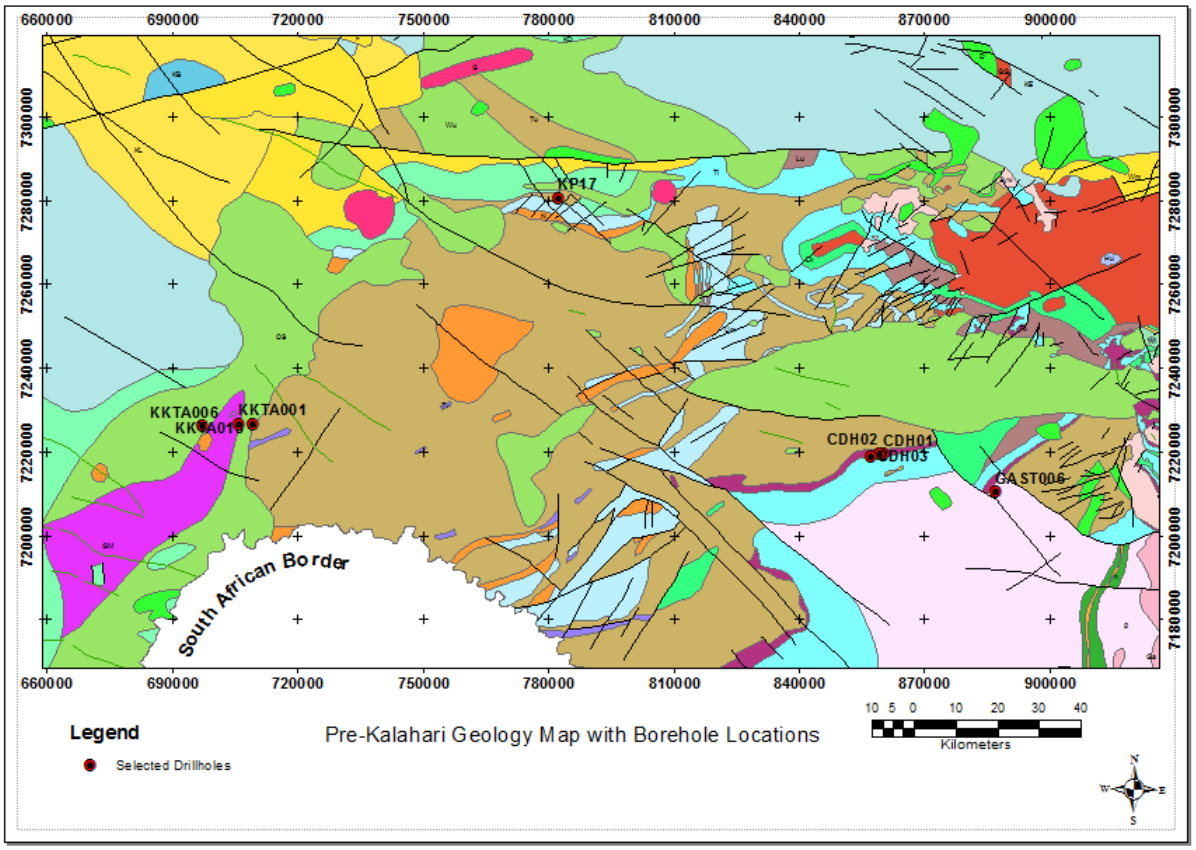

Figure 1.7: 1:250K Geology Map of the study area showing drill hole locations (Rio Tinto Internal report by Mr N O Nkabelane, September 2015).

1.11 Exploration history of the study area

1.11.1 Data Compilation

A comprehensive Rio Tinto Southern Botswana historical data compilation of ironstone prospecting tenure and mapping review was completed between in 2008. An iron occurrence map and database were completed and a listing of historical base metal tenure relinquishment reports identified from prospecting tenure maps from 1995 to present included iron formation logs were reviewed. The latest base metal prospecting tenure map was retrieved in both hardcopy and digital form. The mapping review though confirmed that the local Botswana equivalent of Transvaal group BIFs are fairly extensive in the “Kanye Basin” of southern Botswana and outcrop at a few localities, but for the most part the BIF formations are covered by the Kalahari cover.

1.11.2 Project review

Rio Tinto Exploration tasked a team of experts to identify iron ore targets in specific African countries. Southern Botswana was identified as one of the targets and was ranked highly due to its prospectively and operating environment. Rio Tinto Exploration was then awarded a Prospecting Licence in 2009 and not much work was done due to the global financial crisis (GFC) until late in 2012. The work conducted within the license includes ground geophysical surveys, mapping, and drilling and down hole surveying.

Iron ore exploration in the area of interest in Botswana was never a focus point in the past for Rio Tinto or any other companies. The only exploration done for iron ore was recently done in the eastern sub-basin on ground adjacent to Tshitsane Hill. This included gravity and magnetic surveys and the drilling of around five drill holes on the delineated BIF strike length by Daheng Exploration (a Chinese controlled exploration company).

Exploration in the area of interest, in past was mainly focussed on diamonds, gold (Au), Platinum Group Metals (PGM) and other base metals by companies such as Rio Tinto, De Beers, Molopo Farms Company and Anglo American. This included heavy mineral sampling, airborne magnetic and gravity surveys, ground gravity and ground magnetic surveys and drilling to delineate Kimberlite pipes and test PGM's in Molopo Farms Complex and gold occurrence within the prospecting areas. The other main focus area of exploration was in an area south of the northern sub-basin between the eastern and western sub-basin on the Bushveld correlated Molopo Farms Complex for PGM's. This included a number of geophysical surveys and core drilling. On the BIF outcrop on Janeng Hill a small drilling program in the 1960's was conducted to explore for asbestos and manganese.

1.11.3 Historical Mapping of Botswana's Transvaal Equivalent Strata

Transvaal equivalent strata have been mapped in southern Botswana as far west as the Kalahari Suture Zone in the area of Mabuasehube Pan, west of Kokong, and at Kokong; the Kokong Transvaal based on borehole intersections alone. The northern boundary of Transvaal Group appears to be about the latitude of Jwaneng, extending just south of and parallel to the east-west trending Palala Shear Zone-

Zoetfontein Fault. The Kanye Basin was mapped by Crockett (1969, 1972) as the northern salient of the Northern Cape Basin and contains the Botswana equivalent of the Northern Cape Basin's Griqualand West Sequence (Carney, Aldiss, and Locke, 1994). Tombale (1986) and Mapeo (1990) mapped the more westerly and southern sections of the Kanye Basin as being the "Taupone Group Dolomite" a correlative of the Chuniespoort Dolomite in South Africa, with the Masoke Formation BIF and Kgwakgwe Chert formations being equivalent to the Penge Iron formation of the Chuniespoort Group. Further east in the Kanye Basin, Tombale's Segwagwa Group correlates with the Pretoria Group of the Transvaal Supergroup. It's also noted that it's probably Segwagwa Group rocks inferred for the extreme far west of the Kanye Basin at Mabuasehube Pan, as upper Transvaal Pretoria group rocks were mapped there.

The Masoke Formation of the Taupone Group is probably the closest Botswana equivalent to economic RSA iron formations and is up to 400m thick (Carney, Aldiss, and Locke, 1994). Uplift and erosion of Transvaal equivalent sediments over the Lobatse Arch is thought to have reduced the value of Botswana iron formations relative to their South African equivalents, but the Kalahari covered Taupone Group north of the Knapdaar occurrence is thought to be most prospective for economic iron occurrences (Carney, Aldiss, and Locke, 1994). This generally north-south trending band of Taupone Group would also appear to include the exposed BIF outcrop at Motsoye Hill (Figure 2), as a strike-slip fault of 25-30 kms offset appears to have moved the Taupone group strata to the west-northwest of the Knapdaar occurrence, in the vicinity of the Motsoye Hill BIF occurrence.

CHAPTER 2 GEOLOGY AND STRATIGRAPHY OF TRANSVAAL SUPERGROUP

2.1 Introduction

2.1.1 Definitions

Iron-formations are thought to be chemical sedimentary rocks consisting essentially of silica and iron in the form of oxides, carbonates, silicates and sulphides. A great majority of the known IF are mostly confined to the Precambrian, which are also well banded with alternating layers of chert/ quartz and iron minerals. Therefore, they are commonly called as Banded Iron-Formations (BIF). BIF exhibit diverse physico-chemical characteristics which make any formulation of exact definition difficult. Attempts, however, have been made in that direction. James (1954) has defined iron formation as "chemical sediment, typically thin bedded or laminated, containing 15 per cent or more iron of sedimentary origin, commonly but not necessarily containing a layer of chert". Gross (1965) has used the term in a more general way for all stratigraphic units of layered or laminated rocks that contained 15 per cent or more iron, iron minerals being interbanded with chert and the banded structure being in conformity with the banded structure of the adjacent. The weakness or limitations of above definitions are as follows:

I. The sedimentary rocks defined as banded ferruginous quartzite and banded chert although contain iron far less than 15 per cent seem to have a genetic relationship with typical banded iron-formation and a gradation in properties from the banded iron-formation to the banded ferruginous quartzite to the banded chert is well established (Beukes, 1973). Hence, 15 per shales for the definition although they are a part of the iron-formation and considered as its sulphide facies. Similarly, many non cherty, sulphidic and carbonaceous sediments are considered to be an integral part of the iron-formation although they do not come under the definition (Goodwin, 1973).

II. As far as the mineralogy and the iron content are concerned there exist not much difference between the iron-formation and younger iron-stone and the above definition never distinguish one from the other (Goodwin, 1973). Considering the wide range of rock types with diversified properties that go into one definition, it is felt unnecessary to try for an exact one. Roughly it can be presumed to be a sedimentary rock either from a chemical or from a biochemical precipitates of Precambrian origin, mostly banded or laminated, mostly a chert band alternating

with a band of iron minerals, and containing almost all elements in trace quantities except iron and silica. Iron-formations are called differently in different parts of the world. Wide diversity in character and different degree of metamorphism has made the task to evolve a common scheme of nomenclature more difficult. An adhoc committee on nomenclature was formed at Kiev Symposium which made a good attempt in that direction (Brandt et al, 1973). Iron-formation (IF) or Banded iron-formation (BIF) is the most common name used in USA, Canada, Australia and South America, and is mostly used in a lithologic sense. When the words are capitalized and non-hyphenated like Iron Formation, it implies the corresponding stratigraphic unit (Brandt et al, 1973; Kimberley, 1978).

The oxide facies of the iron-formations are known as Jaspilite in USA and USSR, as banded iron stone in South Africa, as Itabirite in South America and Western Africa, and Banded hematite quartzite (BHQ) and Banded magnetic quartzite (BMQ) in India. The term banded ferruginous quartzite (BFQ) is used for iron-formation when iron percentage is less than 15 per cent but its use in USSR is generally for oxide and silicate facies. The term banded chert is used when iron per cent is negligibly small (Beukes, 1973). In addition to these, other local names in which the iron-formation is also known are ferruginous chert, banded hematite jasper, Jasper bar, calico rock, and zebra rock (Eichler, 1976).

2.1.2 Geographical distribution

Iron-formations are widely distributed and occur in almost all continents of the world. They are mostly confined to the Precambrian Shield Areas and occupy a prominent place in their stratigraphy.mIn North America, it is found both in the Canadian Shield and in USA. Abitibi Volcanic segment, Swayze Area, Gogma Area of Michipicoten, Lake Superior Area and Kirkland Lake Area are prominent fields of iron-formation on the Canadian Shield (Goodwin, 1973). The major iron-formation of the United States are confined to the Lake Superior region, which is the southernmost margin of the exposed Canadian Shield, in the districts of Minnesota, Wisconsin, Michigan, Menominee, Marquette, Gogebic,Mesabi and Gunflint. It is also found in the northern Rocky Mountains where the Precambrian rocks form the core of the ranges in Hontana, Wyoming and South Dakota. Few deposits of younger age are also found

in the south western states of Arizona, Colorado and New Mexico (Bayley and James, 1973).

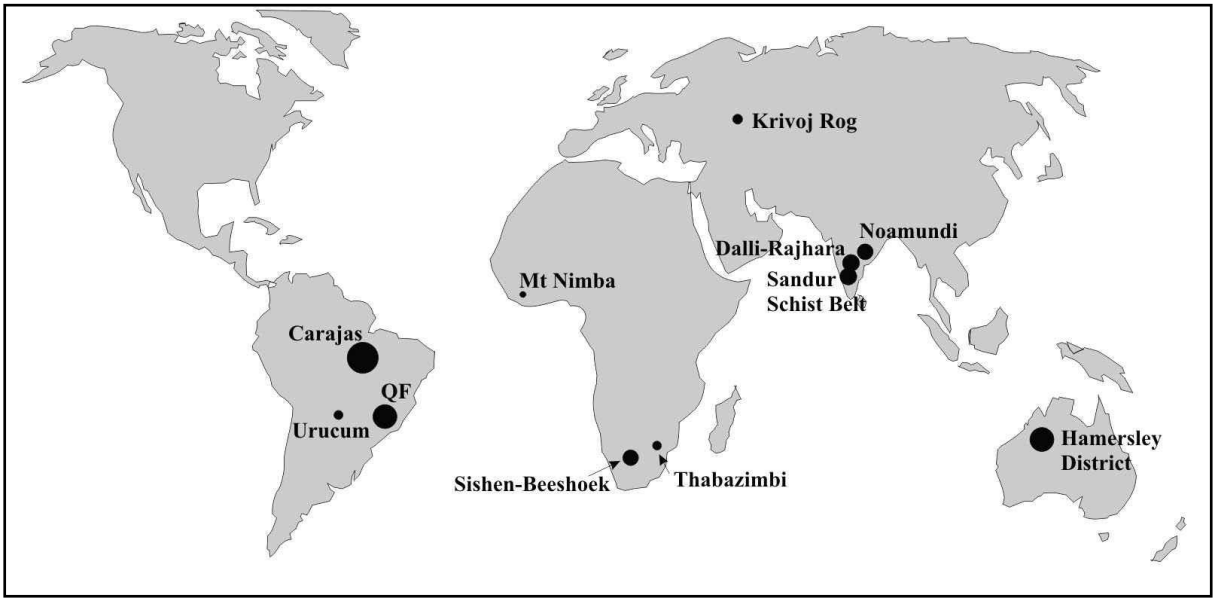

Figure 2.1: Locality map illustrating the distribution of important high-grade hematite ore deposits.

Most widely known iron formations in South America occur in the states of Minas Gerais, Brazil. It is also found as a great deposit in Serra dos Carajas of Brazil, and Morro do Urucum and Serrania de Mutun of Brazil-Bolivia border. Other iron-formations of South America are the Imataca complex of Venezuela, and few deposits of Chile and Uruguay (Dorr, 1973). Most of the iron-formations of Africa are confined to South Africa and classified into four tectono-sedimentary units such as:

I. The greenstone belts of the Kaapvaal and Rhodesian cratons,
II. The Limpopo metamorphic belt,
III. The cratonic basin of Pongola, Witwatersrand and Transvaal Supergroups, and
IV. The Damara Mobile belt (Beukes, 1973). It is also found as
V. Group, Mauritania and in Liberian Shield of West Africa, (James, 1973).

Major iron-formations of Australia are: the iron-formations of Yilgarn Block and Pilbara Block of Western Australia, the iron-formation of the Hamersley Basin of Western Australia, iron-formations of the Cleve Metamorphics of South Australia, haematite rich sediments of the Yarnpi Sound area of Western Australia, the Roper Bar and Constance Range iron-formations of the Northern Territory and Queensland

and the Holowilena iron-formations and Braernar iron-formations of South Australia (Trendall,1973).

Iron-formations of Europe and Asia are mostly confined to USSR and India. In USSR, it occurs mainly along a trend which can be followed between the coastal regions of the Azou Sea in the south and the Kola Peninsula in the north. The deposits of Krivoy Rog, Krurnenchung within Ukrainian Shield and those of the Kursk Magnetic Anomalies (KMA) are well known iron-formations. The Precambrian iron-formations also occur in Urals and the Asiatic parts of the Soviet Union (Alexandrov, 1973).

Iron-formations of India occur in several states of India and major types are classified into two main groups as:

I. The iron-formation of the Dharwar Group, and
II. The iron-ore series of Bihar, Orissa and Madhya Pradesh.

Most of the iron-formations lie close to the border of the Cratonic masses now surrounded by younger fold belts and platform sediments as in between South America and Africa, and between Australia and India. Therefore, perhaps, the segmentation and drifting of Gondwanaland mass has followed a Precambrian fault belt which was perhaps the basin of the deposition of iron-formation (Gross, 1973; Eichler, 1976).

2.1.3 Distribution in time and space

The distribution of iron-formation in the geological time scale involves the age determination which forms a major problem in the case of banded iron-formations because of the negligible concentration of elements present in it which are essential for the radiometry dating. However, the probable age range is determined by dating the associated meta-sedimentary and meta-volcanic rocks which includes the underlying basement rock, rocks lying just above the iron-formation and the igneous intrusions. Direct dating by K-Ar, Rb-Sr and U-Pb techniques have been tried by many. The age determination by K-Ar and Rb-Sr generally proves to be the age of post-depositional metamorphism whereas dating by U-Pb claims to give values close to that of sedimentation (Goldich, 1973, James 1983).

Despite the weakness in basic data the average age range of the iron-formations have been established and can be classified into four age groups as:

I. The middle Archean (3500 Ma - 3000 Ma),
II. The late Archean (3000 Ma - 2600 Ma),
III. The early Proterozoic (2600 Ma - 1900 Ma), and
IV. The late Proterozoic to early Phanerozoic (750 Ma - 450 Ma).

I. Deposits of early and middle Archean are 3000 Ma.

The oldest iron-formation is considered to be Isua iron formation, Greenland with an age of at least 3750 Ma (James, 1983). These iron-formations are interbedded with quartzite strata that represent the oldest rocks of the supra crustal origin. The other important iron-formations belonging to this group are Irnataca complex, Venezuela (3400 Ma - 3000 Ma); the Pilbara and Yilgarn blocks of Western Australia (close to 3000 Ma); the Ukranian Shield of Greater Krivoi Rog (3500 Ma- 3100 Ma) and the iron-formation of India both belonging to the Dharwar Group and the Iron-Ore series of Bihar and Orissa with a probable age range (3200 Ma - 2700 Ma), (Goldich, 1973; James, 1983).

II. Deposits of late Archean i.e. (3000 Ma – 2600 Ma)

The well known iron-formations falling under this age group are: the iron-formation of the Superior Province of the Canadian Shield, (2750- 2700 Ma), the Sekakvian, Bulavayan and Sharnvayan system of Zimbabwe (2750- 2700 Ma), the Witwatersand Supergroup of South Africa (2650 Ma), and the eastern Keralia on the Baltic Shield (2800 Ma.) (Goldich, 1973; James, 1983). The Indian iron-formations of both Dharwar group and the Iron-Ore series of Bihar and Orissa, and the iron-formation of Yilgarn Block of Western Australia are sometimes included in this group instead of middle Archean because of the uncertainty in their age (Goldich, 1973). Most of the iron-fonnations of this group fall within the brief interval of (2750-2700 Ma) indicating an epoch favourable for iron-formation.

III. Deposits of early Proterozoic age (2600 - 1900 Ma)

The early Proterozoic was the major epoch in the iron sedimentation and stands as a milestone in the history of the earth. The six most important iron-formations of the world fall into this group. They are: the vast iron-formation of the Lake Superior Region Canada-USA (2200-2000 Ma); the Labrador Trough and its extension of Canada (2200-2000 Ma); Krivoy Rog and Krush Magnetic Anomaly (KMA) of USSR

(2200 - 1900 Ma); Transvaal system of South Africa, Minas Gerais of South America and the Hamersley area of Western Australia (2200 - 1900 Ma). Most of these major iron-formations fall within an age range of 2200-1900 Ma representing a very favourable time period for the deposition of iron-formation (Goldich, 1973; James, 1983).

IV. Deposits of late Proterozoic and early Phanerozoic age

These iron-formations are very rare. A few deposits are there in Nepal and Brazil. They are also found in the Maly Khinghan and Uola areas of far eastern USSR. Some appear to be Archean types associated with contemporaneous volcanism and otters bear an ill defined relation to the late Proterozoic glaciations. The most notable example of the iron-formation related to the deposits of possible glaciogenic origin is that of the Rapitan Group, Canada, (James, 1983).

The spatial distribution or initial tonnage of iron formations cannot be precisely determined. The margins of errors in these estimations are certainly very large although there are reports on these here and there in the literature. James (1983) has also given a good account of these for some well known iron-formations. Problems associated in the estimation of spatial distribution are deformations and erosion over periods of time in billions of years, incomplete geological mapping and viability of geological assessment in connection with the geometry. James (1983) has also given a graphical picture of their spatial abundance to indicate that the 90 per cent of the total deposit belong to early Proterozoic which we call as the Superior-type. In terms of number of stratigraphically distinct bodies the minor abundance peak of late Archean is most notable. These deposits number in thousands but very minor in their initial tonnage and are called the Algoma type. Similarly, the Phanerozoic are also not that abundant (James, 1983).

Banding is the most distinct lithological feature of the Precambrian banded iron-formation although its origin is yet controversial. Bands rich in iron minerals alternates with bands rich in chert. Bands are quite variable in their continuity, thickness and mineralogical make up, giving a heterogeneous character to the rock formation. Band thickness varies from less than 1 millimetre to several 1 centimetres and continuity varying from few meters to several kilometres. A long continuity of nearly 300 km is well marked in iron-formation of Hamersley Group and at places of South Africa and India.

Metamorphism and orogenesis has blurred many of its primary features and tectonic deformation has generated many structural features like folding. Trendall (1973) has recognised three scales of banding. These in order of decreasing scales are macro banding, meso-banding and micro-banding. Large scale macro-bands are due to the alternation between thin layers of shales and thick layers of band cherty iron-formation, the thickness ranging between 0.6 – 15 centimetres. Meso bands represent the alternative bands of sharply defined iron rich and iron poor layers, thickness varying from few millimetres to several centimetres. Micro bands represent thin banding of iron minerals and chert within a meso-band, thickness varying between 0.2 - 2 millimetres. They are also known as verves (Trendall, 1973). The micro-bands within a chert meso-band consist of iron minerals and in bedding planes that forms the adjacent meso-bands. Red micro bands are due to very fine disseminated haematite, bluish grey micro-bands are for specular hematite, grey and black micro-bands are due to magnetite, while and yellow micro bands are for carbonates, green micro bands are due to chlorites and dark grey micro-bands for carbonaceous materials (Alexandrov, 1973).

Iron-formations are sometimes classified as one component, two components or three component systems depending upon the number of rock forming minerals (except chert). They contain iron mineral in one component system which is either hematite or magnetite or carbonate with associate carbonaceous materials. In case of two component system, micro-bands consist of any two above minerals forming laminae alternating with each other. In case of three component system, one mineral remains as a subordinate to the other two and never forms a micro-band of its own (Alexandrov, 1973).

Iron rich shales also show rhythmic banding of barren quartz or jasper layers alternating with shaly (or silicate). Layers, micro-bandings are quite conspicuous in barren chert (quartz) band and appear as thin laminae of siderite or magnetite. As the iron rich shales grade into iron-formations, carbonate quartz layers or shaly layers are replaced by ore layers (Melnik, 1982). The bandings are usually parallel. However, angular unconformities sometimes exist due to erosion during deposition.

Certain iron-formation exhibit cross bedding and ripple marks to indicate their deposition under a shallow water condition.

Other sedimentary features like slumping, sedimentary breccia and micro faulting are well marked in many iron-formations. Sedimentary structures like scour and fill structure and pre-lithification slump structures like shrinkage and cracks are also marked at places. Development of above structures is due to compaction, desiccation and digenetic alternation of amorphous precipitates (Gross, 1972). Algal structures have been observed in iron formation of USA (Bayley and James, 1973) and in Kuruman iron formation, Transvaal Supergroup South Africa (Beukes, 1973). A remarkable feature of the Hamersley iron-formation is the occurrence of lenticular, biconvex chert lenses along the bedding planes of the evenly banded iron-formation (Eichler, 1976).

Iron-formations having oolitic and granular structures are mostly restricted to the Proterozoic types (Beukes, 1973; Gross, 1972). Granular textures are common in slightly metamorphosed banded iron-formation of the Lake Superior region (Bayley and James, 1973; French, 1973), and in Kuruman and Penge iron formation of South Africa (Beukes, 1973). The granular textures are most uncommon in BIF of USSR · (Alexandrov, 1973). The granules are either spherical or ellipsoidal and consists of iron silicates (Greenalite, minnesotite and stilpnomelane), chert and magnetite in variable proportion. In most of the cases, rocks containing granules grades gradually into oolitic rocks in which oolites are rimmed with hematite (Bayley and James, 1973; Eichler, 1976).

Indian iron-formations are well banded and are either banded hematite quartzite (BHQ) or banded magnetite quartzite (BMQ). BHQ consists of alternating layers of haematites and chert or Jasper with layers varying in thickness from 1 to 20 mm (Melnik, 1982). BMQ are very irregularly banded and cherts are medium to coarse crystalline. Brecciation have been marked in the iron-formations of Bababudan area and in Iron-Ore Series of Orissa, Quartz veins containing quartz of different texture with coarsely crystalline hematite cutting across the bedding planes are common features in many iron-formations (Picharnutu, 1974; Krishnan, 197 3).

2.1.4 Stratigraphy

Stratigraphy of iron-formations differs from one deposit to the other in their lateral continuities, thicknessesh and stratigraphic sequences. Even the stratigraphic sequences in a particular deposit are not completely uniform throughout and have different stratigraphic columns in different parts of the same basin. In spite of these

difficulties, the generalization in the stratigraphy of iron-formation within the deposits and among the deposits has been tried by many investigators. Major iron-formations belonging to the Proterozoic are quite extensive. Laterally they extend from some hundreds to thousands of kilometres and thickness varying from few hundreds to thousands of meters. Whereas most of the Archean iron-formations seem to be very much limited in their lateral continuities and thicknesses because of metamorphism, tectonic deformations and segmentations. Their lateral continuities at present stand at several kilometres and thicknesses in range of 10 to 100 meters (Gole and Klein, 1981).

The Archean iron-formations are associated with various volcanic rocks which include pillowed andesites, tuffs, pyroclastic rocks or rhyolitic flows and greywacke. Iron formations usually lie over the felsic volcanics and are in turn covered by basic volcanics. Thin beds of graphitic schist and black carbon rich mud stones containing appreciable amount of lead, zinc and copper are interbedded with iron-formations. They are presumed to have been derived from tuff and volcanic ash and collected in depressions in the depositional basins (Gross, 1972). Goodwin (1973) has reconstructed the stratigraphy of the Hichipicoten basin. In the eastern and central part of the basin, the lowermost mafic volcanic is overlain by pyroclastic rocks followed by the unit of iron-formation which is origin overlain by mafic volcanics. This is followed by a discontinuous unit of clastic sediments overlain by a younger mafic volcanics. In the western section of the basin, the lowermost mafic volcanics are overlain by a thick clastic sediment, the unit of iron-formation re~ining just inside the clastic sediment which is again overlain by younger mafic volcanics. So the iron-formation in the central and eastern part is in between mafic and felsic volcanics whereas in western part it is inside clastics. In the western part:, the iron-formation represent its oxide facies and is typically composed of interbedded chert magnetite and jasper (hematite chert) enclosed in greywacke mudstones. The central IF representing the carbonate facies consists of in descending order a thick band of tended chert, thin sulphidic and thick carbonate layer.

2.1.5 Classification

The Precambrian banded iron-formations have been classified into two major groups based on their lithologies, rock associations and depositional environments (Gross,

1965, *1913,* 1980). The iron-formations belonging to the Archean age are associated with volcanic rocks and/or greywackes, and are mostly probably deposited in inter-cratonic basins of synclinal types. These iron-formations are associated with greenstone belts and are known as Algoma types. On the other hand, the iron-formations of the early Proterozoic time that are associated with quartzites, lime rock and black shales and devoid of any direct volcanic association are known as the Superior type or the Animikie type. These were perhaps formed in intra-cratonic continental shelf environments of miogeosynclinal types. These superior types are quite thick and sufficiently extensive in their lateral extent compare to the Algoma type (Garrels et al, 1973; Lepp, 1975). A comparison between these two major types of iron formation has been made by Gross (1913) and Eichler (1976). This twofold classification of the Precambrian banded iron-formation has its own limitations (Trendall, 1968; Gale and Klein, 1981):

I. There are many iron-formations younger than 1800 Ma that never come under this classification. Therefore, Garrel et al, (1970) has classified the Precambrian iron formations as:
(a) Archean type, (b) Animikie type, and (c) Post Animikie type;

II. The present scheme of classification has not recognized the similarities among iron-formations but largely based on differences in their stratigraphic and tectonic settings (Kimberley, 1978);

III. The Lake Superior types are usually presumed to be a relatively near shore deposit but there are many deposits belonging to this group that were usually formed in a deep water offshore conditions as assumed in case of the iron-formation of the Hamersley Pas in (Gross, 1980);

IV. Some Superior type iron-formations like that of Hamersley Group art: also associated with volcanic rocks;

V. Iron-formations confined to high grade granulite. These are highly folded magnetite quartzite metamorphosed under granulite facies condition, and occur in association with quartzite, mica schist, marble and meta-Volcanics engulfed in tonalitic gneiss (Radhatrishna et al, 1986). Therefore, it is quite natural that the iron-formations with their divergent characters cannot be exactly classified although a broad classification to above two major types is quite prevalent.

2.1.6 Mineralogy

Banded iron-formations are characterized by alternative bands of iron-minerals and chert. Iron because of its variable oxidation state is very sensitive to environmental conditions and, therefore, can form different minerals in response to the available environmental conditions like Eh, pH and concentration of different active species like CO2, S, SiO2 and others. Post depositional processes like digenesis metamorphism and, of course, weathering, changes the initially formed precipitate to primary and secondary minerals. So the present mineralogy of the iron-formation could be a product of initial condition; and subsequent post depositional changes that it is bound to ur1dergo. James (1954, 1966) has classified the iron-formation based on its mineralogy into four different facies such as oxides, carbonates, silicates and sulphides, depending upon the dominant iron mineral it carry with. These facies are extreme cases and are gradational giving rise to mixed facies.

I. Oxide Facies

The main oxide minerals that make the oxide facies are mostly hematite (Fe_2O_3) and magnetite (Fe_3O_4). The oxide facies can, therefore, be divided into two subtypes – banded hematite quartzite and banded magnetite quartzite. The banded hematite rocks consist of alternating bands of hematite and chert. Haematites' are well crystalline and the degree of crystallinity depends upon the degree of metamorphism it has undergone. Sometimes haematites show oolitic structure, indicating their deposition in shallow water conditions. The banded magnetite rods not only forms alternate bands of magnetite and chert but also contains layers varying proportion of iron silicates, carbonates and chert. The magnetite sub facies; therefore, go with slightly higher proportion of MgO, CaO, MnO, CO_2 and FeO/Fe_2O_3 than its hematite counterpart. In an Eh & pH stability diagram, hematite occupy a wider field of high Eh and high pH whereas magnetite is confined to a narrow field of low Eh and high pH conditions and overlaps with the field of silicates. Its formation and its area of stability is subjected to the activity of CO_2, S, and SiO_2 and, therefore always associated with carbonates, silicates and sulphides.

II. Carbonate Facies

The dominant iron mineral which makes this facies is iron carbonate, siderite ($FeCO_3$). It also contains other minerals like Ferro-dolomite, ankerite and calcite as

accessories. It consists of alternating layers of carbonates and chert and looks like a carbonate counterpart of oxide facies. They do not show oolitic structure, therefore, must have deposited below the level of wave action. These carbonate facies are usually associated with carbonaceous materials and pyrites and are, therefore, seem to be slightly rich in P_2O_5 and SiO. They mostly grades into either oxide or sulphide facies. Although the gradation of carbonate to sulphide facies is common, the gradation from carbonate to oxide is rare. The stability field of carbonate facies, in the Eh and pH stability diagram, remains in between the stability field of oxide and sulphide facies which explains the above facts.

III. Silicate Facies

Silicate facies of iron-formation consists of different iron silicates depending upon the degree of metamorphism the rock has undergone. The iron silicates are mostly greenalite, minnesotaite, chlorite, iron amphiboles of greenalite - commingtonite series, orthopyroxene and iron olivine called fayalite. Greenalite is believed to be the primary silicate which has given rise to other silicates in the course of metamorphism. Their formation also depend on the availability of other oxides like Al_2O_3,TiO_2, CaO, Na_2O, K_2O and MgO. The silicate facies can be grouped as granular and non-granular. In the Eh and pH stability field diagram, the silicate field overlaps the stability fields of magnetite, carbonates, and sulphides and, hence, closely associated with them. Pyrite is also sometimes found as an accessory mineral. It is not quite clear, the conditions that would permit the precipitation of iron and silica as one phase rather than as separate phases (James, 1954; Melnik, 1982).

IV. Sulphide Facies

The main mineral in the sulphide facies is disseminated pyrite with small amount of pyrrhotite and minor siderites in black carbonaceous shales. They may contain chert layers here and there. All sulphide facies contain abundant carbon and clastic material indicating their formation in deep water condition where oxygen was not sufficient to decompose organic matter (Goodwin, 1973). Sulphide facies are mostly restricted to the Archean iron formation (Eichler, 1976).

2.2 Regional Geology

The Kanye basin of Botswana, Transvaal basin in the Transvaal geographic region and Griqualand West in the Northern Cape Province of South Africa (figure 2.2) contain lithostratigraphically similar deposits (Armstrong et al., 1991; Eriksson et al., 1995; Altermann and Nelson, 1998). Stratigraphic units in the Transvaal Sequence can be correlated between the Transvaal and Griqualand West basins (Beukes, 1977, 1986; Hälbich et al., 1993; Eriksson et al., 1995; Martin et al., 1998), where volumetrically significant carbonates and siliciclastic rocks are overlain by BIF deposits which are in turn overlain by a thick sequence of predominantly clastic sedimentary rocks (Altermann and Nelson, 1998). In the Northern Cape Province, the Transvaal Sequence consists of a chemical sedimentary rock package (Ghaap Group) unconformably overlain by a mixed volcanic-chemical-clastic rock package of the Postmasburg Group (Beukes, 1986). The angular unconformity is directly overlain by a glacial tillite (Makganyene Diamictite) that is separated from the overlying Postmasburg Group by a low-angle unconformity (Altermann and Hälbich, 1991).

The Transvaal Sequence overlies the ca. 2715 Ma Ventersdorp Supergroup, and is in turn overlain by red beds of the Olifantshoek Group (siliciclastic-rock package). Beukes (1983) suggested that the deposition of the Transvaal Sequence in the Northern Cape Province was controlled by three major tectono-sedimentary elements, and as a result, basin-facies rock packages developed at the western and south western margin of the Kaapvaal Craton, whereas platform-facies rock packages (including platform edge) developed parallel to the Griquatown Fault Zone and northwards to the Korannaberg fold belt (Beukes, 1986). Altermann (1997) demonstrated that this fault is younger than the basin and had no influence on basin development. As a result, the Griqualand West basin is subdivided into the Ghaap Plateau (Beukes, 1983; platform facies) and Prieska sub-basins (Beukes, 1983; basin facies) because of their different development (Altermann and Nelson, 1998).

The Schmidtsdrif Subgroup forms the base of the Ghaap Group, and consists of upward-fining siliciclastic rocks representing subtidal to tidal-flat deposits that were subsequently drowned (Beukes, 1977). Carbonate deposition was established and developed into a major rimmed carbonate shelf on the Kaapvaal Craton (Beukes, 1987). Altermann and Herbig (1991) suggested that the Griqualand West basin

experienced its highest subsidence rates in its central parts. However, to the north of the Griquatown Fault this was accommodated by stromatolitic growth and carbonate accumulation (building the Ghaap Plateau) that maintained shallow marine conditions, whereas south of the fault, peritidal flats were often exposed to erosion and as such, prevented the accumulation of a thick pile of carbonate strata. Subsequent transgression from the west resulted in deeper water conditions. Therefore, carbonate build-up is represented by a stromatolitic-carbonate sequence (Campbellrand Subgroup) deposited in a subtidal, shallow-water setting dominated by strong currents within the Ghaap Plateau sub-basin, whereas deposition of intertidal and supratidal clastic-carbonate facies and stromatolitic facies (Altermann and Herbig, 1991; Höferle et al., 2000) of the Nauga Formation occurred in the Prieska sub-basin. The transition between the underlying carbonate build-up and the overlying BIF is gradational (Hälbich et al., 1992).

In the Ghaap Plateau sub-basin, the transition zone consists of contorted, cryptal laminated limestone–dolomite with mudrock partings, grading upward into interbedded mudrock, fine-grained carbonate and siderite-rich BIF (Tsineng Member), together they form the Gamohaan

Formation of the Campbellrand Carbonate Sequence (Klein and Beukes, 1989). These rocks are overlain by deeper water BIFs of the Asbestos Hills (Asbesheuwels) Subgroup. In the Prieska sub-basin, the decline in carbonate sedimentation was accompanied by siliciclastic in flux that culminated in the deposition of the Naute Shales, which was in turn followed by deposition of the Asbestos Hills Subgroup iron formations. BIF deposition in a basin-slope environment is interpreted as a response to the progressive deepening of the basin (Martin et al., 1998), and the rise in sea level attributed to a major transgression (Beukes, 1987).

The Asbestos Hills Subgroup has been the subject of many detailed mineralogical, sedimentological and geochemical studies (e.g. Beukes, 1980, 1983,1984, 1986; Van Wyk, 1987; Klein and Beukes, 1989; Beukes and Klein, 1990; Horstmann et al., 1990; Hälbich et al., 1993; Horstmann and Hälbich, 1995). This subgroup comprises the rhythmically banded

Kuruman Iron Formation (i.e. banded iron formation) and the clastic-textured, shallow-water ortho and allochemical Griquatown Iron Formation (i.e. granular iron formation; GIF) defined by the Danielskuil and Pietersburg Members. The 210m thick Kuruman Iron Formation (range 150–1700 m) is subdivided into four members. At its

base, the Kliphuis Member (ankerite-banded chert with shale partings) is followed by the rhythmically banded Groenwater (chert and oxide-rich BIF) and Riries Members (siderite-rich BIF), and capped by an intraclastic iron formation, the Ouplaas Member, which is interpreted to have formed in a shallow-water platform environment. The Groenwater Member comprises four subunits representing three clastic sediment and BIF cycles (Matlipani zone together with the Whitebank zone, Elgan zone and Derby zone), with the last two cycles dominated by volcanically derived stilpnomelane mudrock interbedded with chert. This coupling is repeated in the overlying Riries Member, which also has three clastic sediment and BIF cycles, the uppermost of which (Alphen zone) contains grainstone bands. The Kuruman Iron Formation is interpreted to represent shallowing-upwards deposition (initially in deepwater) and is conformably overlain by the Griquatown Iron Formation that consists of lithofacies types deposited in a shallow epeiric sea (Beukes, 1984). A shallowing-upward cycle commenced during the deposition of the Griquatown Iron Formation (Beukes and Klein, 1990), and in the Prieska sub-basin the iron formation grades upwards into siliciclastic rocks of the Koegas Subgroup (Beukes, 1986) that was deposited mainly in shallow marine to deltaic environment (Altermann and Hälbich, 1991). Uplift and erosion occurred prior to the deposition of the Makganyene Diamictite, which sits unconformably on the Koegas Subgroup in the Prieska sub-basin and, the Griquatown Iron Formation in the Ghaap Plateau sub-basin.

Subsequently, the Makganyene Diamictite is disconformably overlain by submarine Ongeluk lavas and hyaloclastites (base of Postmasburg Group), which are in turn conformably overlain by mudrocks, subordinate sandstones and bedded sedimentary-Mn deposits of the Hotazel Formation (Beukes, 1986). The Penge Iron Formation is stratigraphically equivalent to the Asbestos Hills Subgroup (Beukes, 1973; Eriksson et al., 1995; Cheney, 1996). It outcrops in the Transvaal Province within the contact metamorphic aureole of the Bushveld Complex (Miyano and Beukes, 1984), where BIF deposition (fourth transgressive cycle) followed that of the Malmani carbonates, which document three transgressive cycles (Altermann and Nelson, 1998). Hälbich et al. (1993) defined five internal subdivisions within the iron formation, which started with a chert-shale facies that graded into banded iron-oxide facies (with lower chert-rich and upper shale-rich zones), banded iron-silicate facies,

banded iron-oxide facies, and a carbonate-rich, interlayered chert and shale zone, which is discordantly overlain by clastic sediments of the Pretoria Group.

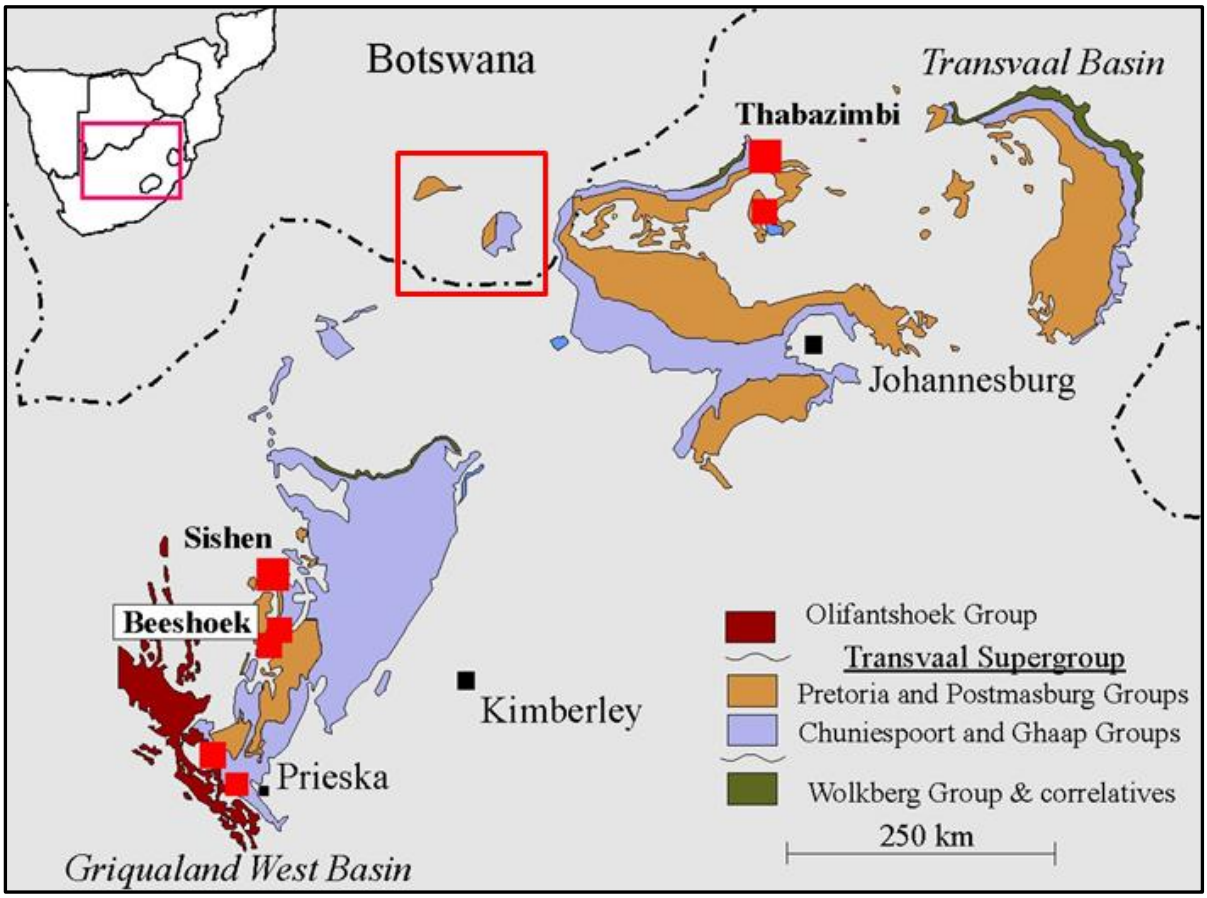

Figure 2.2: Location and regional geological setting of Griqualand West Basin, Transvaal Basin and Molopo-Kanye Structural Basin in Southern Botswana.

The succession preserved in the three structural basins in Southern Africa is generally similar, with correlation being best for the lower chemical sedimentary units, and poorest for the upper clastic sedimentary and volcanic lithologies (Table 2.1). In the Griqualand West Basin BIF occurs in the Asbestos Hills Subgroup, whilst the lateral equivalents in the Kanye Basin are ironstone and associated chert of the Masoke Formation, and in the Transvaal Basin the Penge Iron Formation hosts the high grade Thabazimbi iron-ore deposits (Eriksson et al, 2006). Whereas in the Transvaal Basin BIF is confined to the Penge Formation, there are successive BIF units in the Asbestos Hills Subgroup (Ghaap Group) of the Griqualand West Basin.

The Kanye basin of Botswana, Transvaal basin in the Transvaal geographic region and Griqualand West in the Northern Cape Province of South Africa (Figure 2.2) contain lithostratigraphically similar deposits (Armstrong et al., 1991; Eriksson et al., 1995; Altermann and Nelson, 1998). Stratigraphic units in the Transvaal Sequence

can be correlated between the Transvaal and Griqualand West basins (Beukes, 1977, 1986; Hälbich et al., 1993; Eriksson et al., 1995; Martin et al., 1998), where volumetrically significant carbonates and silicic-clastic rocks are overlain by BIF deposits which are in turn overlain by a thick sequence of predominantly clastic sedimentary rocks (Altermann and Nelson, 1998).

The Kanye Basin was mapped by Crockett (1969, 1972) as the northern salient of the Griqualand West Basin and contains the Botswana equivalent of the Northern Cape Basin's Griqualand West Sequence (Carney, Aldiss, and Locke, 1994). Tombale (1986) and Mapeo (1990) mapped the more westerly and southern sections of the Kanye Basin as being the "Taupone Group Dolomite" a correlative of the Chuniespoort Dolomite in South Africa, with the Masoke Formation and Kgwakgwe Chert formations being equivalent to the Penge Iron formation of the Chuniespoort Group. Further east in the Kanye Basin, Tombale's (1986) Segwagwa Group correlates with the Pretoria Group of the Transvaal Supergroup. It's also noted that it's probably Segwagwa Group rocks inferred for the extreme far west of the Kanye Basin at Mabuasehube Pan, as upper Transvaal Pretoria group rocks were mapped there.

2.3 Stratigraphy of the Transvaal Supergroup

The stratigraphy of the Transvaal Supergroup was described by Button (1986) and Beukes (1978; 1980; 1983; 1984; 1986; 1987) and represents 8km thick succession composed of siliciclastic, chemo-sedimentary, and volcanic rocks. In the Griqualand West Basin, the Transvaal Supergroup is subdivided into the chemo-sedimentary Ghaap Group and the volcano-sedimentary Postmasburg Group. These can be correlated with basal Chuniespooort and overlying Pretoria Groups in the Transvaal area (Table 2.1 by J.M Moore et al., 2012).

Table2.1: Comparisson of the lithostratigraphy of the Transvaal Supergroup in Griqualand West, Kanye and Transvaal Basins (J.M Moore et al., 2012)

Griqualand West basin			Kanye basin			Transvaal basin		
Group	Formation	Age (Ma)	Group	Formation	Age (Ma)	Group	Formation	Age (Ma)
(Olifantshoek)			Segwagwa	Lomugau		Pretoria	Rayton	
	Lucknow	*<2228 ± 25*[a]		Monotoholwane	*<2193 ± 20*[j]		Woodlands	
				Gatsepane			Magaliesberg	*<2205 ± 13*[k]
				Mogapinyana	*<2236 ± 13*[j]		Silverton	
	Mapedi/Gamagara			Tsatsu			Daspoort	*<2233 ± 15*[k]
				Tlaameng			Strubenkop	
				Ditojana	*<2239 ± 20*[j]		Dwaalheuwel	
	Manganore/Wolhaarkop			Kgwakgwe			Hekpoort	2224 ± 21[c]
							Boshoek	
							Timeball Hill	2316 ± 7[l]
							Rooihoogte	
Postmasburg	Mooidraai	2394 ± 26[b]					Duitschland	*<2424 ± 12*[k]
	Hotazel							
	Ongeluk	2222 ± 13[c]						
	Makganyene	*<2436 ± 7*						
Ghaap	Koegas (Subgroup)	2415 ± 6[d]	Taupone	Masoke		Chuniespoort	Penge	2431 ± 31[i]
								2480 ± 6[e]
	Griquatown	2431 ± 31[e]						
	Kuruman	2460 ± 5[f]						
	Gamohaan	2521 ± 3[g]		Ramonnedi			Frisco	
	Kogelbeen/Papkuil						Eccles	
	Fairfield/Reivilo						Lyttelton	
	Monteville	2555 ± 19[h]					Monte Cristo	
	Lokammona						Oaktree	2550 ± 3[m]
								2583 ± 5[m]
	Boomplaas							
	Vryburg	2642 ± 3[i]		Black Reef			Black Reef	2642 ± 2[i]

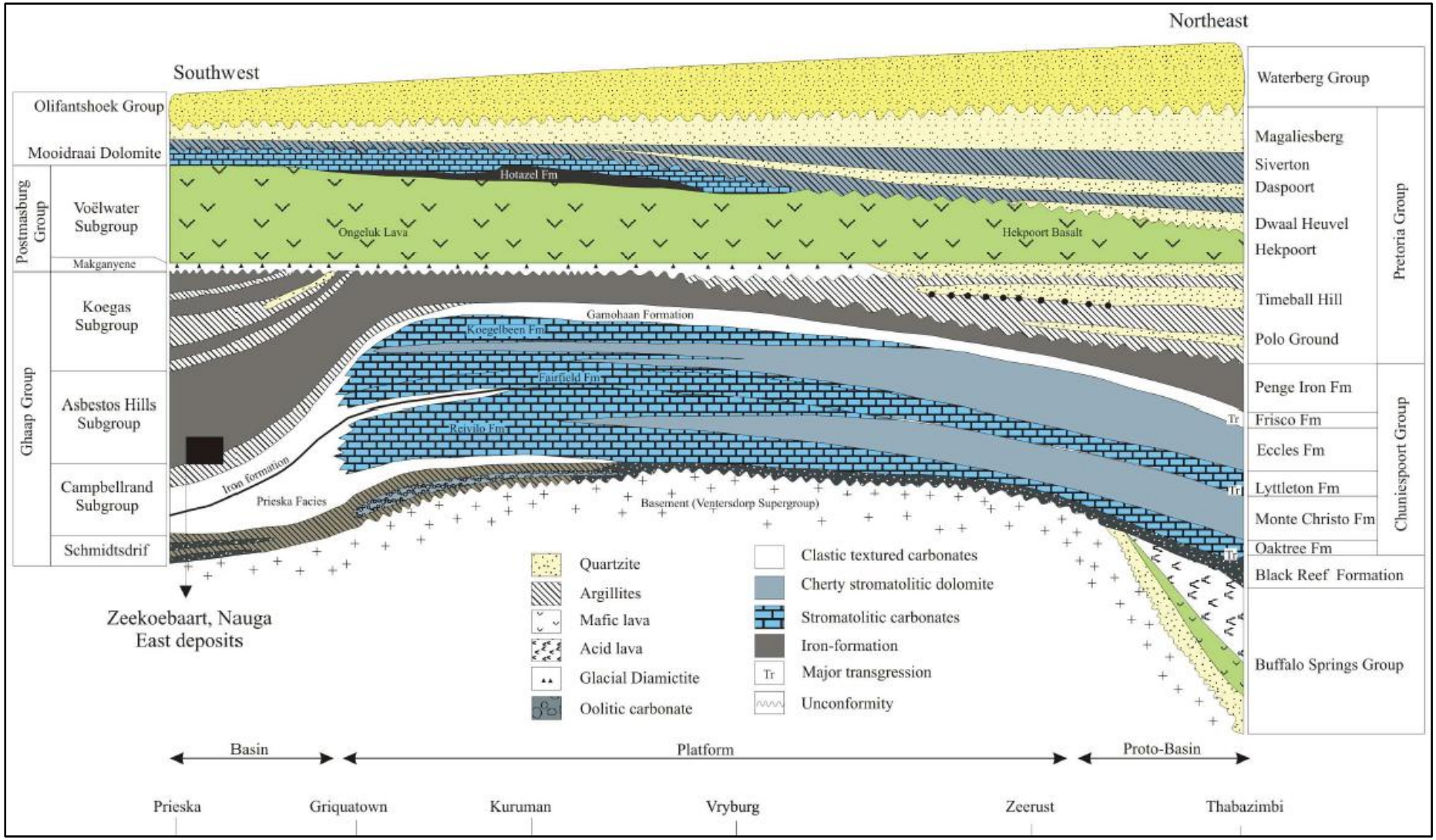

Figure 2.3: Stratigraphic cross-section of the Transvaal Supergroup, from Prieska to Thabazimbi (modified after Beukes, 1983

Deposition the Transvaal commenced at 2669±5Ma (Gutzmer & Beukes, 1998) with the mostly fluvial siliciclatic rocks of the Vryburg Formation in the Griqualanad West area or at 2588 (McMartin etal., 1998) with the Black Reef Formation in the Transvaal area; up to 2km thick Wolkberg and Buffalo Springs Groups in the Griqualand West region. A possible correlative of the Wolkberg and Buffalo Springs Groups in Griqualand West area is the Geelbekdam Member in the Vryburg Formation (figure 2.2), which is also separated by an unconformity from the rest of the Vryburg Formation (Coetzee, 2001), figure 2.3.

2.3.1 Ghaap Group

2.3.1.1 Schmidtsdrift Subgroup

The Schmidtsdrift Subgroup forms the base of the Ghaap Group, and consists of upward-fining siliciclastic rocks representing subtidal to tidal-flat deposits that were subsequently drowned (Beukes, 1977). Carbonate deposition was established and developed into a major rimmed carbonate shelf on the Kaapvaal Craton (Beukes, 1987). Beukes (1979) subdivided the Schmidtsdrift Subgroup into the basal Vryburg Formation, interpreted by Beukes (1986) to represent fluvial to marginal marine deposits, consisting of shales, siltstones, quartzites, carbonates and basaltic andesitic amygdaloidal lavas. Altermann and Siegfried (1997) interpret oolitic sands to have been transported and consequently favour a deeper subtidal depositional environment.

The Boomplaas Formation, however, is not developed in the basinal facies of the Prieska area (as indicated in figure 2.2). The upper Lokammona Formation is composed of banded siderite lutites overlying the tuffaceous siltstone, carbonate oolites and stromatolite reef deposits (Beukes, 1983). The deposits are interpreted to indicate a marine regressive cycle over the Boomplaas Formation (Altermann and Siegfried, 1997). Gutzmer and Beukes (1998) dated the Vryburg Formation at 2650±8 Ma. Banded iron-formation overlying the dolostone are micro-, messo-, and macrobanded with single laminae being of large lateral consistency (Beukes, 1983, 1984). Only in the southernmost part of the Griqualand West area is the Asbestos Hills Subgroup conformably overlain by interbedded iron-formation and siliciclstic rocks of the Koegas Subgroup (Beukes, 1986).

SUPER GROUP	GROUP	SUBGROUP	FORMATION	LITHOLOGY	APPROXIMATE THICKNESS (IN METRES)
TRANSVAAL	POSTMASBURG	VOELWATER	Mooidraai	Dolomite, Chert	250
			Hotazel	Mn, Fe-Formation	
			Ongeluk	Andesitic lava	900
			Makganyene	Diamictite	50-150
	GHAAP	KOEGAS	Nelani	Shale	240-600
			Rooinekke	Fe-formation	
			Naragas	Quartz-wacke, shale	
			Kwakwas	Riebeckitic shale	
			Doradale	Fe-formation	
			Pannetjie	Quartz-wacke, shale	
		ASBESTOS HILLS	Griquatown	Clastic textured Fe-formation	200-300
			Kuruman	Microbanded Fe-formation	150-750
		CAMPBELLRAND	Gamohaan	Sparry limestone, shale	1500-1700
			Kogelbeen	Dolomite, limestone	
			Klippan	Cherty dolomite	
			Papkuil	Dolomite	
			Klipfonteinheuwel	Cherty dolomite	
			Fairfield	Sparry dolomite	
			Reivelo	Micritic dolomite	
			Monteville	Dolomite, limestone, shale	
		SCHMIDTSTDRIF	Lokammona	Shale	10-250
			Boomplaas	Dolomite, limestone, shale	
			Vryburg	Quartzite, lave, shale	

Figure 2.4: A simplified stratigraphy of the Transvaal Supergroup in the Griqualand West Basin (modified after Beukes and Smit, 1987; Dorland, 1999).

2.3.1.2 Campbellrand Subgroup

The Campbellrand Subgroup comprises predominantly dolomite with subordinate interbedded chert and limestone with one or two thin BIF beds. Overall thicknesses vary from 2 000 m in the north to 550 m in the south (Beukes and Gutzmer, 2008). The Campbellrand Subgroup follows conformably on the Lokammona Formation of the Schmidtsdrift Subgroup. Beukes (1980, 1983, and 1987) further sub-divided this group into two main facies, namely the Prieska facies and the Ghaap Plateau facies, also known as the basinal and platform facies respectively (Figure 2.2). The platform

facies consist of the basal Monteville Formation, followed by Reivilo, Fairfield, Klipfontein Hills, Papkuil, Kogelbeen and the top Gamahaan Formations. These formations extend laterally into the basinal facies consisting of the Nauga and Naragas Formations.

The depositional environment of the Campbellrand was interpreted by Beukes (1980, 1983) to have been a stable shallow marine platform and basin, provided by the Kaapvaal Craton.Therefore, carbonate build-up is represented by a stromatolitic-carbonate sequence (Campbellrand Subgroup) deposited in a subtidal, shallow-water setting dominated by strong currents within the Ghaap Plateau sub-basin, whereas deposition of intertidal and supratidal clastic-carbonate facies and stromatolitic facies (Altermann and Herbig, 1991; Höferle et al., 2000) of the Nauga Formation occurred in the Prieska sub-basin.

The transition between the underlying carbonate build-up and the overlying BIF is gradational (Hälbich et al., 1992). In the Ghaap Plateau sub-basin, the transition zone consists of contorted, cryptalgalaminated limestone–dolomite with mud rock partings, grading upward into interbedded fine-grained carbonate and siderite-rich BIF (Tsineng Member), together they form the Gamohaan Formation of the Campbellrand Carbonate Sequence (Klein and Beukes, 1989). These rocks are overlain by deeper water BIFs of the Asbestos Hills (Asbesheuwels) Subgroup. In the Prieska sub-basin, the decline in carbonate sedimentation was accompanied by siliciclastic influx that culminated in the deposition of the Naute Shales, which were in turn followed by the iron formations. BIF deposition in a basin-slope environment is interpreted as a response to the progressive deepening of the basin (Martin et al., 1998), and the rise in sea level attributed to a major transgression (Beukes, 1987).

2.3.1.3 Asbestos Hills Subgroup

The BIFs of the Kaapvaal craton carry some of the world's deposits of crocidolite asbestos and iron and manganese ores. Applying the stratigraphic nomenclature of Beukes (1978, 1980), the Asbestos Hills Subgroup of Griqualand West comprises a lower Kuruman and upper Griquatown Formation, and these are correlated at member level across the craton with Penge Formation in the North-eastern portion of the Transvaal basin (Beukes, 1983). The Masoke Formation is regarded as the equivalent unit in the Kanye basin (Table 2.1). The Asbestos Hills Subgroup

comprises the rhythmically banded Kuruman Iron Formation (BIF) and the clastic-textured, shallow-water ortho and allochemical Griquatown Iron Formation (referred to as granular iron formation; GIF) defined by the Danielskuil and Pietersburg Members.

The approximately 210m thick Kuruman Iron Formationis interpreted to represent shallowing-upwards deposition (initially in deep water) and is subdivided into four members. At its base, the Kliphuis Member (ankerite-banded chert with shale partings) is followed by the rhythmically banded Groenwater (chert and oxide-rich BIF) and Riries Members (siderite-rich BIF), and capped by an intraclastic iron formation, the Ouplaas Member, which is interpreted to have formed in a shallow-water platform environment. The Groenwater Member comprises four subunits representing three clastic sediment and BIF cycles (Matlipani zone together with the Whitebank zone, Elgan zone and Derby zone), with the last two cycles dominated by volcanically derived stilpnomelane mudrock interbedded with chert. This coupling is repeated in the overlying Riries Member, which also has three clastic sediment and BIF cycles, the uppermost of which (Alphen zone) contains grainstone bands (Figure 2.3).

The Griquatown Iron-formation consists of interbedded orthochemical and allochemical íron-formation unitsdeposited in a shallow epeiric sea (Beukes, 1984). Siderite and greenalite lutite interbedded with grainstone, grainlutite and disclutite (edgewise conglomerate) constitute the Danielskuil and Skietfontein Members which interfingers basinwards with the Middelwater Member consisting of riebeckitic minnesotaite- greenalite lutite. The metamorphic grade and structural deformation of the sequence increase basinwards and the minnesotaite is considered to represent a metamorphic equivalent of greenalite (Beukes, 1980a). A shallowing-upward cycle commenced during the deposition of the Griquatown Iron Formation (Beukes and Klein, 1990). The top of the Griquatown Iron Formation is formed by chertbanded greenalite lutites of the Pietersberg Member.

The Manganore Iron Formation

BIFs occurring on the Maremane dome and its proximities has been named the Manganore Iron Formation (Beukes, 1983), which is commonly interpreted to represent slumped remnants of the Asbestos Hills Subgroup preserved in palaeo-karst/sinkhole structures in the Campbellrand Subgroup dolomites formed during a hiatus preceding the deposition of the Gamagara Formation. Widespread iron mineralisation occurs above the BIF along an unconformity plane, i.e. the Gamagara unconformity. The Manganore Iron Formation is thus thought to represent an altered and mineralised equivalent of the Asbestos Hills BIFs.

2.3.2 Koegas Group

In the Prieska sub-basin, The Griquatown iron formations grade upwards into siliciclastic rocks of the Koegas Subgroup (Beukes, 1986) that were deposited mainly in shallow marine to deltaic environment (Altermann and Hälbich, 1991). These in turn grade upwards into chloritic claystone, siltstone and quartz wackes of the Pannetjie Formation of the Koegas Subgroup situated to the south of the Griquatown fault zone. Deposition of the Koegas siliciclastics was thus synchronous with the upper part of the Griquatown Iron-formation.

The iron formations and siliciclastic of the Koegas Subgroup thus appear to conformably overly the Griquatown Iron Formation. At the base of an upward-coarsening iron formation – siliciclastic sedimentary cycle are the Pannetjie, Doradale, Kwakwas, Naragas, and the Rooinekke Formations (Beukes, 1983). The Koegas Subgroup represents the top of the Ghaap Group, and is covered with a regional unconformity by the Makganyene glacial deposits of the PostmasburgGroup (Figures 2.2 and 2.3). The Koegas Subgroup appears to represent a distal (marine) facies, in the west and at the base of the Makganyene massive diamictites.

2.3.3 Postmasburg Group

The Postmasburg Group idevelops on the western edge of the Maremane dome and in the Kalahari manganese field. It comprises from the base the Makganyene diamictite, Ongeluk andesite, manganiferous Hotazel iron formation, and finally Mooidraai dolomite at the top. The red bed succession of the Mapedi and Gamagara Formations has a marked basal erosional unconformity towards the underlying

Postmasburg Group lithologies, but is conformably overlain by shallow marine quartzites of the Lucknow Formationthat constitute the top of the Transvaal Supergroup in the Griqualand West (Beukes et al., 2002).

Two facies are present in the Makganyene diamictite, the first comprising massive to poorly bedded diamictite, pebblysandstone and siltstone, shale and mudstone. These are interpreted as piedmont glacial and glacio-fluvial assemblages (Beukes, 1983, Visser 1971). The second facies occurs along the western margin of the Kaapvaal craton and can broadly be described as containing stacked cycles of graded bedded diamictite-greywacke-siderite bandlutite (Beukes, 1983). The presence of striated chert fragments and pebbles have been interpreted to be of glacial origin (Visser, 1971; De Villiers and Visser, 1977; Van Wyk, 1980) and interpreted as glacio-marine deposits (Beukes, 1983). The laterally extensive Ongeluk lavas (figure 2.2), which comprise essentially tholeiitic basaltic andesites, were extruded under water in a marginal basin within the continental setting of the Kaapvaal craton (Schütte, 1992). The lavas have been dated at 2239 ± 90 Ma (Armstrong, 1987) and 2223 ± 13 Ma (Cornell *et al*, 1995). In the Kalahari manganese field the Ongeluk lavas are confined to the Dimoten syncline, where they are overlain by the cyclic manganiferous BIF of the Hotazel Formation of the Voëlwater Subgroup.

2.3.4 Olifantshoek Supergroup

After a period of erosion the Olifantshoek sequence was deposited. The Olifantshoek Supergroup consists of a thick (~1500 m) sequence of quartzites, shales and andesitic lavas, which have been thrust eastwards over lithologies of the Postmasburg Group. This succession is considered to have formed in terrestrial environments under tropical lateritic weathering conditions and contain excellent examples of ancient lateritic soil profiles (Gutzmer and Beukes, 1998). The unit attains maximum thickness and development in ancient karstic dissolution structures in carbonate of the Campbellrand Subgroup on the Maremane Dome along the Gamagara Ridge (Da Silva, 2011).

At the base is the Mapedi Formation with basal conglomerate and interbedded lavas and shales. This is followed by the arenites of the Lucknow Formation. Locally, the Mapedi and Lucknow Formations are known as the Gamagara Formation with the

basal Doornfontein Conglomerate Member and the Paling Shale Member. Stratigraphically higher, the Olifantshoek Group comprises the Neylan Quartzite Formation at its base and is overlain by the Hartley Lava, Volop Quartzite and Top Dog Quartzite Formations. The Neylan Formation has a prominent polygmictic conglomerate at its base. It overlies a major unconformity along which incised valleys are developed (Tinker et al., 2002). The Hartley Formation comprises both mafic and felsic lavas with latter having being dated at 1928±8Ma (Cornell et al., 1998). The overlying Volop Group comprises conglomeratic to coarse red to purple poorly sorted quartzites. In contrast, the upper Top Dog Formation of the Volop Group is represented by light grey rather well-sorted orthoquartzite with shale interbeds. It is conformably overlain by a very thick succession of the fine to coarse quartzites of the Groblershoop Group (Van Niekerk, 2006)

CHAPTER III GEOLOGY OF THE STUDY AREA

3.1. Introduction

Field mapping was conducted in three main areas with known outcrops, Most of the project area is covered by younger Kalahari cover. Prominent BIF outcrops in the area of interest include: Janeng Hill (to the South-west), Tshitsane Hill (to the North-east), Ukwi and Moretlwa Hills (both to the East).

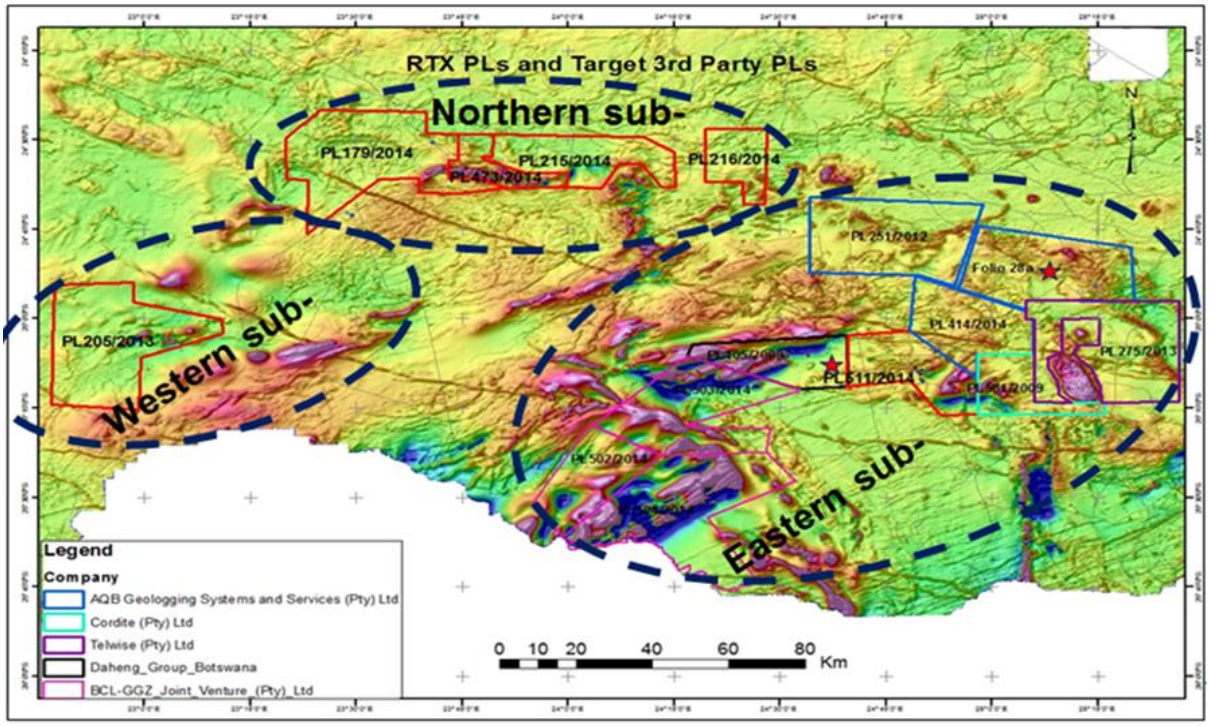

Figure 3.1: Locality map showing the three areas within the study area with most outcrops (Janeng Hill, Tshitsane and Moretlwa Hills).

3.2. Tshitsane Hill area

The local geology of Tshitsane Hill comprises of six major units in succession clearly distinguishable from each other (Figure 3.4). At the base of this succession is Kanye Volcanic Formation that is overlain by the Black Reef Quartzite Formation outcropping near the Kanye town. The 'Black Reef Quartzite' is in turn overlain by a package of dolomite followed by chert and chert breccia respectively. The chert breccia is overlain by a BIF unit with sharp contact to the underlying dolomite. At the top of the succession is series of light-grey, brown and dark grey shale with common diabase intrusions.

The Most of the mapping was focused to the SE and NE of the hill; no outcrops were mapped on the western side of the hill. The geology of Tshitsane is comprised of two main Groups i.e. Taupone and Segwagwa Groups. Four main lithologies were identified during the mapping which includes Kanye vocanics at the base followed by Ramonnedi dolomite which is in turn overlain by chert-breccia followed Iron formation. These units are overlain by a shale unit outcropping to the NE of the hill; the contact between the underlying BIF and shale is gradational. This shale unit is intruded by dolerite and gabbro sills of post-Transvaal age which are locally abundant in Lobatse-Ramotswa area and also occur further west around Kanye and Moshaneng, (Aldiss and others 1983).

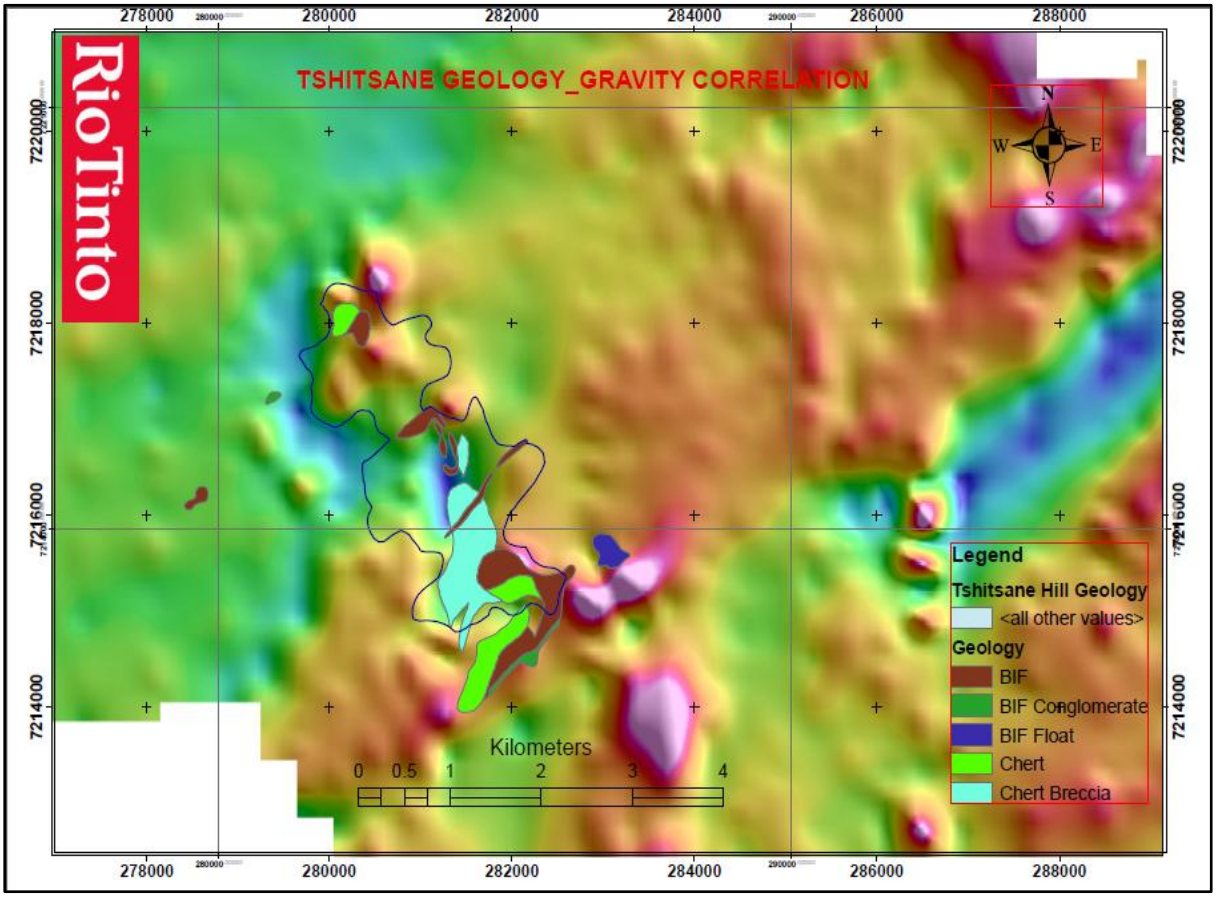

Figure 3.2: Tshitsane Hill geology map super-imposed on the gravity image, the map shows all four main outcrops of Tshitsane Hill area.

The central (main) outcrop comprises similar jaspillitic BIF with mostly gentle to moderately steep east to south-east dips (20-50 degrees) with occasional steeper south dips (60-70 degrees south), (figure 3.2.). It is not clear if the latter represents overturned bedding. There are several folded zones. Fold hinges generally plunge

gently to moderately SE, with steep SW dipping axial planes. The BIF along the western side of this outcrop is more cherty and thicker banded, while the BIF along the eastern side contains more brecciated zones.

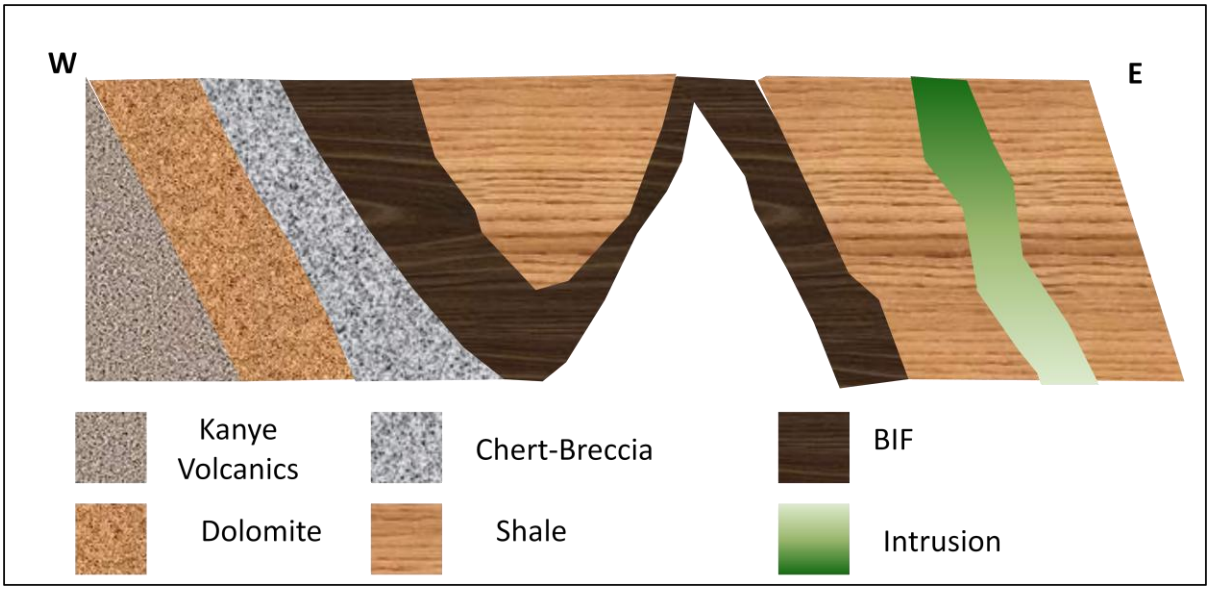

Figure 3.3: A cross-section W-E across Tshitsane Hill area, the strata youngs towards ENE, with intrusive into Segwagwa shales.

The southernmost outcrop comprises mostly steep (65-75 degrees) east to SE dipping red jaspillitic BIF. Occasional open to tight folds have fold hinges that plunge moderately to steeply east with axial planes that dip steeply to the ESE to SSE. At this location the chert breccia, which outcrops to the SE of the BIF overlies the BIF suggesting that the sequence at this location may be overturned.

A fourth outcrop slightly northwest of central (main) also comprises jaspillitic BIF and ferruginous banded chert. Particularly the western side of this outcrop is predominantly ferruginous banded chert with moderate ESE dip (26-53 degrees). The chert grades upwards into typical red jaspillitic BIF also with moderate ESE dip (32-58 degrees). Occasional areas of folding show that fold hinges plunge gently SE to S, with steeply easterly or westerly dipping axial planes. Locally there are areas where the BIF is enriched in iron.

Plate 3.1: A: a mineralised section of the core drilled in the Tshitsane Hill. B: a sampled section of the core.

3.2.1 Black Reef Formation

The 'Black Reef Quartzite' forms a marker unit developed at or near to the base of the Transvaal Sequence/ Supergroup throughout most of the outcrops in South Africa. Although, the outcrop pattern suggest conformity with the overlying Transvaal beds and it shows upward gradation into them, SACS (1980). In Botswana, the basal bed is normally a conglomerate.

3.2.2 Taupone Dolomite Group

This composite unit is made up of lower dolomite-chert sequence which overlain by ferruginous shale and banded, ferruginous and stromalitic chert. Some of the distinctive facies represented by bedded and oolitic limestones interbedded with

chert. The chert is locally clastic and also shows signs of slumping and brecciation. Upwards, the chert become more ferruginous and show stromalitic structures.

3.2.3 Segwagwa shale

The Ditlhojana Formation at the base of the Segwagwa Group, is an argillaceous and arenaceous formation characterised by carbonaceous and pyritic shales, siltstones, sandstones and medium – coarse grained white and ferruginous quartzites with a rare chert-clast conglomerate (Key, 1983). It is overlain by ferruginous shales of the Tlaameng Formation which are in turn overlain by massive, fine grained, amygdaloidal and non-amygdaloidal basaltic – andesitic lavas of the Tsatsu Formation. GAST005 and GAST006 drilled at of Tshitsane hill intersected brownish and yellowish ferruginous shale. While a water borehole drilled by a local farmer about 2 km NE of GAST005 and GAST006 intersected a black coloured and carbonaceous shale unit.

3.2.4 Intrusions

These mainly compromise isolated intrusions with basic to intermediate compositions. Dolerite and gabbro sills of post-Transvaal age are locally abundant within the project area and also occur further towards Kanye Town and Moshaneng village. Dolerite and Gabbro sills in the Woodlands formation of the Lobatse-Ramotswa area most probably injections from Bushveld Complex, although Key (1983) various ages of the intrusions occur in the same area. Gabbro from a sill near Kanye (Aldiss and others 1989) is coarse-grained and contains about 25% of olivine together with plagioclase. These sills appear to be mafic in nature and can be assigned to amphibolitic group (Beukes 1978). It has been observed where the dykes and sills are in contact with the surrounding BIF, that the BIF has been displaced. The dyke has a greyish appearance in weathered surfaces and a brownish colour with green patches.

3.2.5 Masoke Iron Formation

Two units were distinguished, mainly on the basis of thickness of bands in the iron formation. BIF at the study area generally has good development of micro and meso bands. Thin banded iron formation has meso bands generally thinner than 1cm, while thick banded BIF has meso band thicker than 10 cm and up to 30cm. Both BIF

types are generally non-magnetic and are red coloured. The outcropping rocks suggest a clean BIF with only iron oxide and silica as the rock forming minerals. The dominant (and only) iron oxide is hematite and is fine grained. Silica is present in the form of chert (generally red colored) and quartz in breccia zones.

The first type consists essentially of micro- and meso banded autochthonous iron-formation whereas the second type, which conformably overlies it, consists of clastic-textured iron-formations. The former is conformably underlain by dolomite and limestone of the Campbellrand Subgroup, whereas the latter is conformably overlain by siliciclastics. In turn the iron-formation displays many similarities with the clastic-textured iron-formations of the Griquatown iron formation as described by Beukes (1984). The Kuruman and Griquatown Iron-formations are silicified and oxidized to jasperoids (Beukes, 1980a) down to depths of several tens of metres below the present surface.

3.3 Structures

The structure of the Transvaal Supergroup rocks in Southern Botswana is significantly different to that of the Griqualand west basin. The Kheiss orogeny, which forms the main N-S grain of the Sishen area, is only developed in the extreme western part of the map area, and rocks affected by it are nearly entirely covered by younger sediments. The main structural trend in Southern Botswana is ENE-WSW, and the orogeny responsible for this is older than the Kheiss orogeny.

3.3.1 Basement structures

The main structural grain in the basement rocks (greenstone belts of the Kraaipan Group) is N-S to NNW-SSE, and is nearly perpendicular to the main grain of the Transvaal Supergroup. The outcrop patterns of the BIF's in these greenstone belts suggest that they are largely synclinal (D1). The NNE to N grain of the belts is reactivated later as NNE trending faults which offset the units of the Transvaal Supergroup and the Molopo Farms Complex, but not the Waterberg Group.

3.3.2 Structure of the Transvaal Supergroup.

Minor tilting accompanied by erosion must have affected the rocks between deposition of the Taupone and Segwagwa Groups. This is reflected in progressive

erosion of the Masoke BIF towards the north suggesting uplift across a broadly E-W to NW trending line roughly through the centre of the map area.

3.3.3 Folds

The main fold structures in the map area are doubly plunging NE to ENE trending broad synclines and narrow sheared anticlines (D2) which affected the rocks up to the Segwagwa Group as well as the Molopo Farms Complex. The inferred outcrops of the latter follow the trend of these folds, with local steep dips up to 40 degrees in the limbs of these folds. This suggests that at least in the west, D2 post-dated emplacement of the complex at 2.04Ga. However in the east, Mapeo and Wingate (2009) postulate that D2 predates intrusion of the Segwagwa-Masoko Igneous complex at 2.05Ga. This means that either D2 was broadly contemporaneous with the emplacement of the complex, or that the latter interpretation is incorrect, and that the ovoid shape of these intrusions is the result of interference of D2 and D3. Folds developed during the later event (D3) in this area trend around N and are responsible for the elongated ovoid shape of the Segwagwa complex. D3 folds also affect rocks of the Segwagwa Group (Upper Transvaal), but not the Waterberg Group. Interference of D2 and D3 in the western part of the map formed the doubly plunging synclines described above with measured fold hinges plunging from 20 degrees ENE to 15 degrees west.

3.3.4 Faults

Map scale NNE to NE trending faults offset the units including the Molopo Farms Complex, but not the Waterberg Group over distances up to 40km on the map, although the true offset is likely to be much less. These faults reactivate the older trend in the basement rocks of the Kraaipan Group. Apparent sinistral and dextral offsets occur on faults with the same orientations, suggesting that true displacements are dip slip (possibly normal). The easternmost fault is interesting, in that the dip of the Transvaal stratigraphy changes from north on the western side of the fault to SSE on the eastern side. This suggests scissor movement with progressively increasing displacement to the SSE. This fault also cuts the Segwagwa Syncline (D3).

Smaller scale NE trending faults predate and are cut by the NNW trending block faults, and also predate the emplacement of the Segwagwa-Masoko Complex and therefore must be older than 2.05Ga. Examples are the Taupone, Ramonnedi and Segwagwa faults of Mapeo and Wingate (2009). These faults probably postdate deposition of the Transvaal Group, however some affect only the rocks up to the Lower Transvaal, and others affect rocks up to the top of the Segwagwa Group. Mapeo (1997) indicates reverse movement on these faults. Small scale thrusts in the same area are possibly of the same generation and are indicative of an N to NNW directed compressive regime.

Waterberg Group rocks are preserved in much more open E-W to WSW trending synclines (limb dips of maximum 15 degrees), suggesting a renewed phase of open folding along the same trend of D2 after deposition of these rocks. These rocks are also affected by rare N-NE and NW trending faults and fractures which also affect the Karoo strata.

Plate 3.2: Showing banded iron formation at Janeng Hill. Left is thin micro-banded BIF and right is thick meso banded BIF

3.3.5 Breccia zones and small scale faulting

Brecciation of the iron formation is common at Jwaneng Hill. The breccias comprise angular fragments of jaspillite in a matrix of recrystallised white quartz or recrystallised iron oxide (Figure2. 8). Breccia's are often confined to narrow, dyke-like zones which strike in a common northerly trend and dip steeply to the west

(average orientation is 275/70). Width is mostly of the order of 20-50cm. Rare; small northerly trending faults with steep westerly dips and mostly apparent sinistral offsets are subparallel to these breccia zones.

Plate 3.3: Breccia pod consisting of jaspillite fragments in white quartz matrix (left) and N trending breccia dyke with iron oxide

3.3.5 Veins

Thin quartz veins with specularite cross cut all structures described above. In many outcrops they occur in two distinct orientations. One set strikes NW with a moderate to steep NE dip, the other set strikes N with a subvertical to steep westerly dip.

The presence of specularite in the intergranular space of the sandstones of the Waterberg Group suggests that this event post-dated deposition of these units.

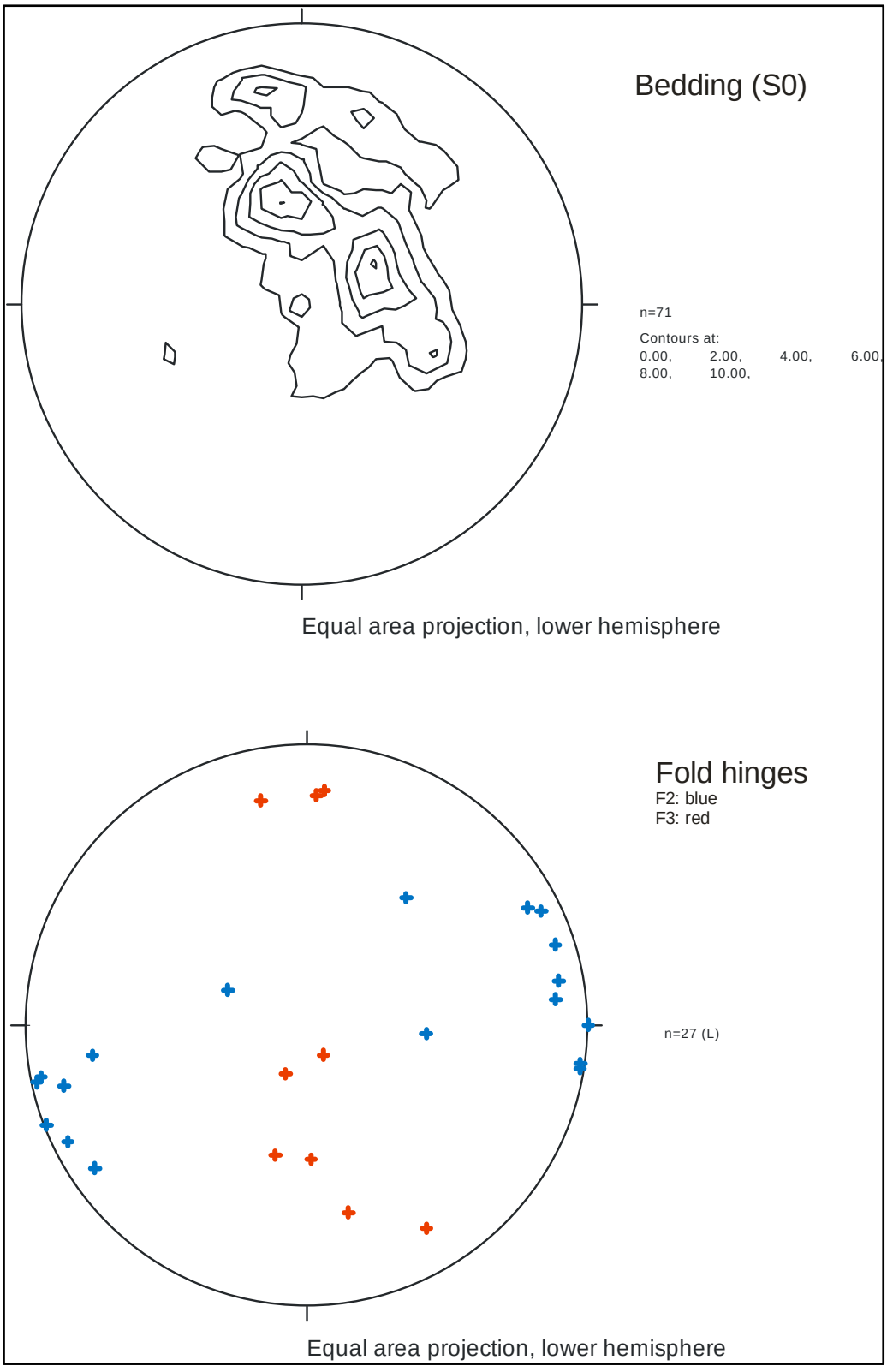

Figure 3.4: Stereoplots of bedding data (top: poles to bedding) and fold hinges from the Jwaneng Hill area.

The combined structural data for Tshitsane Hill shows that poles to bedding are distributed along a poorly developed girdle suggesting relatively open folding along

easterly plunging fold axes. The measured fold hinges also plunge from east to south. From the limited data it is not clear if this represents one event, or more than one event. Two main trends of BIF were mapped: 0° to 90° NE with general dips averaging 40° to 55° NE. The other mapped trend of BIF have generally dips ranging from 30° to 50° SE; the strike ranges between 90° to 180° SE. These BIFs have a thin sleeve of the BIF breccia which is thought to have developed at Karoo times. The contact between the BIF breccia and BIF is sharp.

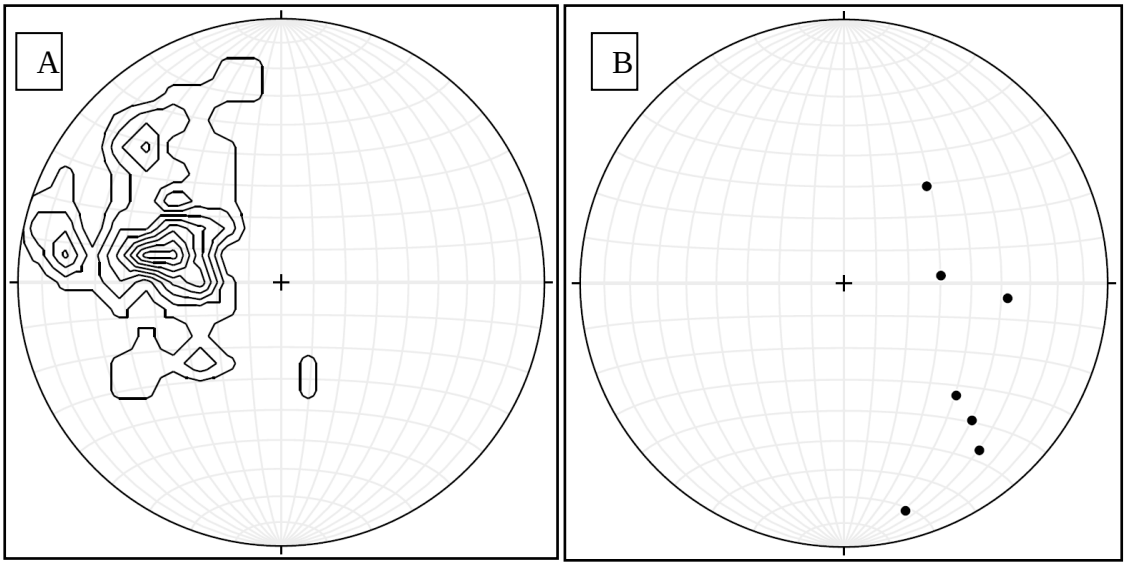

Figure 3.5: Stereo plots (lower hemisphere, equal area) of the Tshitsane hill area. Left **(A)** poles to bedding contoured, right **(B)** fold hinges

Two major lithologies were mapped: Masoke Iron Formation and Chert (and chert breccia). Tshitsane Hill is made up of four main outcrops (Figure 3.1). Most of these comprise jaspillitic (oxidised) iron formation with occasional outcrops of chert breccia and ferruginous chert. The northernmost outcrop comprises jaspillitic BIFs with a moderate (30-40 degrees) NE to ENE dip. This is underlain by chert breccia which shows occasional crude bedding and a gentle northerly dip. The chert breccia is strongly hematitized and contains local stockwork hematite veinlets.

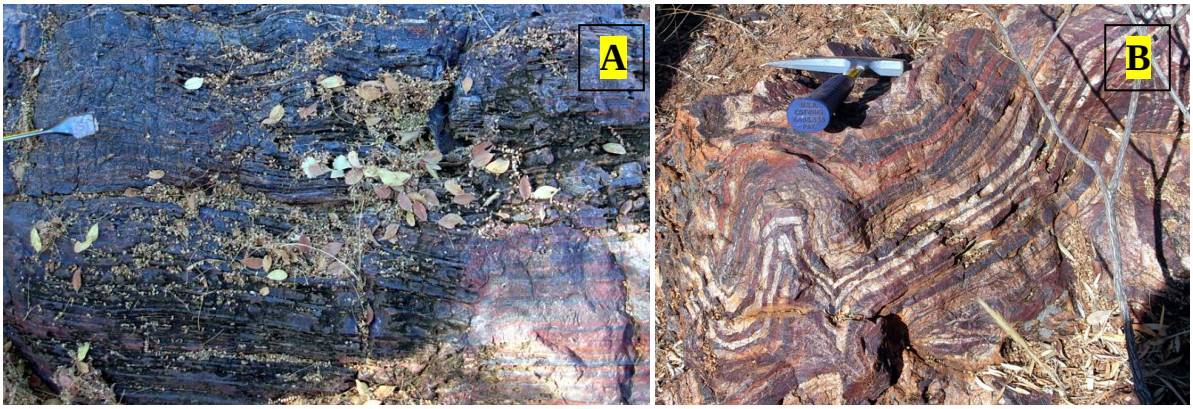

Plate 3.4: A: Red BIF in contact with darker, Fe-enriched iron formation. B: Folded red jaspillitic BIF Tshitsane Hill.

Chert and chert breccia were mapped around the centre of the hill and towards the NE edge of the hill. Chert breccia has about 10% of Fe-rich float. Chert is mostly banded to ferruginous and it does not have obvious structural measurements; it however mimics the structural measurements of the overlying BIF. In places the texture shows crystal growth which may imply open-space filling.

From mapping of Tshitsane Hill the sequence is interpreted to young ENE from the hill with dolomites/chert breccias and Kanye Volcanic to the west and BIF followed by shale that is intruded by dolerite and gabbro sills of post-Transvaal age as referred by, Aldiss and others 1983.

Plate 3.5: BIF outcrop at Tshitsane Hill.

Plate 3.6: (a) BIF conglomerate with angular fragments and hematitic matrix, Karoo age (b) Micro-banded BIF outcrops of Masoke Iron at Tshitsane Hill

Plate 3.7: (A) Tshitsane Hill BIF, characterised by micro-banded, siliceous and jasperllitic **(B)** Kgwakgwe chert breccia intersected during drilling characterised by ferruginous matrix, this breccia was underlain by a dolomite unit intersected in the same bore hole drilled to the NE of Tshitsane.

3.3 Ukwi and Moretlwa Hill areas

Moretlwa Hill is a low hill with mainly outcrop of a low Fe-grade BIF conglomerate. Rare sub crops of BIF have gentle N to NW dips (14-27 degrees). A small reliable outcrop shows steeper ENE dips (33-50 degrees), suggesting that the BIF is folded about north to N to NE plunging fold hinges. The BIF is messo-banded and brecciated in places.

There are more extensive outcrops of the Masoke iron formation outcrop on Ukwi hill. The BIF here dips gently to the WNW to N (15-28 degrees) with open folding about gently north-east plunging fold hinges. The BIF is messo banded, with jaspillitic iron formation containing elongated chert pods. Chert breccia was encountered which underlies the BIF.

3.4. Janeng Project area

The only outcropping Precambrian rocks in the Janeng Tenement area comprise isolated outcrops of thinly and thickly banded BIF from the Transvaal Supergroup (Masoke Iron formation), and red to purple-coloured quartzite. These are overlain by calcrete, clays and unconsolidated sands of the Kalahari Formation. Water boreholes in the area have intersected both the quartzite of the Olifantshoek/ Waterberg Group and the rocks of the Transvaal Supergroup.

Two units were mapped at Janeng Hill: BIF and chert breccia, these units are underlain a jasper breccia. BIF at Janeng Hill generally has good development of micro and messo bands. The Janeng Hill is mainly composed of highly contorted hematitized micro BIF (plate 3.3a), similar in nature to the Kuruman Iron Formation. The iron formation dips at 35 degrees towards the SE. On the dip slope of the outcrop secondary massive jasper bands crosscuts bedding in the iron formation. From the historic log J2 drilled right on top of Janeng Hill it is clear that hematitized BIF is underlain by a jasper breccia that in turn is underlain by a chert breccia similar to the Wolhaarkop breccia locally found in the Maremane Dome area. BIF has messo bands generally thinner than 1cm, while lutitic BIF has thicker bands, more than 10 cm and up to 30cm. The remainder is mostly silica, with very low contents of deleterious elements.

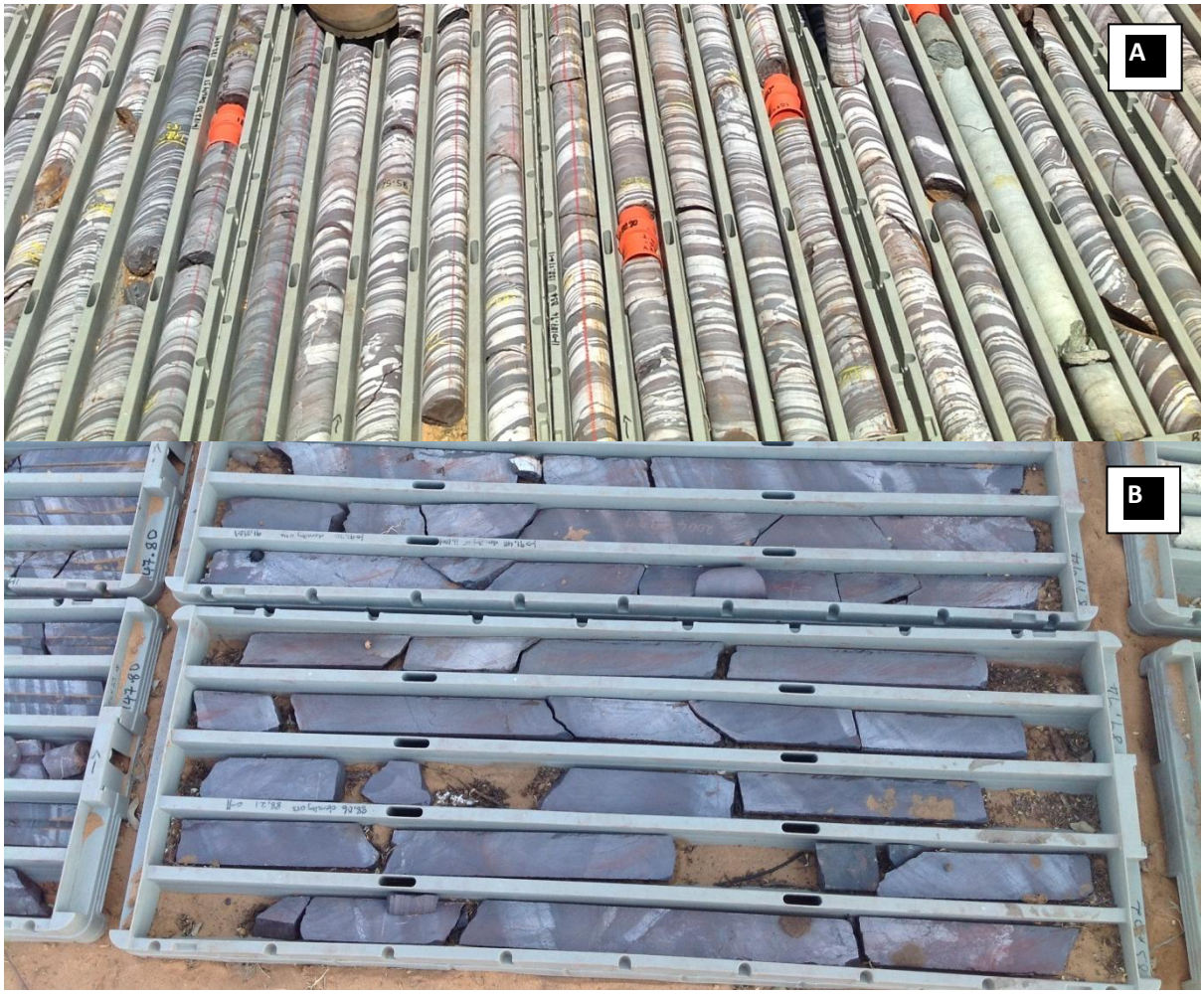

Plate 3.8: Photos of Janeng Hill area core of KKTA001, **(A)** Hematitized thinly laminated and micro-banded Iron Formation in lower part of core, **(B)** Thick bedded and lutitic hematitized Iron Formation in top part of the core.

The BIF at Janeng Hill is generally non-magnetic and are red colored. The outcropping rocks suggest a clean BIF with only iron oxide and silica as the rock forming minerals. The dominant iron oxide is hematite and is fine grained. The thickness of the iron formation at Jwaneng Hill, reconstructed using an average southerly dip of degrees is minimal. Iron formation was also intersected in a waterbore 500m south of the outcrop which could indicate (if dips remain south) a much thicker iron formation. One recent bore east of Jwaneng Hill also intercepted jaspellitic BIF.

3.5 Selected drill holes and samples

Five drill holes were selected and logged at different locations in the project area. From the logged drill holes twenty-six core samples were carefully selected. The selected samples represent major lithologies (BIF, chert, chert breccia and shale) in the study area. Selected drill holes are KKTA013, KKTA001, KKTA006, KP17 and GAST006 as presented in figure 3.5.

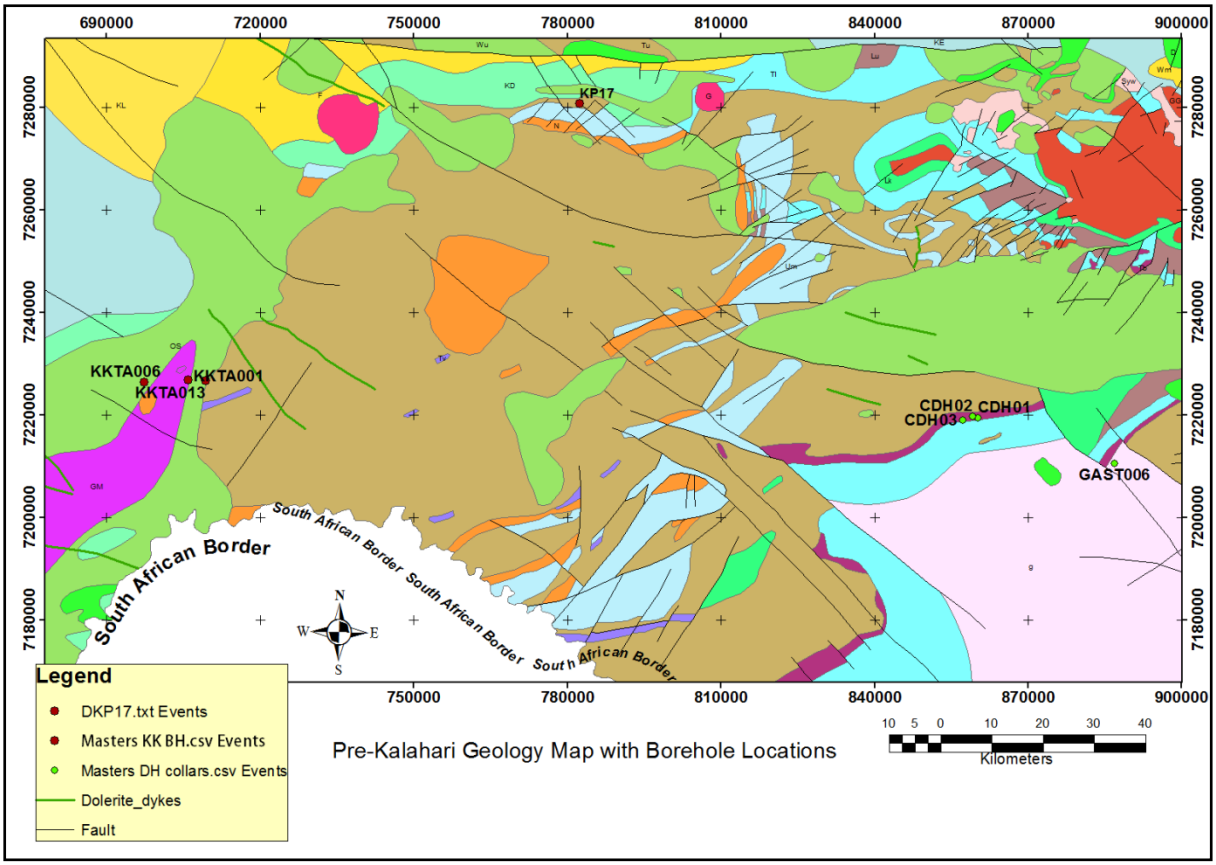

Figure 3.6: Sampled bore hole location map on 1:250k geology of the study area.

3.5.1 Core logging

Diamond drill hole KP17 was inspected at the Botswana Geological Surveys core facility in Kang. This hole is important because it intersected iron formation which is intruded by ultramafic rocks of the Molopo Farms Complex. The location for this drill hole is 791875mE, 7275365mN east of Konkwa Pan.

Table 3.1: Log of core KP17

Depth			
From	**To**	**Lithology**	**Remarks**
0	69	Kalahari	kalahari sand and calcrete rubble
69	137	Ultramafic	non to weakly magnetic
137	139	Ultramafic	fructured and veined ultramafic rock with magnetite veins (magnetic)
139	142.5	Breccia	Brecciated rock with occasinal magnetite and chert bands (BIF assimilation)
143	145.8	Ultramafic	Occasional magnetite veins
146	149.6	Breccia	subrounded clasts of chert, contain pyrite and pyrhotite
150	155	Ultramafic	
155	157	Breccia	
157	174.8	BIF	micro and messo banded magnetite -rich BIF
175	176.6	Hybrid zone	A gradation contact between BIF ultramafic
177	277	Ultramafic	weak to non magnetic
277	280	Ultramafic/ Hybrid zone	BIF diffuse banded rock, variable and magnetic
280	294	BIF	magnetite-rich BIF with micro and messo banding
294	298.5	Ultramafic	pyroxinite with pyrrhotite
299	300.5	BIF	
301	311	Carbonate	foliated, mylonitic, massive grey dolomite and abundant pyrite
311	326	Quartzite	Altered

The following observations were made from KP17: Molopo Farms intrusive rocks are characterised by metre-wide zones of hybrid and breccia rocks on the contacts with the Transvaal Supergroup rocks.

In the BIF zones, the bedding angle to core varies from 45 to 60 degrees with an average of probably of the order of 45-50 degrees. Borehole KP17 was drilled vertically. Total intercepts of BIF in KP17 (including hybrid and assimilated zones) are 139-176.6m (37.6m) and 277.0-300.5m (23.5m). BIF in KP17 looks texturally very similar to the BIF at Janeng and at Ukwi Hills.

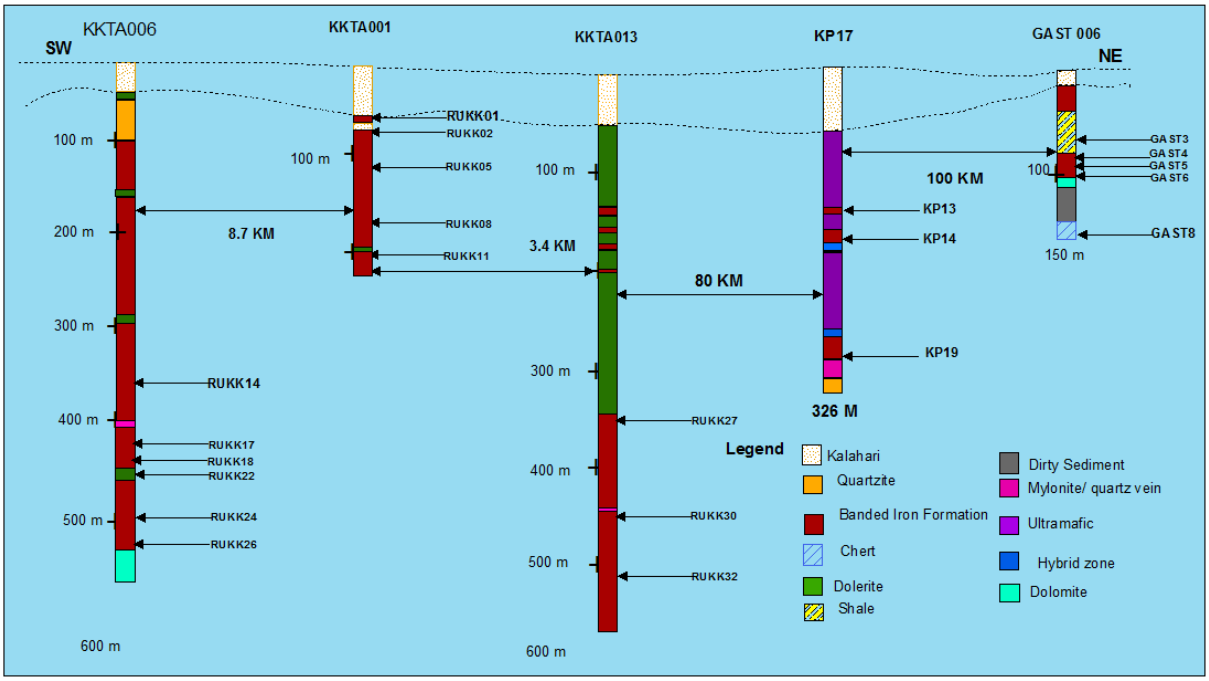

Figure 3.7: Sketch displaying all five selected drill holes and sample locations on each drill hole.

Kokotsha drill holes log

Table 3.2: KKTA001 Log

Depth			
From	**To**	**Lithology**	**Remarks**
0	36	Kalahari	sand and laterite
36	74	BIF	Granular and lutitic, slighlty oxidised and thickly banded (`30cm to 70cm)
74	194	BIF	thin alternating chert and hematite bands and

			brecciated
194	194.7	Mafic	Intrusion
194.7	236.76	BIF	brecciated and contoured iron formation

Drill core KKTA001 was drilled through 33m of Kalahari cover; this was immediately followed by a 3m thick unit of weathered, cobbly, and pebbly and poorly sorted ferruginous (BIF) conglomerate. This overlies 20m thick unit of brecciated BIF which is hematitic, veined and with quartz infill the fractures. The top part of this hole is iron formation characterised by granular and lutitic, slightly oxidised and thickly bedded (~30cm to 70cm); 33m-70m. Below this unit is a thinly laminated iron formation: 70m-194. It is characterised by thing alternating cherty and hematitic bands; and is also intensely fractured. This iron formation was terminated by a dolerite intrusion, whilst the drill hole ended in brecciated and contoured BIF at 236m.

Table 3.3: GAST006 Log

Depth			
From	**To**	**Lithology**	**Remarks**
0	7.5	Kalahari	Overburden
7.5	35.34	Conglomerate	conglomerate of chert and BIF clasts in a calcareous goethite matrix (pre-Kalahari unconformity)
35.3	71.55	Shale	Laminate, yellow and aluminous shale
71.6	72.26	Shale	maroon friable clay rich shale
72.3	75.6	BIF	Bracc iated BIF, weakly magnetic and hematitized
75.6	96.8	BIF	cherty BIF, finelt banded
96.8	104.7	Carbonate	dolomite, shaley, weathered and highly fructured
105	133	Sediment	dirty sediment
133	149.3	Chert breccial	chert breccial, iron Fe-rich matrix with angular chert fragments

Table 3.4: KKTA006 Log

Depth			
From	**To**	**Lithology**	**Remarks**
0	30	Kalahari	
30	61	Quartzite	brownish-red, clean and mature and medium grained
61	62	Intrusive	
62	117	Quartzite	
117	151	BIF	messo-banded
151	152	Intrusive	
152	196	Vein	quartz vein
196	283	Intrusive	
283	285	BIF	brecciated, chloritized and remobilised iron with hair-line lamination of magnetite
285	311	BIF	BIF and mylonite, highly brecciated
311	358.42	BIF	brecciated with quartz grains and veinlets; messo-banded, chert and jasper
358.42	392.1	Vein	quartz vein
392.1	392.33	BIF	magnetite-rich BIF, messo-banded, chloritised, interlayering of chert and specularite
392.33	422.57	BIF	Altered BIF
422.57	428	Mylonite	
428	485.78	BIF	laminated, remobilisd iron,
485.78	488.47	Intrusive	dolerite, medium grained
488.47	531.03	BIF	mainly micro-banded, brecciated with pyrite flecks
531.03	531.63	Mylonite	highly chloritized
531.63	541.01	BIF	contored messo banded, micro baned

In drill core KKTA006, the iron formations are in sharp fault contact with a massive recrystallized grey dolomite that in turn is intruded by a diabase near the end of the hole. The iron formation displays crackle brecciation in proximity to the basal fault. The brecciation is similar to that in lower KKTA001. KKTA001 is located alongside a major fault (evident from geophysical surveys), whereas both KKTA006 and

KKTA013 are distal to the fault. This is apparent from haemititization of iron formations in KKTA001.

Table 3.5: KKTA013 log

Depth			
From	**To**	**Lithology**	**Remarks**
0	55	Kalahari	calcrete and sand
55	78	Intrusive	slightly magnetic
78	92	Goethite	
92	138	Intrusive	Magnetic
138	140	BIF	Magnetic
140	159	Intrusive	magnetic dolerite
159	160	BIF	
160	174	Intrusive	magnetic dolerite
174	177	BIF	
177	193	Intrusive	magnetic dolerite
193	195	BIF	
195	349	Intrusive	with quartz veins and magnetic
349	438	BIF	haematitic wit veins
438	439	Mylonite	with pyrite grains
439	556	BIF	Griquatown with chert pods and lutitic
556	574	BIF	Kuruman, brecciated
574	576	BIF	Brecciated

3.5.2. Correlation of drill holes

Haematitized thinly laminated and micro-banded iron formation appears to characterise the lower part of the drill cores, whereas thickly-bedded and lutitic hematitized iron formation dominates the top part of the cores. In contrast to the iron formation intersected KKTA001, the iron formations in cores KKTA006 and KKTA013, intersected at depth of about 350 m, appear as typical micro-banded and

lutitic iron Formation with no pervasive haemititization. Rather the iron formations are highly magnetic, and contain abundant siderite and iron silicates.

GAST006 intersected a succession below the Kalahari cover that is virtually identical to that associated with high-grade Sishen-type karst deposits on the Maremane dome. The iron formation is highly disturbed and hematite-rich and overlies a ferruginous chert breccia very similar in composition and appearance to the Wolhaarkop Breccia. It is overlain by hematitized iron formation displaying increasing hematite contents upwards in the succession. The field visit supported the observations made at the core yard. Especially at Ukwi hill the contact between micro-banded iron formation and lutitic iron formation are well exposed. The iron formations dip to the north and although haemititization appears, they are relatively undeformed indicating that they are probably in normal gradational contact with the carbonates below.

This observation is in contrast to the highly deformed iron formation intersected towards the base of KKTA001 and KKTA006 along with the overlying chert breccia. Similar chert breccia with larger clasts of highly contorted micro-banded haematitized iron formation outcrop in the Tshitsane Hills. These breccias are probably located in dissolution karst structures in underlying Campbellrand dolomite. All in all the Ukwi-Tshitsane Hills area displays geology that is very similar to that of the Sishen area on the Maremane dome. The area could thus be considered highly prospective for discovering karst-hosted Sishen-type iron ore deposits.

In drill core KKTA006, the iron formation is in sharp fault contact with a massive recrystallized grey dolomite that is, in turn, intruded by a diabase near the end of the hole. The iron formation displays crackle brecciation, this brecciation is similar to that observed in the lower part of core KKTA001.

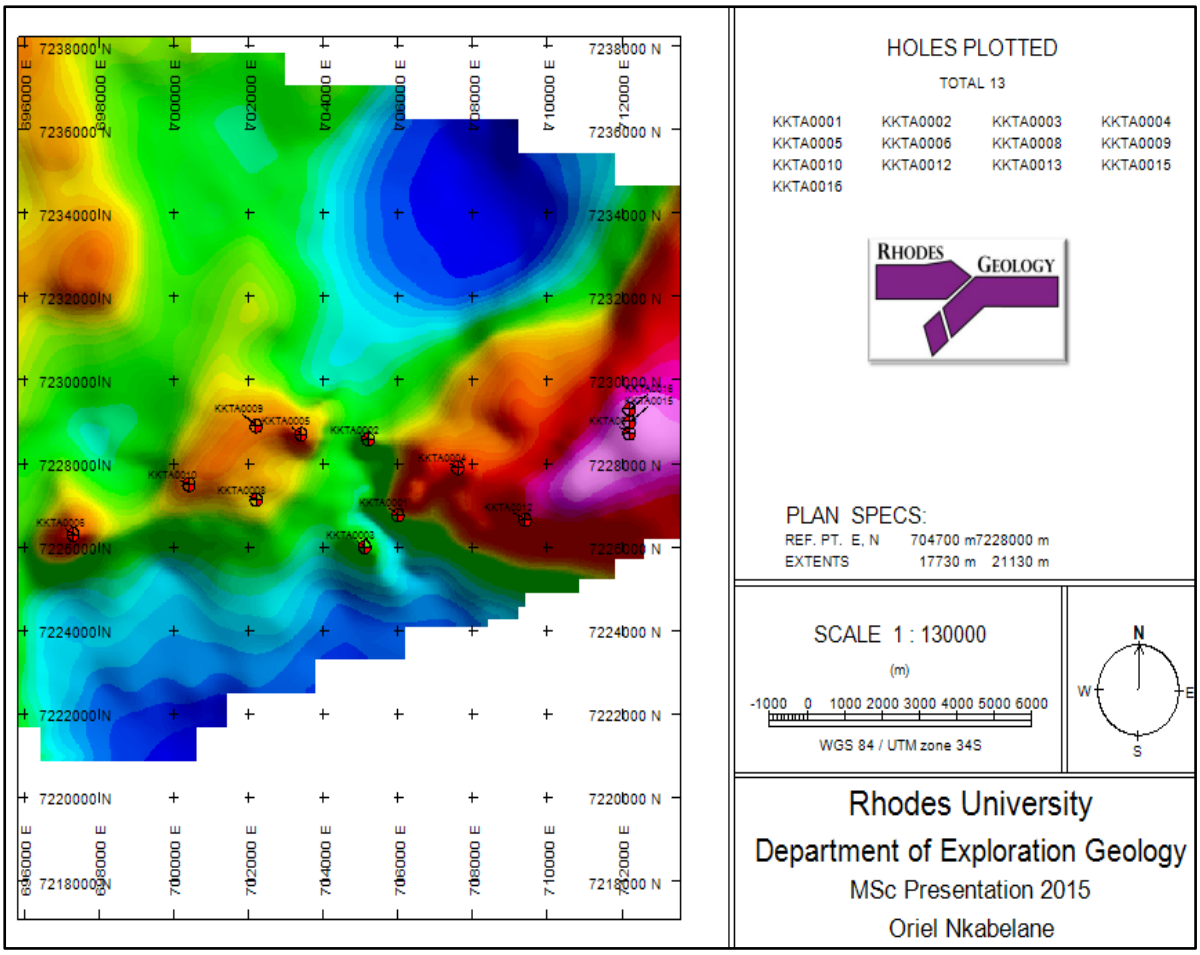

Figure 3.8: Collar locations map of Kokotsha Project (KKTA drill holes). These were drilled on 'magnetic low' and 'gravity highs' anomalies.

Finally it is most important to note that according to geophysical analyses of the project area, as outlined in the early chapters, KKTA001 is located alongside a major fault whereas KKTA006 and KKTA013 are distal to the fault. It would thus appear as if the hematitization of the iron formations in core KKTA001 are related to fluid movement along the fault zone. However, the process was one of only oxidation of iron minerals to hematite without leaching of silica (chert) and therefore did not result in formation of high-grade hematite iron ore.

Three drill holes were drilled by Rio Tinto Exploration in the project area (KKTA001, KKTA006 and KKTA013). Of the three drill holes, KKTA001 intersected totally haematitized BIF to a depth of about 236m below 40 m of Kalahari cover (table 3.2 and figure 3.4). The upper 50 m or so of the iron formation is composed of hematitized granular and lutitic iron formation that overlies a prominent granular iron formation bed with large granular jasper pods that is in turn underlain by hematitized

micro BIF. Apart from the fact that it is hematitized; this succession is comparable to that of the Kuruman Iron Formation with the Ouplaas Member at its top overlain by GIF. The iron formation in the lower part of the core is contorted and brecciated.

3.5.3 Ukwi and Moretlwa Hills correlations

Historic logs were drilled at Ukwi and Moretlwa; these were drilled by Daheng Exploration. Three drill holes were logged in Gaborone at the premises of Daheng Exploration; the drill holes of keen interest as they intersected Sishen-type stratigraphy. Drill holes selected for logging are CDH1, CDH2 and CDH3 (Figure 3.7).

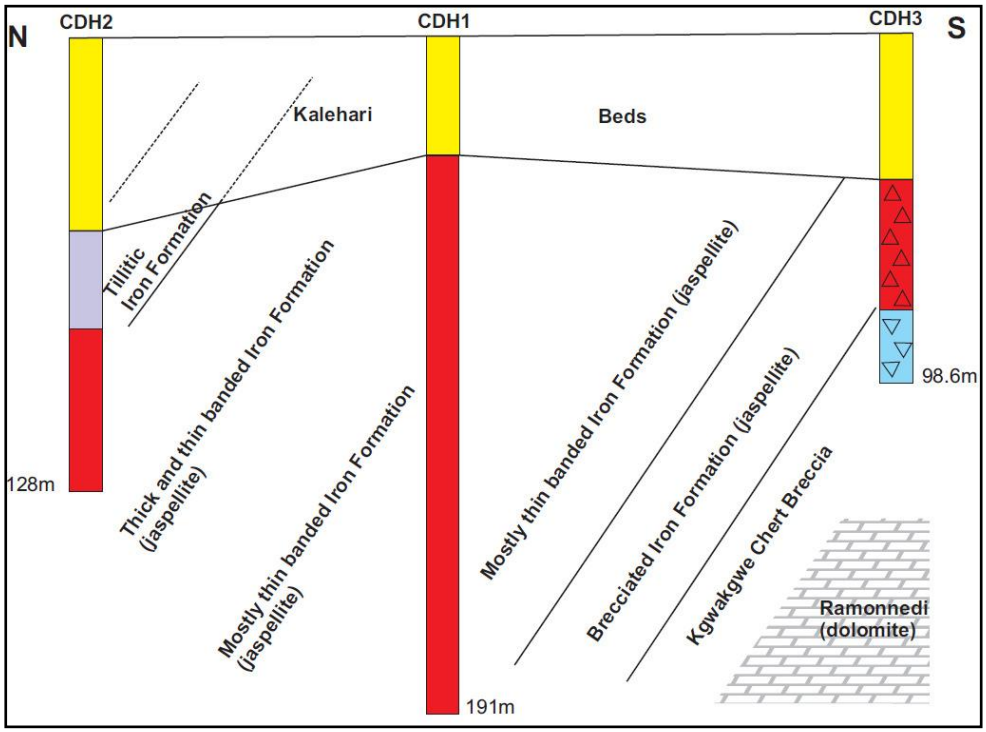

Figure 3.9: Schematic stratigraphic correlation of drill holes CDH1, CDH2 and CDH3 in Ukwi Hill area.

Drill hole CDH1 (255000mE, 7222000mN) intersected a very thick sequence of jaspillitic iron formation. The simplified log of this hole is: 0-33.6 Kalahari. 33.6-46 oxidised BIF. 46-191 end of hole is oxidised red (mostly thin) laminated BIF. There are several narrow zones of haematite enrichment associated with brecciated sections of the iron formation as well as narrow (clay filled) cavities (<20cm).

Drill hole CDH 2 (254000mE, 7222200mN) also intersected only iron formation, however, of slightly different appearance to that of CDH1. The simplified log of CDH2 is 0-54.4

Kalahari, 54.4-82 red jaspillitic BIF with areas of tillitic iron formation 82-128 end of hole, red jaspillitic BIF with some brecciated zones (<20cm thick). This hole has interbedded thick and thin banded jaspillitic.

Drill hole CDH3 (252000mE, 7221400mN) intersected the highest grades of iron formation (this hole is close to RC2) on figure 3.8. The simplified log of this hole is: 0-41.3 Kalahari sand, calcrete, 41.3-49.0 strongly haematised and enriched BIF (direct on the contact with the Kalahari is BIF, slightly further down is hematite enriched BIF. 49.0-78 brecciated lower grade BIF. 78-98.6 end of hole is Kgwakgwe breccia.

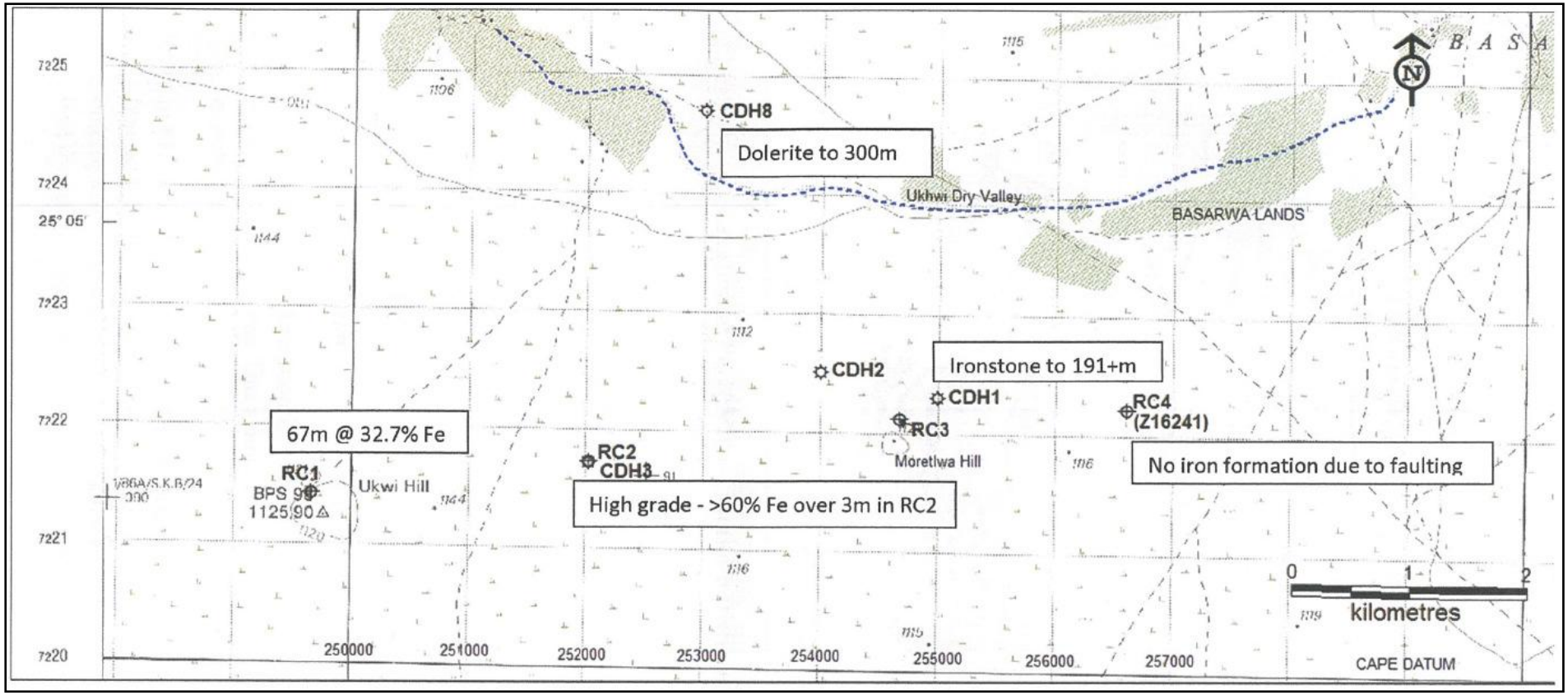

Figure 3.10: bore hole location of Daheng Exploration drilling at Ukwi and Moretlwa Hill area. Three drill holes were selected from this drilling.

The iron formation at Ukwi and Moretlwa Hill dips gently to the N-NNW (5-28 degrees, with an average of about 17 degrees). The north dip suggests that CDH2 intersected the highest stratigraphic part of the iron formation, followed by CDH1 and finally CDH3, which intersected the transition to the Kgwakgwe chert breccia. This unit most likely overlies the Ramonnedi dolomite at depth.

A simplified composite log for the Masoke BIF on the Daheng drilling is given in Figure 3.8. The composite stratigraphy of the Masoke BIF at Ukwi Hill is hence as follows (from top to bottom):

Tillitic Iron Formation (at least 28m thick) followed by interbedded thick and thin-banded jaspillitic iron formation (at least 46m thick), then mostly thin-banded jaspillitic iron formation with thin breccia zones (at least 157m thick) and finally brecciated iron formation (at least 37m thick). The latter immediately overlies Kgwakgwe chert breccia (at least 21m thick) and overlies dolomite of the Ramonnedi formation. The composite thickness of the Masoke BIF in drill core at Ukwi Hill is at least 268m and possibly significantly larger since most holes show only one significant stratigraphic contact. Bedding was generally intercepted at an angle of about 70 degrees, which translated in a minimum stratigraphic thickness of the iron formation of about 252m. This is in accordance with the minimum thickness estimated at Kokotsha of about 172m. The iron formation at Kokotsha and Ukwi Hill is very similar in appearance in that both have a combination of micro and meso banding and both are strongly oxidised.

The iron formations in cores KKTA006 and KKTA0013, intersected at depth of about 350m, appear as “pristine” typical Kuruman and Griquatown iron formation with no pervasive haemititization. Rather the iron formations are highly magnetic and contain abundant siderite and iron silicates. In both boreholes the uppermost few meters of the cores are composed of sideritic granular and lutitic iron formation underlain by podded granular iron formation beds. The underlying iron formation is composed of stacked cycles of micro-banded magnetite-haematite, magnetite-siderite and siderite-magnetite BIF.

The Asbestos Hills Subgroup has been the subject of many detailed mineralogical, sedimentological and geochemical studies (e.g. Beukes, 1980, 1983, 1984, 1986; Van Wyk, 1987; Klein and Beukes, 1989; Beukes and Klein, 1990; Horstmann et al., 1990; Hälbich et al., 1993; Horstmann and Hälbich, 1995). This subgroup comprises

the rhythmically banded Kuruman Iron Formation (i.e. banded iron formation) and the clastic-textured, shallow-water ortho and allochemical Griquatown Iron Formation (i.e. granular iron formation; GIF) defined by the Danielskuil and Pietersburg Members. The ~210m thick Kuruman Iron Formation (range 150–1700 m) is subdivided into four members.

CHAPTER IV PETROGRAPHY AND MINERALOGY

4.1 Introduction

The mineralogy of BIF and GIF from the best preserved sequences is remarkably uniform, comprising mostly silica, magnetite, hematite, Fe-rich silicate minerals (stilpnomelane, minnesotaite, greenalite, and riebeckite), carbonate minerals (siderite, ankerite, calcite, and dolomite), and, less commonly, sulfides (pyrite and pyrrhotite). Chert (and crystalline quartz in metamorphosed IFs) is ubiquitous in all types of IF. In BIF, chert layers are commonly banded, alternating with millimeter-thick laminae of Fe-rich silicate and carbonate minerals. Individual laminae are wavy to wrinkly and, locally, appear to truncate against overlying laminae. In places, chert forms pre compaction nodules draped by compacted laminae, suggesting an early paragenesis for the nodular chert. In GIF, the chert ‘peloids’ show open packing, indicating pre compaction lithification.

Magnetite is widespread in IFs, where it occurs as euhedral, fine- to coarse-grained crystals. It is particularly abundant in cherty Fe-rich layers as laminae comprising dense clusters of inter-grown euhedra. Magnetite commonly is replaced by hematite (termed martite) and locally replaces carbonate minerals. Magnetite is clearly a secondary mineral that formed mostly during the late history of the iron ore formation associated with metamorphism and deformation (Ayres, 1972; Ewers and Morris, 1981; LaBerge, 1964). Hematite is the most common Fe-oxide mineral in IFs, where it typically occurs with magnetite in millimeter to centimetre thick layers. Together with magnetite, hematite defines the lamination in most chert layers. Hematite may also be present in some intercalated mudstones, but in this case, it is much less abundant than magnetite (or pyrite). The timing of hematite growth is texturally ambiguous, although rare hematite spheroids (Ayres, 1972) likely represent some of

the earliest components of Ifs. If they did form very early, then the precursor phase probably was a form of ferric oxyhydroxide, such as ferrihydrite.

Petrographic descriptions of various iron formation types was carried out using a Leica Microscope at transmitted light for gangue minerals and reflected light for ore minerals. Both X-ray Diffraction (XRD) and a Scanning Electron Microscope (SEM) were employed to identify minor minerals and study textures in detail. A total of sixteen polished thin-sections and eight ore-mounts of iron formations were studied petrographically, while the XRD technique was employed to study the bulk mineralogy, as most samples are especially fine-grained. However, it is often not possible to identify specific mineral species, but rather the mineral group. It is for this reason that a combination of techniques was used to understand the mineralogy of the selected samples.

4.2 Microscopic observations and methodologies

Twenty-four drill core samples were selected from five different cores for spatial coverage (figure 4.1). The selected drill holes are: GAST0006, KP17, KKTA001, KKTA006 and KKTA013. KP17 (0-326m) was drilled through Molopo Farms intrusive rocks are characterised by metres wide zones of hybrid and breccia rocks on the contacts with the Transvaal Group rocks. This hybrid rocks are (sometimes brecciated) mixtures of the intrusions and BIF. KKTA001 intersected totally hematitized BIF to a depth of about 236m below 40 m of Kalahari cover. GAST0006 (0m – 149m) is a very interesting core as it intersects both iron formations, dolomite and the chert breccia (table 3.3). Both KKTA006 (0m – 576m) and KKTA013 (0m - 541m) are similar: they both intersect iron formations and thin sleeves of intrusive rocks. KKTA001 is located alongside a major fault (evident from geophysical surveys), whereas both KKTA006 and KKTA013 are distal to the fault. This is especially apparent from the haemititization of iron formations in core KKTA001.

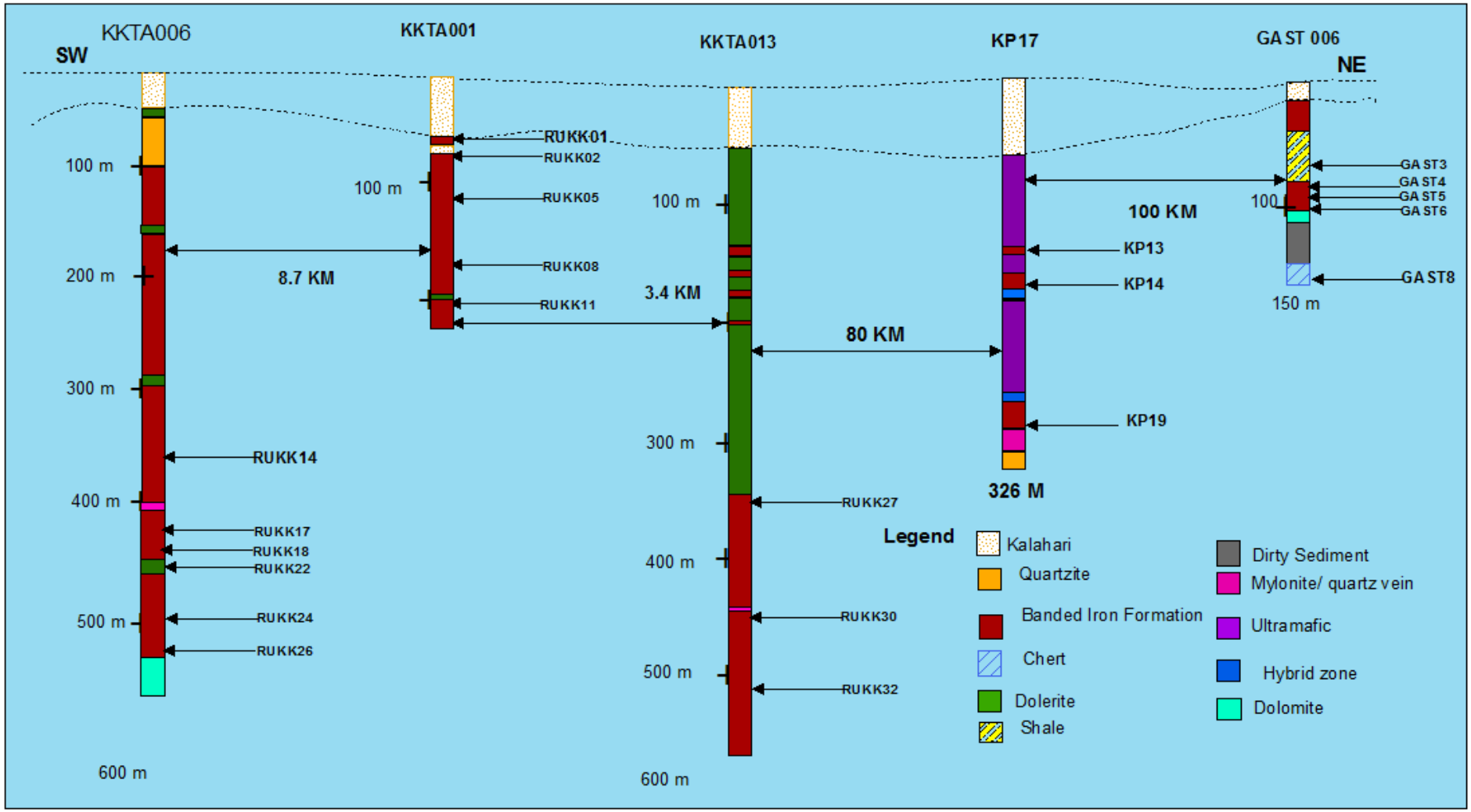

Figure 4.1: Lithostratigraphic columns for the logged boreholes KKTA001, KKTA006, KKTA013, KP17 and GAST0006. The various rock types and thickness variations between the logged boreholes are illustrated.

Reflected and transmitted light examinations of the polished thin section of the BIF samples indicate a bulk rock with an intricate mixture of hematite (~40%), chert (~50%) and other minor minerals (~10%). The haematite occurs as extremely fine grains/crystals, ranging in individual size from <5µm through to rarely 50µm, with most grains. These grains are evenly dispersed throughout a matrix of equally fine-grained chert, albeit with an overall layered distribution (but only rarely as thin continuous laminae). The 5µm grains are dispersed essentially within quartz as a single population together with scattered and layered hematite. Moreover, another population of haematite occurs as “coarse” granular masses, irregularly layered, with grain sizes ranging from 20 to 80µm.

The quartz matrix to the haematite petrographically has a classic micro/cryptocrystalline “cherty” texture, pointing to likely siliceous chemical sediment originally.

For the purpose of mineralogical investigations selected samples from five drill holes were grouped into four main groups (Table 4.2). The selected samples were grouped based on physical and microscopic attributes such as colour, density, texture and hematite-magnetite content and/or presence of silicate minerals (Figure 4.2).

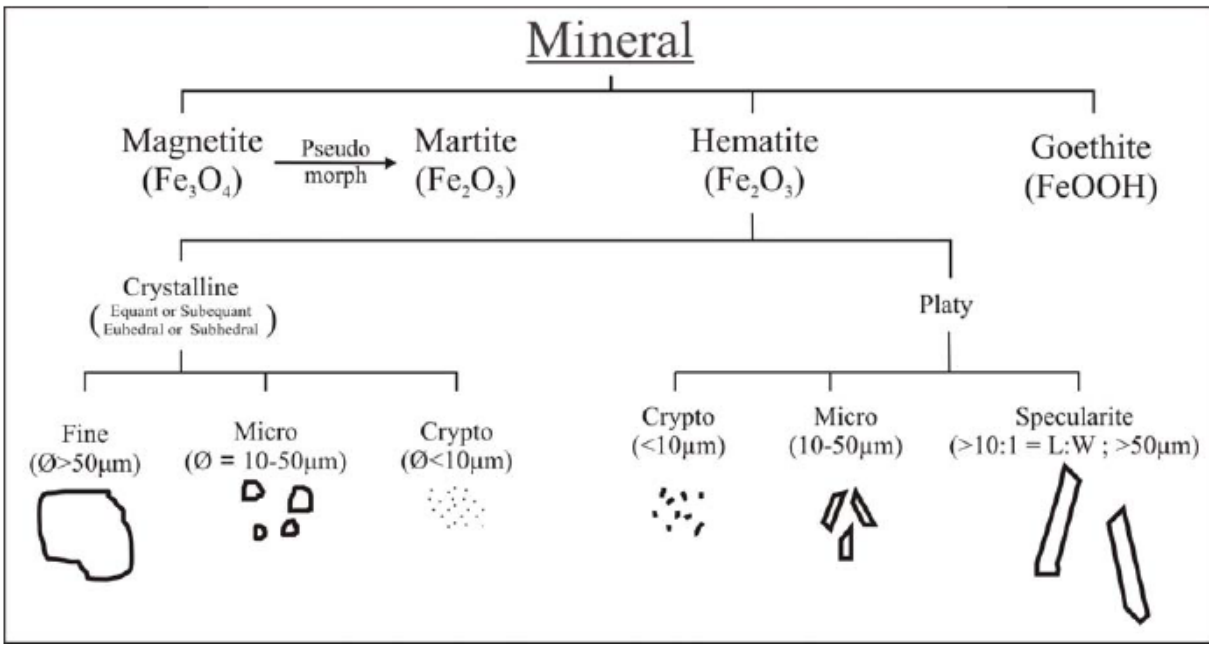

Figure 4.2: Textural generations of different Fe-oxide mineral present in iron ore and BIF. Magnetite is normally transformed to pseudomorphic martite. Goethite is only developed in association with the pre-Kalahari and modern day erosion surface.

Hematite occurs in a variety of forms as indicated in the text (after Mukhopadhyay et al., 2008).

Table 4.1: Categories of iron formations sampled

Group	**Colour**	**Hematite content**	**Silicate content**
Oxidised Iron Formation	Dark red	Moderate	Moderate
Pristine Iron Formation	Light grey	Low	High
Chert Breccia	Cream/red	Low	High
Altered Iron Formation	Dark grey	High	Low

Table 4.2: Selected iron formations samples per category

Pristine IF	**Oxidised IF**	**Altered IF**	**Chert-haematite**
RUKK14	RUKK1	RUKP13	GAST8
RUKK17	RUKK2	RUKP14	
RUKK18	RUKK5	RUKP19	
RUKK22	RUKK8		
RUKK24	RUKK11		
RUKK26			
RUKK27			
RUKK30			
RUKK32			

4.3 Pristine Iron Formation

Pristine iron formations as described in the discussions in chapter 3 were intersected in cores KKTA006 and KKTA0013, intersected at depth of about 350m. The iron formations are highly magnetic, and contain abundant siderite and iron silicates. In both cores the uppermost few meters of the cores are composed of sideritic granular and lutitic iron formation similar to Griquatown Iron Formation underlain by podded and granular iron formation beds that compare to the top Ouplaas Member of the Kuruman Iron Formation.

Samples RUKK32, RUKK14, RUKK24 and RUKK26 comprise BIF and are presumed to be from the same unit. They were all taken at depth (figure 4.1) and

appear “fresh”, highly magnetic and hence most of the iron occurs as magnetite. Some of the samples comprise BIF that has magnetite partially altered to hematite.

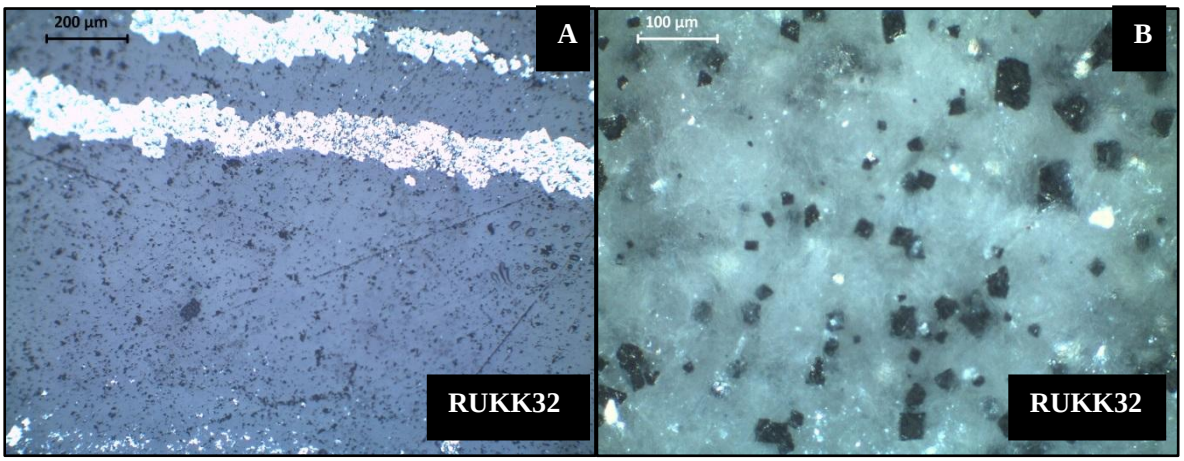

Photomicrograph 4.1: **A:** Sample RUKK 32 consists of alternating bands of magnetite and chert, with clear contacts (x100). Contact between chert layer with minor scattered haematite, and chert-dominated layer**.** Some of the magnetite is slightly altered to haematite. **B:** Euhedral micro-crystals of magnetite evenly dispersed in a chert matrix. The magnetite occurs as extremely fine grains/crystals, ranging in individual size from <5µm through to rarely 50µm, in sample RUKK32 above.

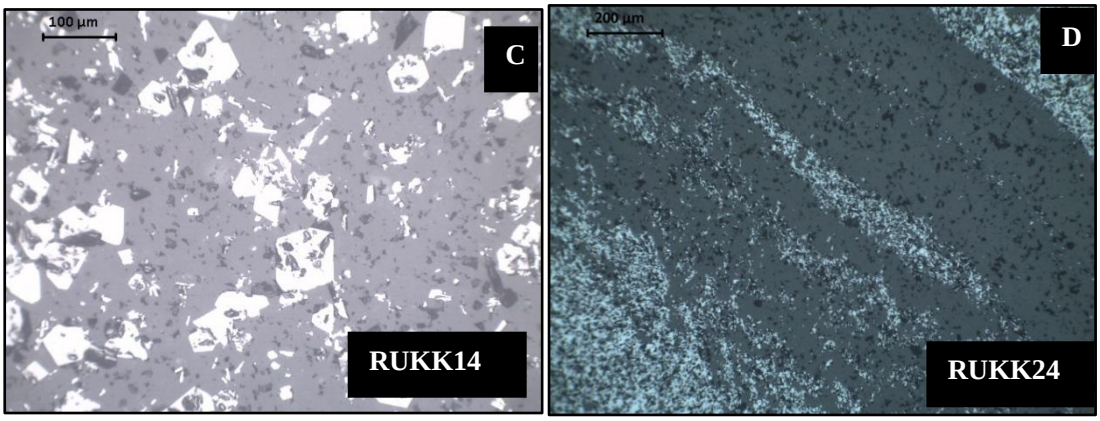

C: RUKK14, This sample is charecterised by euhedral magnetite replicas that are contained within a cherty matrix. Two generations of disseminated hematite namely: ultrafine crystals, and coarser hematite, that tends to replace magnetite. **D: RUKK24**, Homogeneous compact massive and weakly thin bedded, fine cherty-hematite-magnetite BIF. Hematite as dispersed grains 5 to 10mm in size, also weakly layered as euhedral replicas 20 to 50mm after magnetite through host quartz.

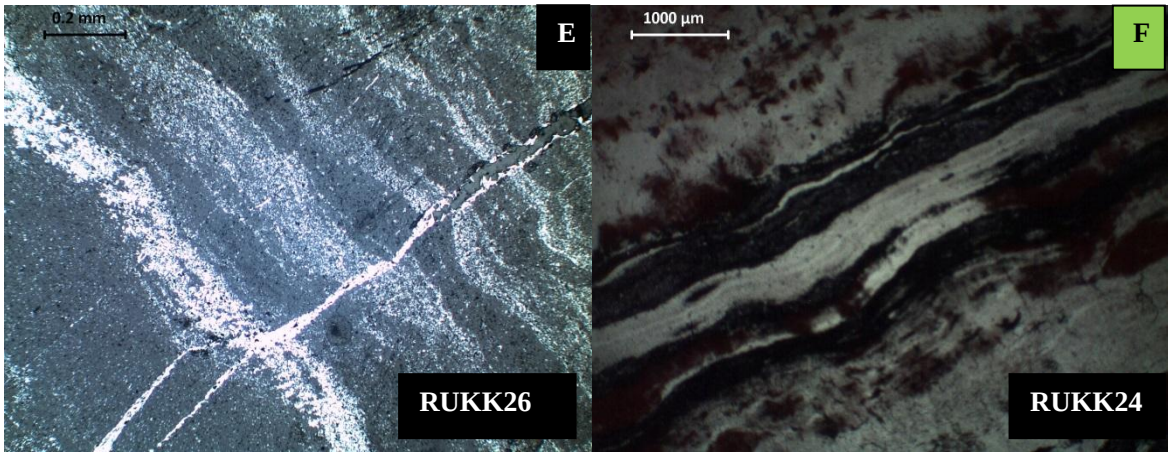

E: RUKK26, Photomicrograph E comprises extremely fine-grained BIF. Very fine hematite forms massive bands in a fine in cherty matrix. Infrequent fine quartz veining crosscuts the massive hematite bands. **F: RUKK24,** Alternating laminae of fine granular magnetite with fuzzy replicas after hematite characterised by fine decussate micaceous, hematite in between.

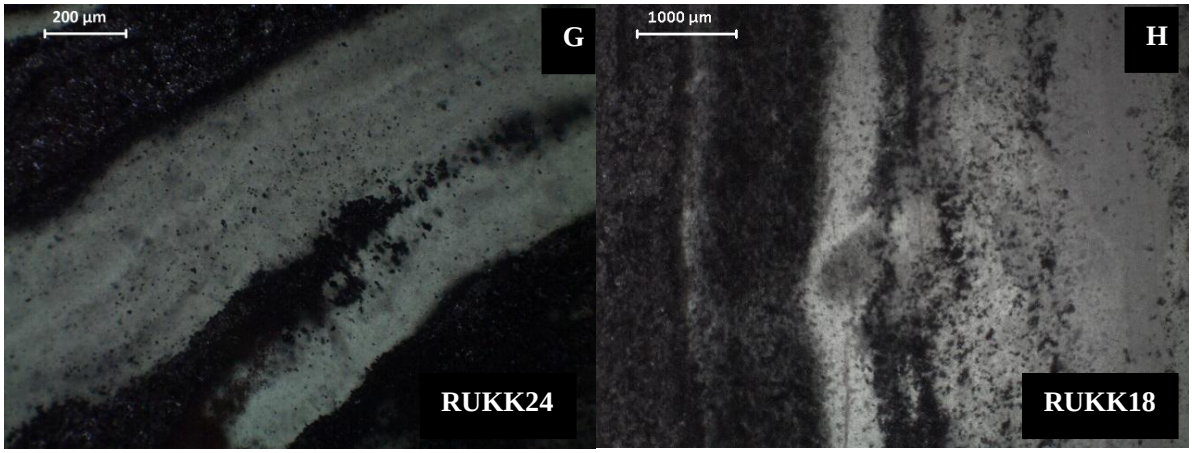

G: RUKK24, Higher magnification showing euhedral magnetite crystals in chert matrix. This is characterised by clear and sharp contacts between the magnetite and chert laminae. However, fine decussate micaceous magnetite crystals are evenly dispersed in the chert matrix. **H: RUKK18,** Photomicrograph showing magnetite crystal evenly dispersed in the chert matrix, the one half the samples is represented by a magnetite rich layer. The magnetite crystal is similar to that of RUKK24, displays euhedral shape.

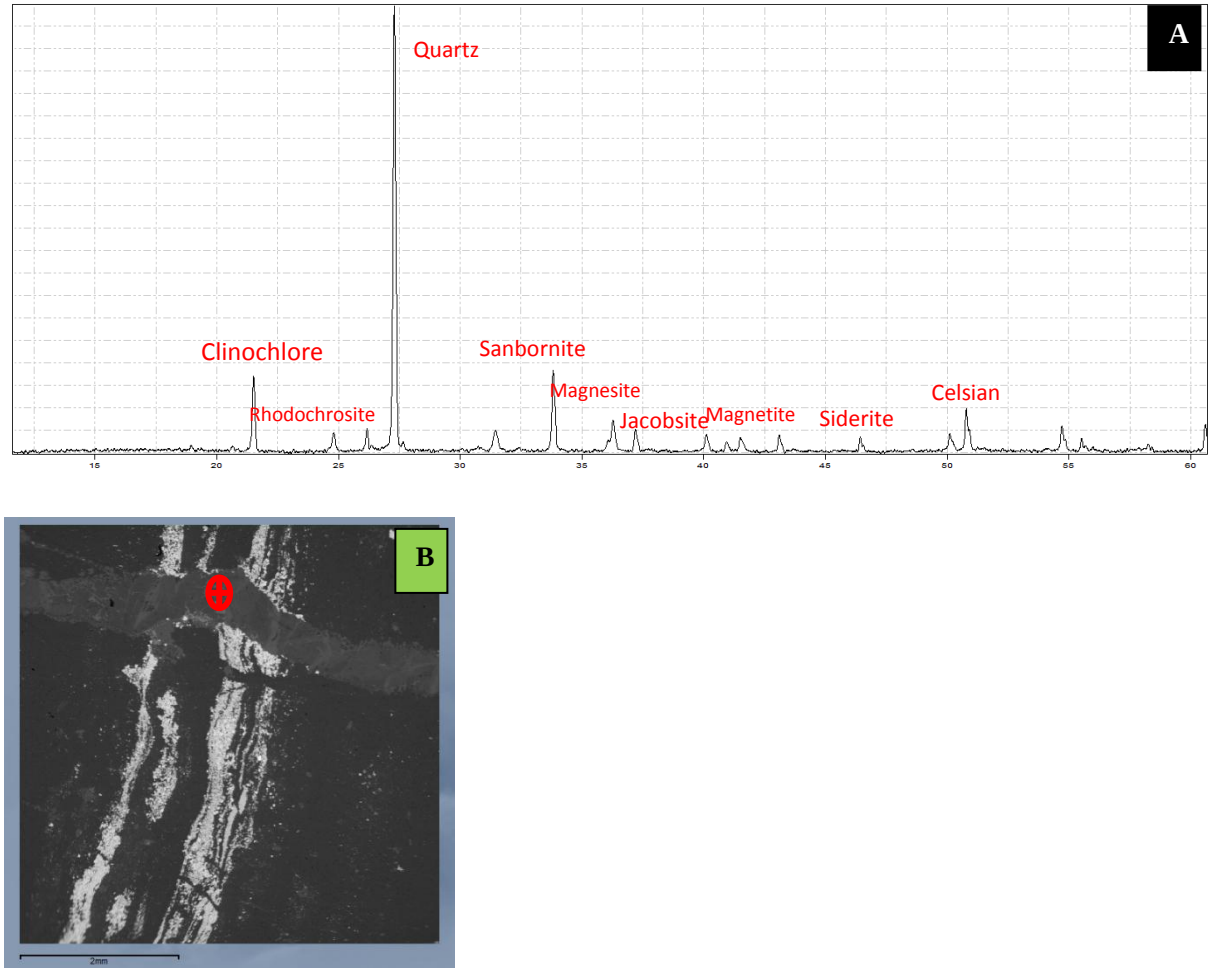

Figure 4.3.1 (RUKK24): Back scatter electron image, XRD and EDS analysis of the fresh BIF. **A.** XRD spectra of BIF, minerals present in RUKK24 are clinochlore (especially in the vein), dominant quartz, magnetite, celsian, rhodocrosite and sanbornite. **B.** Back scatter electron image showing a clinochlore dominant vein and typical banding in iron formation, representative image of fresh BIF.

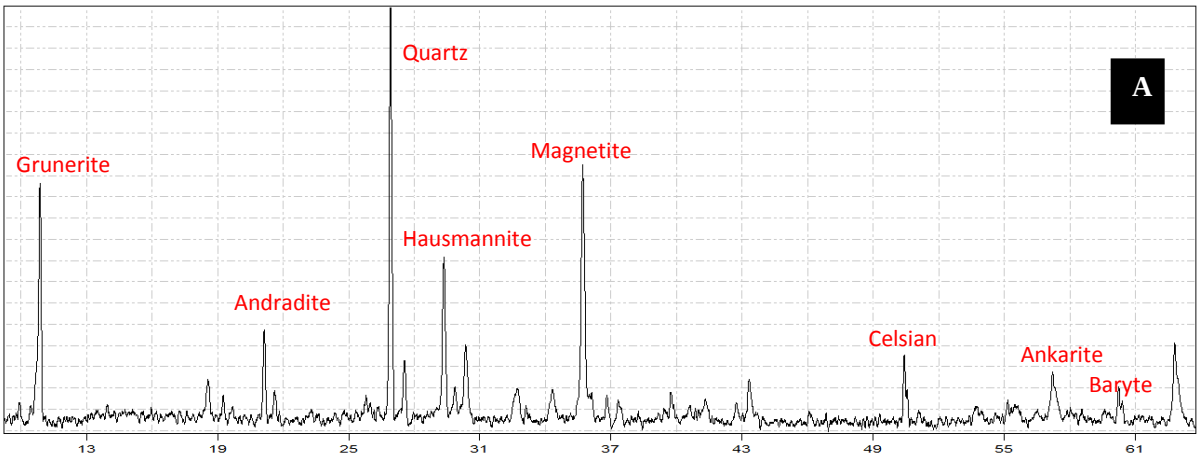

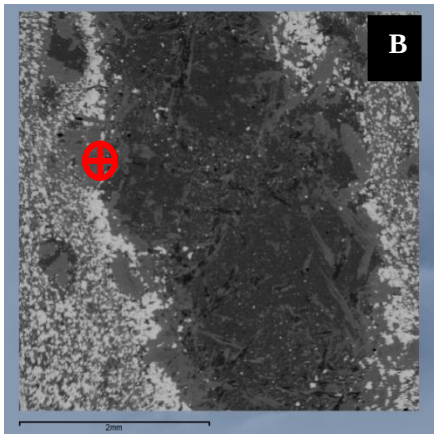

Figure 4.3.2 (RUKK32): Back scatter electron image, XRD and EDS analysis of the pristine BIF. **A**. XRD spectra of BIF, minerals present in RUKK32 are clinochlore (especially in the vein), dominant grunerite, andradite, hausmannite, magnetite and ankarite**.**

C. Back scatter electron image showing radial texture associated with goethite, representative image of fresh BIF.

4.4 Oxidised Iron Formation/partially hematitized BIF

These are described in chapter 3; this chapter will describe microscopic observations. Representative specimens from this type of iron formation consist predominantly of 40-50% chert and 50-60% extremely fine-grained hematite. The latter is from patchy to massive and irregularly layered, variously inter-grown with chert. Abundant fracture networks develop in most samples, with mostly fine to ultrafine decussate, blade- to mica-like grains with minor, slightly coarser-grained platy hematite. At higher magnification, cryptocrystalline chert areas are seen to be crowded by dispersed, extremely fine-grained minerals, possibly Fe-silicates.

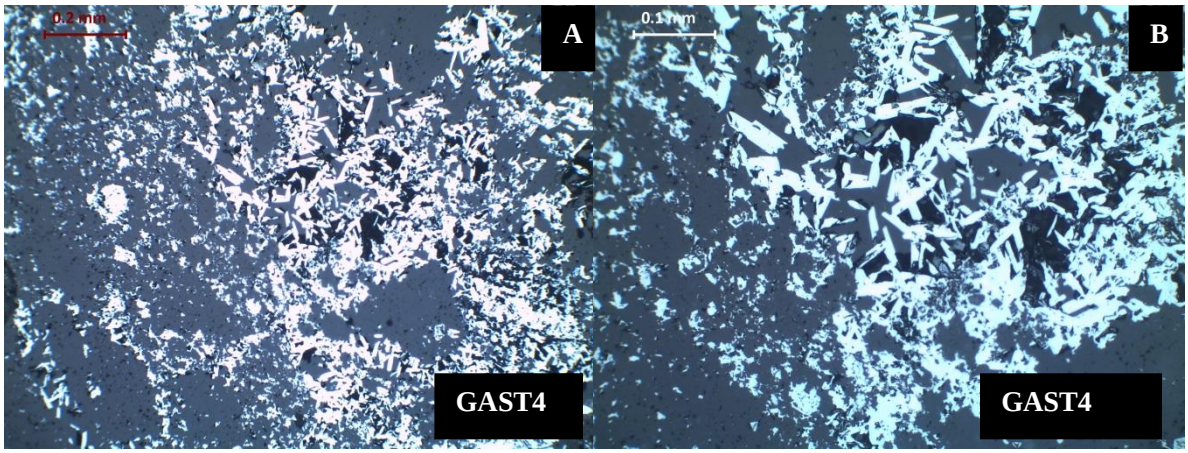

Photomicrograph GAST4 4.2(A). Shows a poorly banded BIF rich in hematite as micro-platy crystals. The banding has local radial textures associated with goethite. **B.** Higher magnification showing platy hematite. Here, hematite occurs as secondary hematite (specularite) along a hydrothermal vein. The lighter colour is associated with goethite haematite.

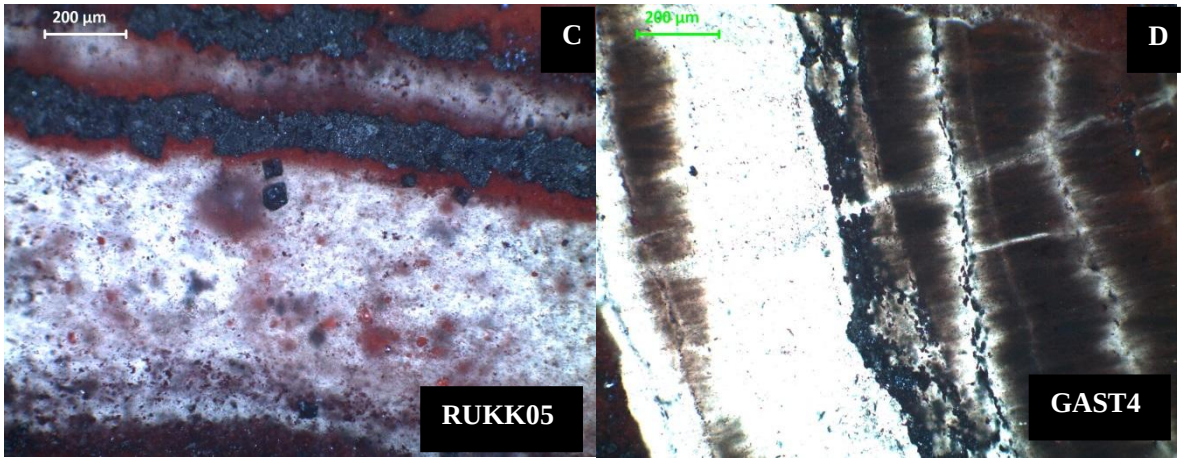

Photomicrographs C & D: Hematitized iron formations, taken under reflected and transmitted light respectively. This specimen consists of homogeneous and massive ultrafine hematite in an apparently siliceous matrix of grey reddish-brown colour. Reflected and transmitted light examination of the polished thin section indicates a bulk rock with an intricate mix of hematite and chert. The hematite occurs as extremely fine crystals, ranging in individual size from <5µm through to rarely 50µm, with all crystals > 20µm seen to be pseudomorphs after euhedral-magnetite crystals.

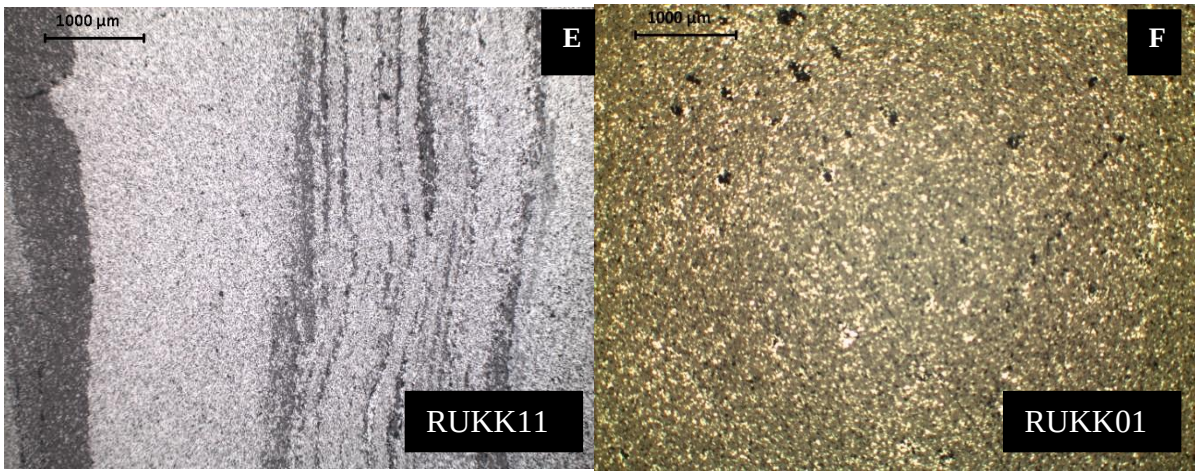

Photomicrographs E& F . Similar to photomicrographs C & D above: Homogeneous, compact, massive and thinly-bedded cherty-hematite BIF. Hematite

occurs as dispersed crystals 5 to 10mm in size, also weakly layered as 20 to 50mm euhedral pseudomorphs after magnetite through the host quartz.

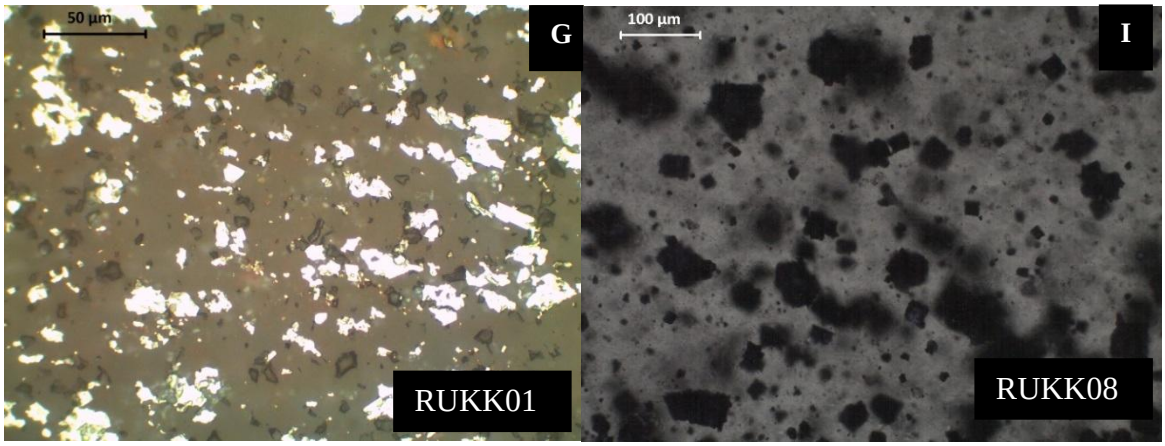

G: RUKK01, Homogeneous compact massive and weakly thinly bedded, fine cherty-hematite specimen. Hematite as dispersed grains 5 to 10mm in size, also weakly layered (not on this scale) as 20 to 50mm pseudomorphs after magnetite. Hematite grains are evenly dispersed throughout a matrix of equally fine chert, albeit with an overall layered distribution on a larger scale.

I: RUKK08, Extremely fine granular population of hematite. These are likely pseudomorphs after coarser original sub- to euhedral magnetite, some with ce residuals of hematite. In moderate magnification (x100), two generations of disseminated hematite can be seen, namely ultra-fine grains, and coarser hematite pseudomorphs after magnetite, set within a micro-crystalline chert matrix.

A

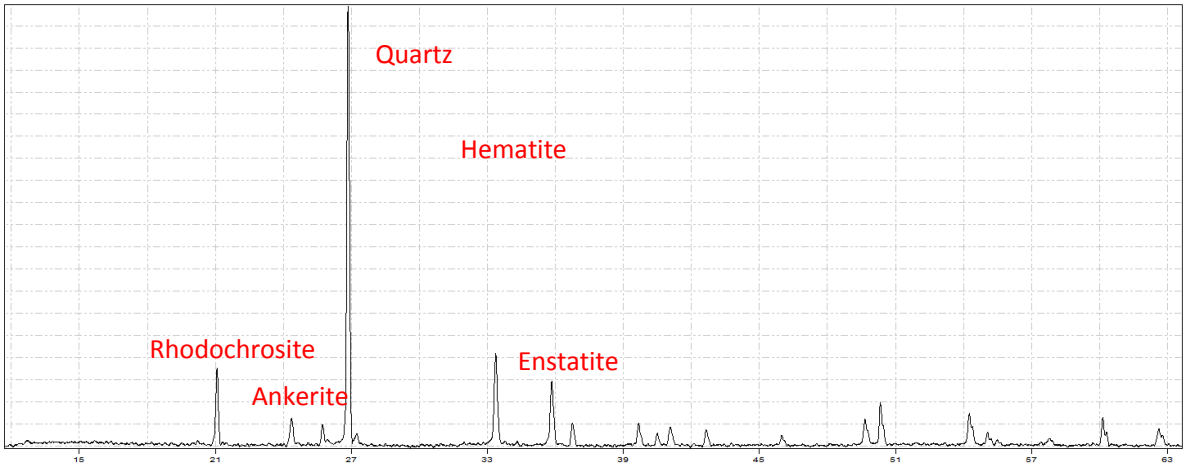

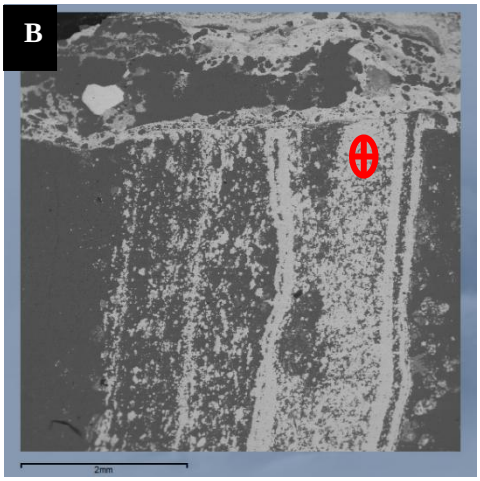

Figure 4.4.1 (RUKK01): Back scatter electron image, XRD and EDS analysis of the oxidised BIF. **A**. XRD spectra of BIF showing minerals present in RUKK01, minerals present are quartz, hematite, ankerite and rhodochrosite. **B.** Back scatter electron image showing typical hematite banding, with minor Mn, otherwise dominated by Fe and SiO, representative image of fresh BIF.

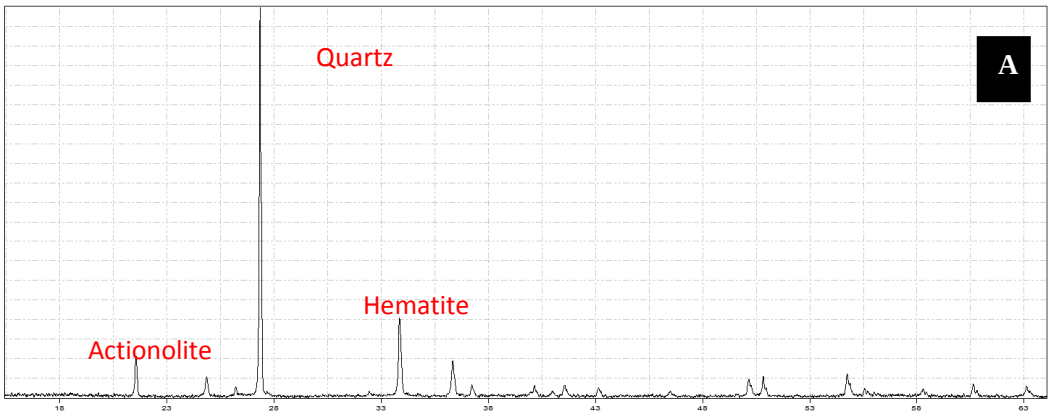

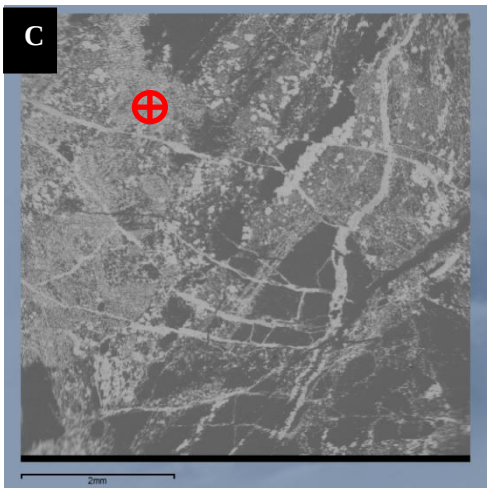

Figure 4.4.2 (GAST04): Back scatter electron image, XRD and EDS analysis of the oxidised BIF. A. XRD spectra of BIF showing minerals present in GAST04, minerals present are quartz, hematite and actinolite. **B.** Back scatter electron image showing typical hematite with micro-joints with quartz filling.

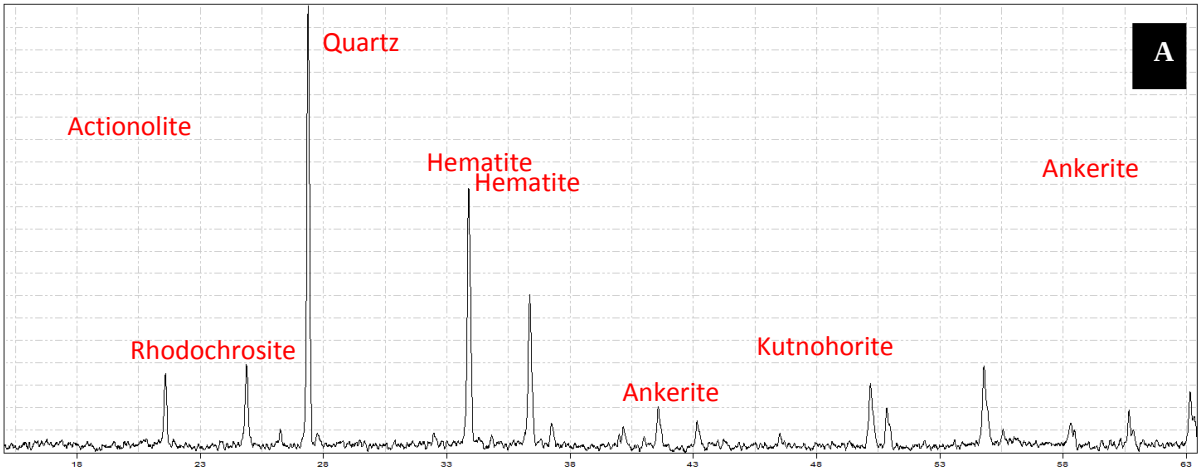

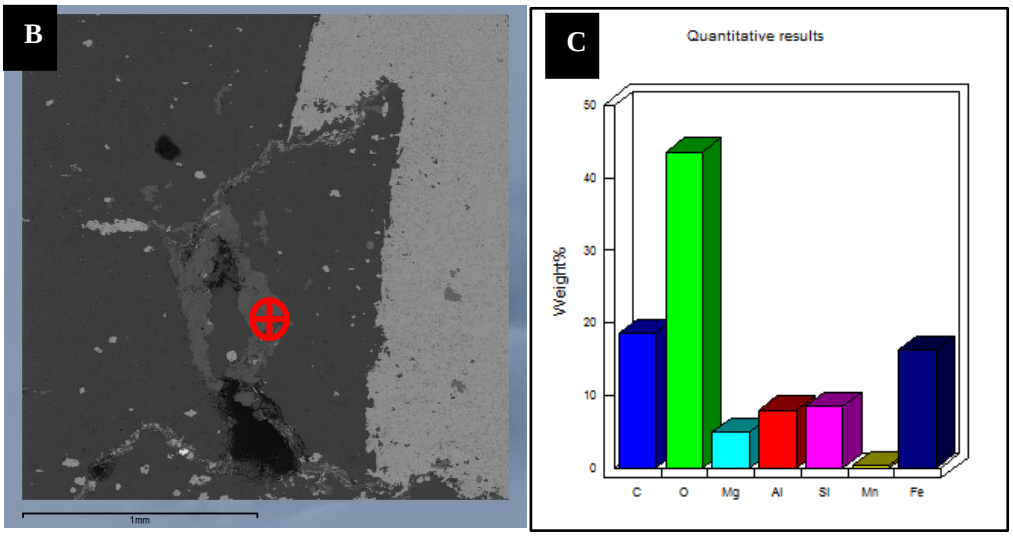

Figure 4.4.3 (RUKK11): Back scatter electron image, XRD and EDS analysis of oxidised BIF. A. XRD spectra of BIF showing minerals present in RUKK11, i.e. quartz, hematite, rhodochrosite, and ankerite. **B**. Back scatter electron image showing micaeous hematite and silica banding. **C.** The quantitative analysis shows the specimen consists of dominant Fe, SiO, Al, Mg and minor Mn while other occur as minor minerals

4.5 Altered Iron Formation

Drill cores from KP17 are characterised by a shear-zone intersected at depth below the intrusive rocks of Molopo Farms Complex. In KP17 drill core the ultramafics contain xenoliths of microbanded magnetite iron formation that appear similar to Kuruman Iron Formation (Beukes, 1980, 1983). This succession is in faulted contact with massive quartz wacke, siltstone and mudstone. The correlation of the massive quartz wacke and mudstone unit appears very similar to that of the Duitschland Formation.

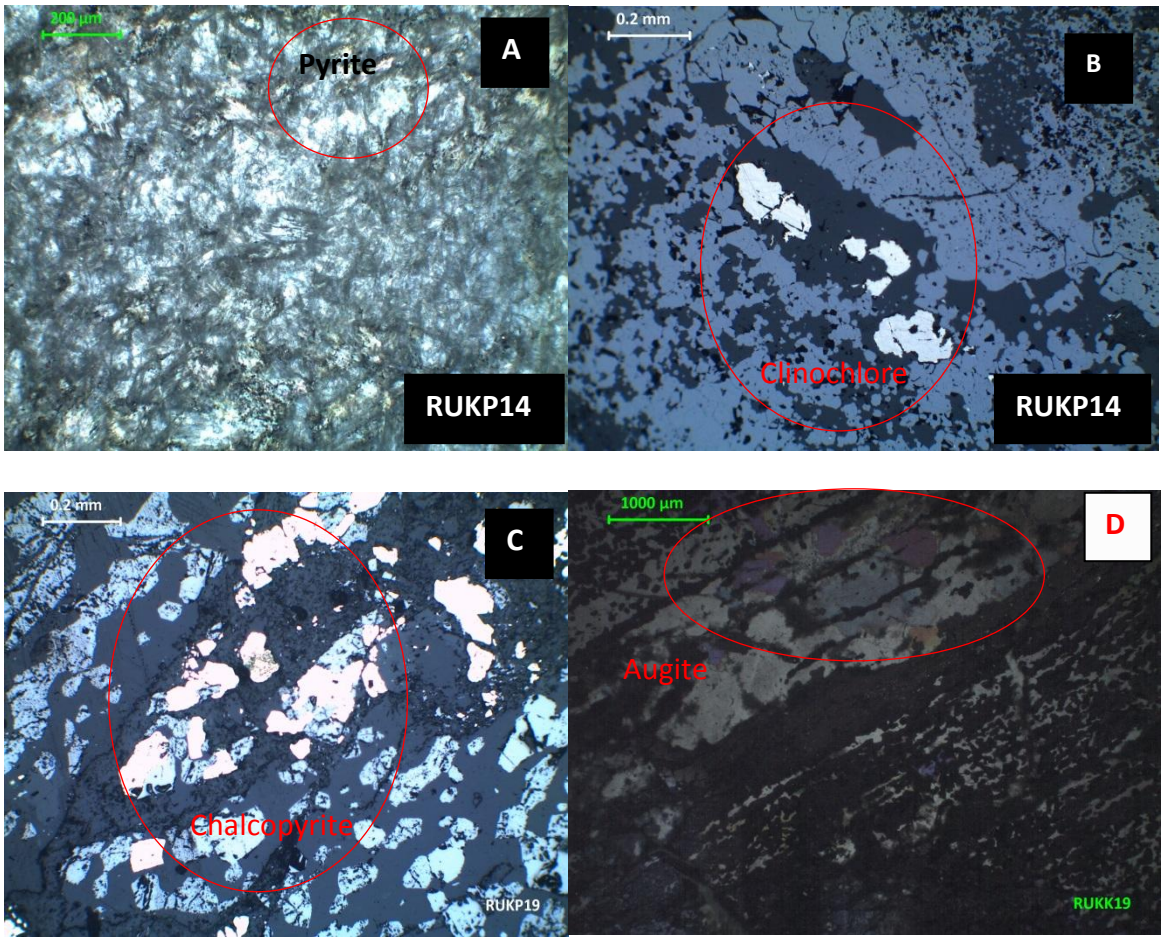

Photomicrograph 4.5.1.A: Reflected light image showing pyrite in bright yellow colour. This specimen is characterised by distinctive pyrite mineralisation with magnetite, with subhedral to euhedral textures. **B:** Reflected light displaying dominant carbonate and silica and minor clinochlore in the veins.**C:** Carbonate and silica rich matrix with sericite and clinochlore. **D:** Alternating bands of magnetite and chert bands, messo and micro banded, with clinochlore.

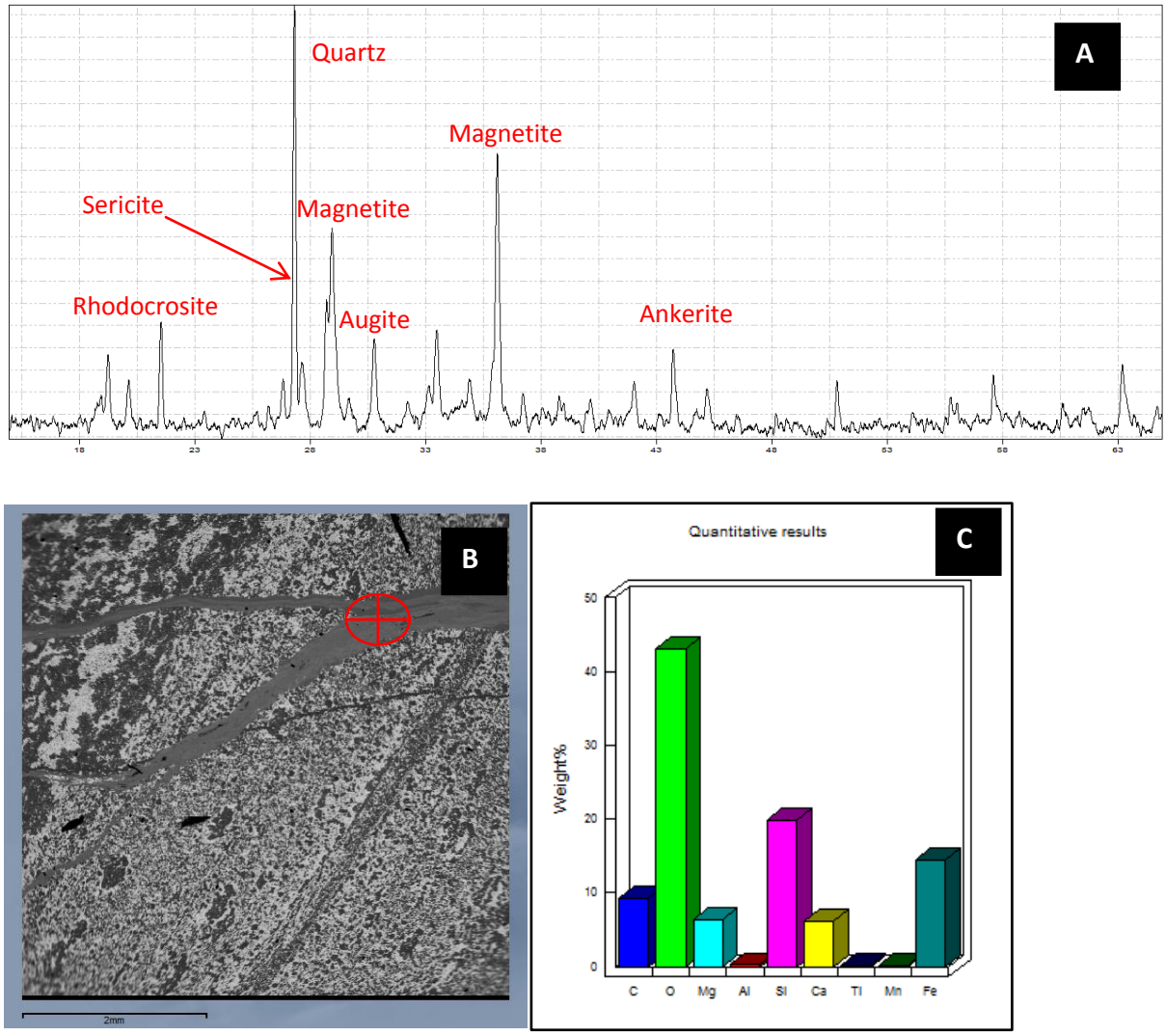

Figure 4.5.1 (KP14): Back scatter electron image, XRD and EDS analysis of the altered BIF, the altered formation has an anomalous Ti. **A**. XRD spectra of BIF showing minerals present in KP14, minerals present are ankerite, rhodochrosite, quartz, magnetite, augite and sericite. **B**. Back scatter electron image showing micaeous hematite. **C**. The quantitative analysis shows the specimen consists of dominant Fe, Si, Al, Mg and minor Mn.

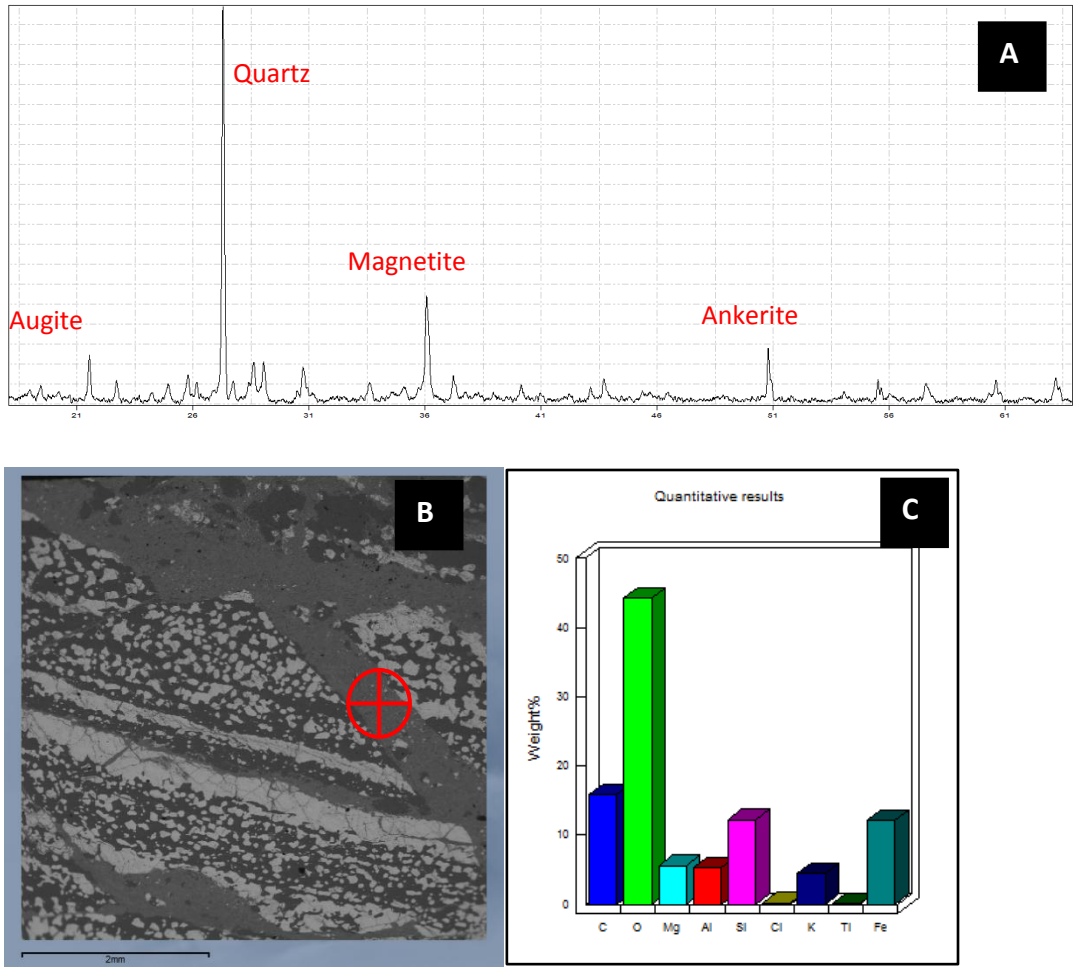

Figure 4.5.2 (KP19): Back scatter electron image, XRD and EDS analysis of the altered BIF**. A.** XRD spectra of BIF showing minerals present in KP19, minerals present are quartz, magnetite, augite and ankerite**. B**. Back scatter electron image showing micaeous hematite and silica banding.

C. The quantitative analysis shows the specimen consists of dominant Fe, SiO, Al, Mg, K and minor Ti.

Samples are dominated by augite from the mafic and ultramafic rocks of Molopo Farms Complex (MFC). These altered BIFs also contain silicates of calcium, sodium, magnesium, iron and aluminium and occasionally contains zinc, manganese and titanium impurities. Its chemical formula is $(Ca,Na)(Mg,Fe,Al)(Al,Si)_2O_6$ and it usually has grayish-green, greenish brown and dark brown colour as in the image above (Photomicrograph 4.5.1.B) . Sulphides are also apparently dominant, followed by the chlorite mineral clinochlore. Clinochlore is a basic iron magnesium aluminium silicate that may contain small amounts of chromium. Its chemical formula is $(Mg,Fe^{2+})_5Al_2Si_3O_{10}(OH)_8$ and has a white colour on this KP17 core.

4.6 Hematite-chert facies/Chert Breccia

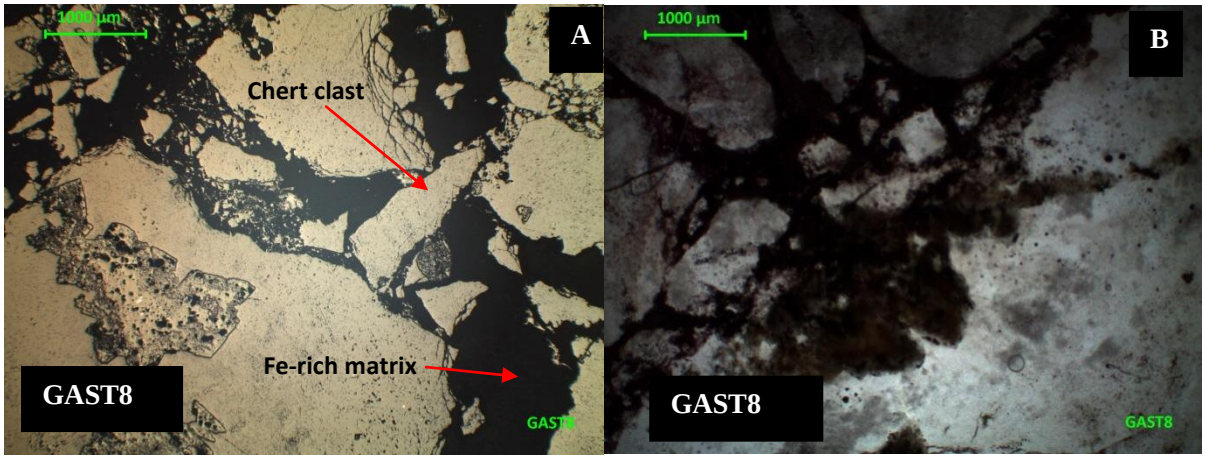

Photomicrograph 4.6.1: (A). GAST8 Reflected light image of chert breccia sampled at the end of GAST006. Irregularly alternating layers within breccia fragments are dominated by chert, and are also rich in extremely fine decussate micaceous hematite, relatively concentrated in the matrix between the chert fragments. **B. GAST8,** Transmitted light image showing dark hematitic matrix between the different chert clasts. In microscopic detail the dark hematite rich matrix, within the breccia fragments, and locally as small fragments, is mostly extremely fine decussate with individual crystal sizes never exceeding 50µm. Coarser hematite occurs sporadically in some layers (and in matrix), as apparent pseudomorphs after magnetite commonly around 0.5mm, rarely up to 2.0mm, and also as less clearreplacement products of original magnetite but converted to compact clusters of ultra-fine decussate hematite. The latter is selectively concentrated within the breccia matrix. Minor fragments of vein quartz also occur in this breccia. One localised occurrence of a cluster of rounded quartz grains with interstitial fine hematite, may represent hematitized clastic sediment.

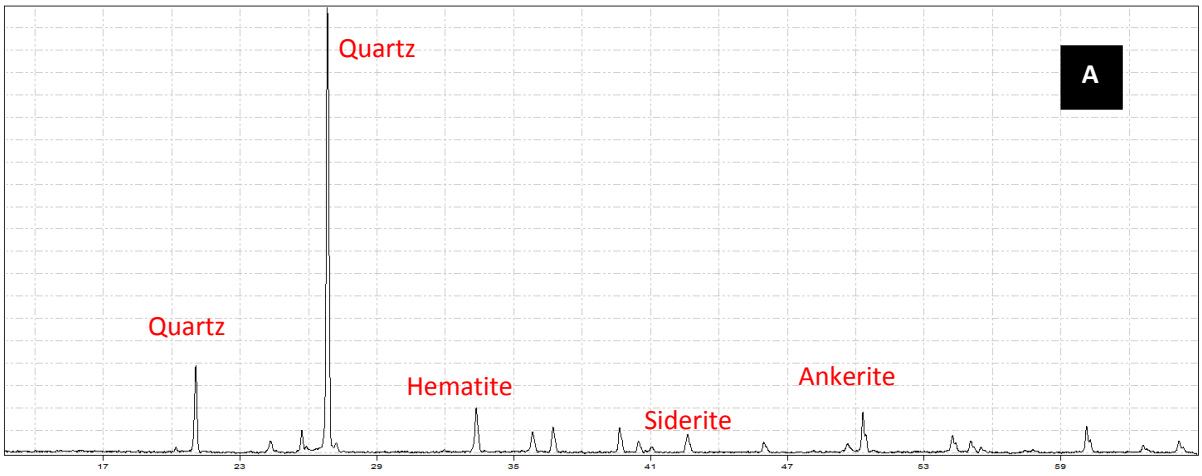

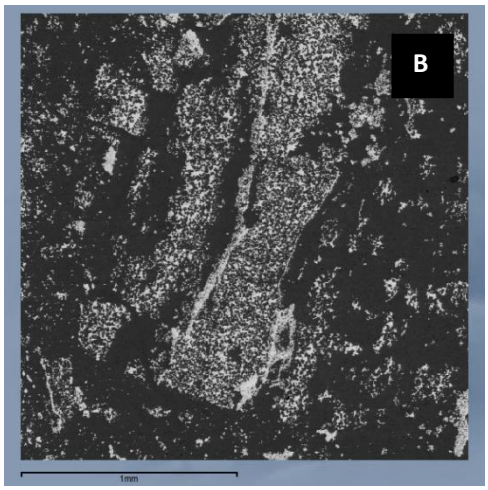

Figure 4.6.1 (GAST06): Back scatter electron image, XRD and EDS analysis of the oxidised BIF. **A.** XRD spectra of chert breccia showing minerals present in GAST06, this specimen is dominated by silica while other minerals such as dolomite, ankerite and sanbornite occur in minor amounts. **B.** Back scatter electron image showing breccia of GAST08.

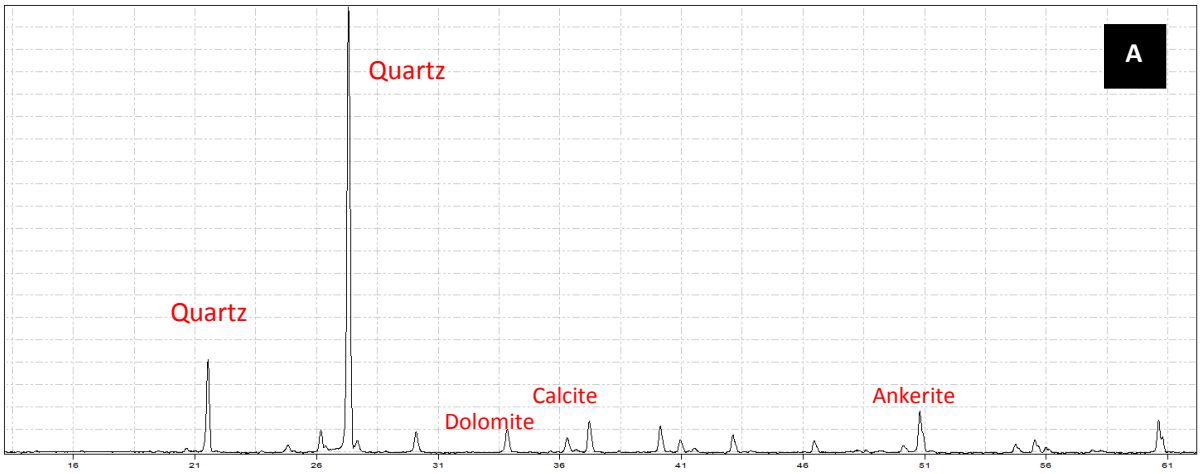

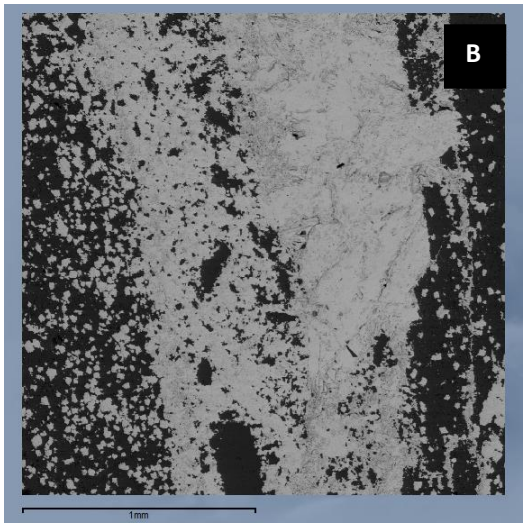

Figure 4.6.2 (GAST08): Back scatter electron image, XRD and EDS analysis of the oxidised BIF**. A.** XRD spectra of chert breccia showing minerals present in GAST08, minerals present are quartz and ankerite. **B**. Back scatter electron image showing breccia of GAST08.

CHAPTER V BULK GEOCHEMISTRY

5.1 Introduction

Twenty-six samples were selected for this study; most of the samples are drill core. Twenty-four these are drill cores, three are outcrop samples while one is drill chips from water-well drilling. The samples comprise of BIF, chert breccia and shale. Whole rock geochemistry analysis was performed on the selected samples. All samples were quartered using a diamond blade-cutter at the Department of Geology, Rhodes University; the one quarter of core was kept while the rest was crushed and pulverised for analysis. Major element analysis was performed by XRF, Rh Tube, and 3kWatt. The detection limit for all oxides is 0.01%.

NAME	Fe_2O_3	Mn_3O_4	TiO_2	CaO	K_2O	P_2O_5	SiO_2	Al_2O_3	MgO	Na_2O	LOI	SUM
RUKK01	43,56	0,04	0,04	0,05	0,04	0,04	56,28	0,41	0,07	bdl	0,08	100,60
RUKK02	51,05	0,04	0,07	0,08	0,08	0,07	48,05	0,84	0,14	bdl	0,24	100,65
RUKK03	38,31	0,04	0,04	0,05	0,05	0,04	61,45	0,53	0,10	bdl	0,14	100,75
RUKK05	56,20	0,03	0,03	0,03	0,03	0,04	43,49	0,59	0,22	bdl	0,17	100,83
RUKK08	42,30	0,03	0,01	0,07	0,02	0,06	58,14	0,16	0,02	bdl	0,03	100,84
RUKK11	75,24	0,02	0,02	0,04	0,01	0,04	25,14	0,12	0,01	bdl	0,01	100,65
RUSS13	47,69	0,19	0,05	1,27	0,06	0,04	49,11	0,54	0,56	0,01	0,54	100,06
RUKK14	48,85	0,03	0,02	0,21	0,05	0,08	51,63	0,23	0,03	0,01	-0,43	100,71
RUKK17	56,15	0,24	0,02	0,31	0,04	0,06	43,09	0,21	0,23	0,02	0,33	100,70
RUKK18	21,34	0,05	0,94	0,18	4,08	0,14	42,93	21,12	4,04	0,05	4,89	99,77
RUKK22	38,18	0,25	0,01	2,14	0,02	0,05	56,74	0,15	0,74	0,01	2,76	101,04
RUKK24	55,19	0,05	0,01	0,52	0,01	0,12	44,40	0,08	0,09	bdl	0,25	100,72
RUKK27	39,52	0,28	0,04	1,37	0,43	0,06	55,19	0,30	2,21	0,78	0,37	100,56
RUKK30	50,15	0,51	0,01	2,63	0,16	0,18	43,02	0,12	3,34	0,16	0,74	101,02
RUKK32	7,27	0,08	0,61	0,11	3,52	0,09	67,39	14,93	0,89	0,03	5,15	100,06
GAST4	38,01	0,02	0,01	0,01	0,00	0,02	62,70	0,05	0,01	bdl	0,09	100,91
GAST5	27,77	0,03	Bdl	0,01	Bdl	0,02	72,90	0,02	bdl	bdl	0,02	100,78
GAST6	7,91	0,16	0,01	3,22	Bdl	0,09	86,73	0,19	0,07	bdl	2,47	100,83
GAST8	39,13	0,77	0,01	1,45	0,03	0,15	56,79	0,08	3,52	0,02	-1,02	100,94
KP13	39,13	0,76	0,010	1,45	0,03	0,15	56,79	0,08	3,51	0,02	1,02	100,94
KP14	45,18	0,36	0,030	5,21	0,07	0,10	45,45	0,37	4,48	0,07	0,48	100,86
KP19	34,67	0,11	0,64	3,13	0,12	0,41	48,04	6,08	4,43	2,00	0,79	100,47

Table 5.1 Major element geochemistry of the assayed sample

5.2 Oxides facies

5.2.1 Major oxides

The main oxide minerals that make the oxide facies are mostly hematite Fe_2O_3.and magnetite Fe_2O_3. The oxide facies can, therefore, be divided into two subtypes – banded hematite quartzite and banded magnetite quartzite. The banded hematite rocks consist of alternating bands of hematite and chert.

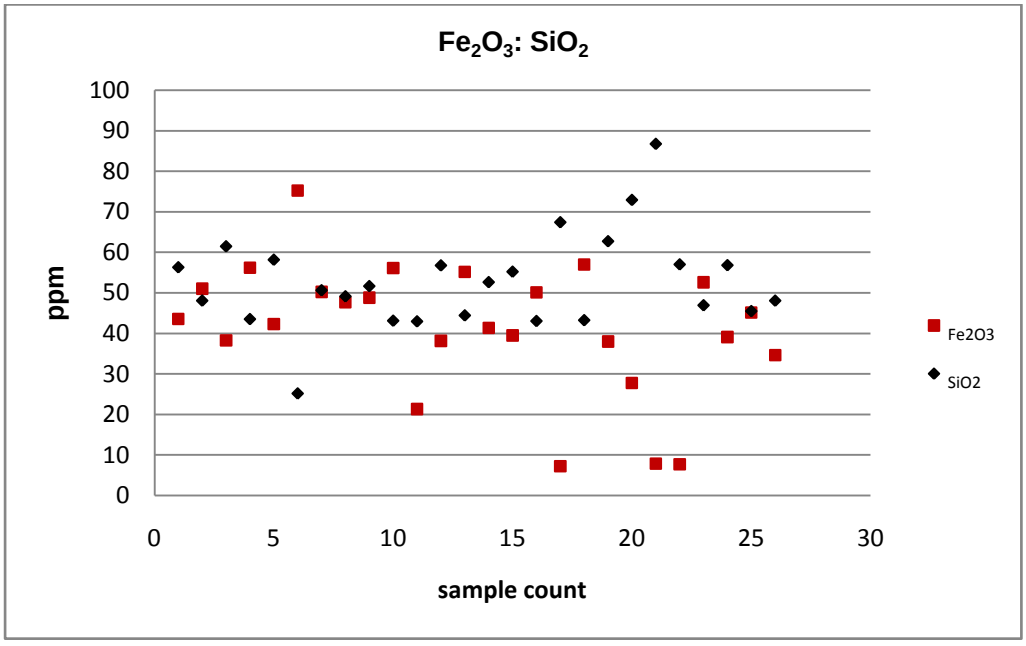

Figure 5.1 Binary plot based of the relationship between SiO_2 and Fe_2O_3.

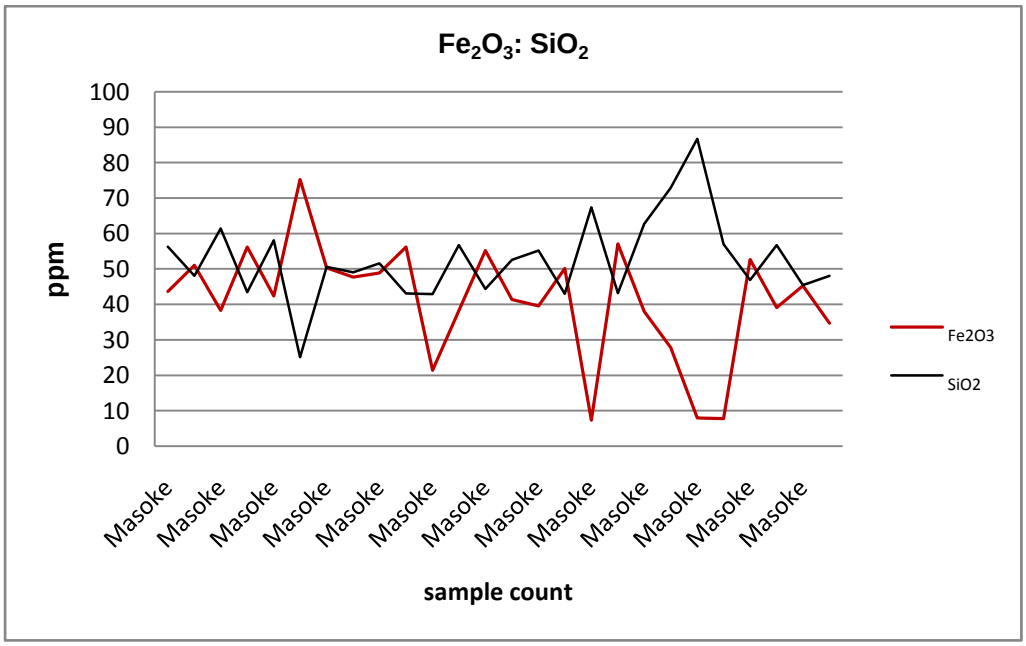

Figure 5.2 Probability plot based on major oxides, SiO_2 and Fe_2O_3.

It is apparent from Table 5.1 that the BIF samples have very similar chemistry. Specifically the major constituents of these BIF are dominated by SiO_2 and Fe_2O_3. Banded iron-formations are characterized by alternative bands of iron-minerals and chert; these rocks are bimodal in nature. Their formation also depends on the availability of other oxides like $Al2O_3$, TiO2, CaO, Na_2O, K_2O and MgO; these are found in minor traces. One sample, however, has typically high Fe_2O_3 (75wt %) as shown in probability plots (figure 5.1, and figure 5.2); and table 5.1 (sample number: RUKK11).

5.2 .2 Minor oxides

Silicate facies of iron-formation consists of different iron silicates depending upon the degree of metamorphism the rock has undergone. Their formation also depends on the availability of other oxides like $Al2O_3$, TiO_2, CaO, Na_2O, K_2O and MgO.

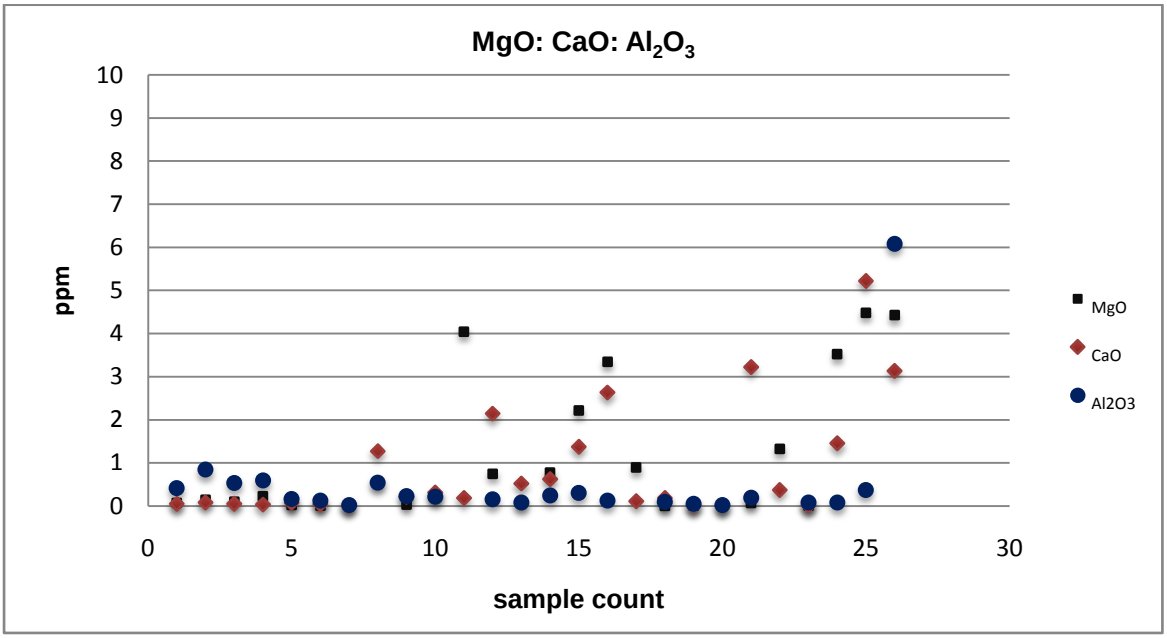

Figure 5.3 Binary plots showing the relationship between MgO, CaO and Al_2O_3.

These samples are clearly Al_2O_3 depleted, while there is good positive correlation between MgO and CaO. The latter plots also show a break between MgO-poor samples (most) and MgO-rich samples (RUKK30, RUKK32, KP13, RUKK22, RUKK18 and KP14). Three of the selected samples have anomalous Al_2O_3 and correspond to shales; these samples are KP19, GAST5 and GAST3. CaO has a smooth plot with most of the BIF having relatively low CaO values (average 0.6wt%)

and KP14 having the highest at 5.2 wt % followed by the chert breccia sample at 3.2 wt%.

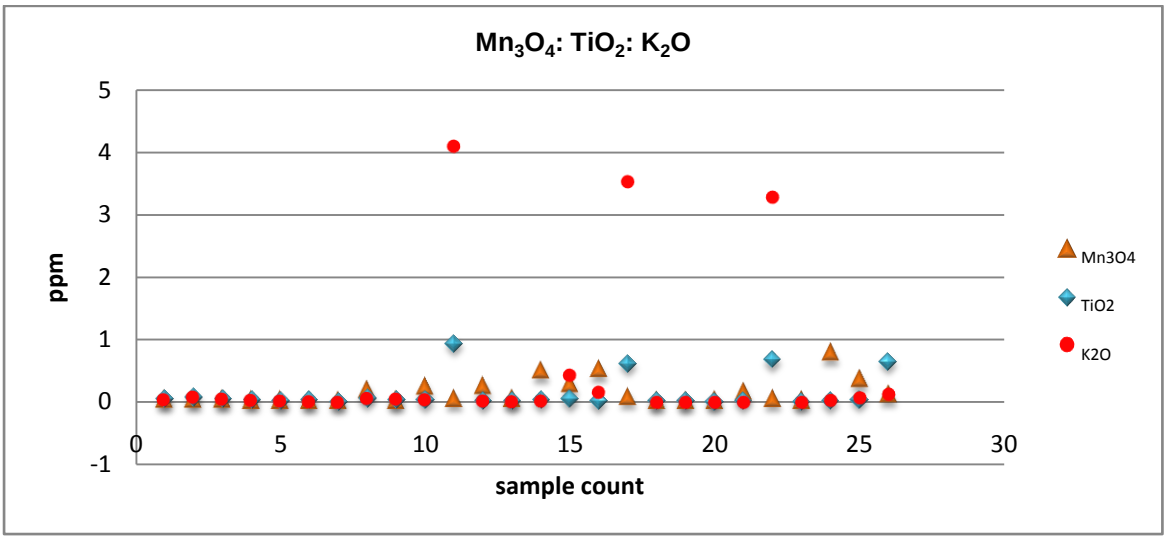

Figure 5.4 Binary and probability geochemical plots with emphasis on minor element oxides. Few associated with KP17 have slightly higher than normal K2O; these samples were collected at the contact of the Transvaal and intruding MFC.

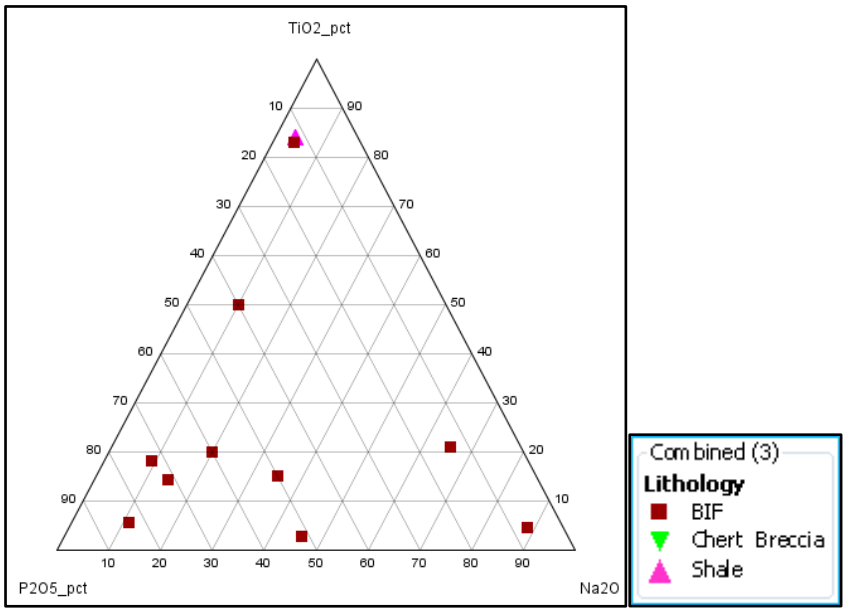

Figure 5.5 Ternary plots per lithology of the collected samples.

It is apparent from the plot that RUKK30 and KP19 which are both BIFs have high Na_2O. While RUKK22 and GAST3 which are BIF and shale respectively have anomalous TiO_2. The rest of the BIFs are characterised by higher P_2O_5 and are depleted in both TiO_2 and Na_2O.

In terms of major element geochemistry presented in table 5.1 above, sample GAST6 and GAST8 have similar major element values. They are characterised by high SiO_2 and very low Fe_2O_3 and they are also depleted in Al_2O_3. These two samples are essentially highly siliceous portions of chert breccia. Samples GAST6 and GAST8 are characterised by moderate Mn (as Mn_3O_4) which is important, as Mn is known to be found in the dissolution breccia found in the Griqualand West Basin (Schalkwyk, 2005). The binary geochemical plots of Figs. 5.2 and 5.3 show relations of different lithologies against total Fe oxide in terms of major element chemistry which reflects their petrogenetic compositions.

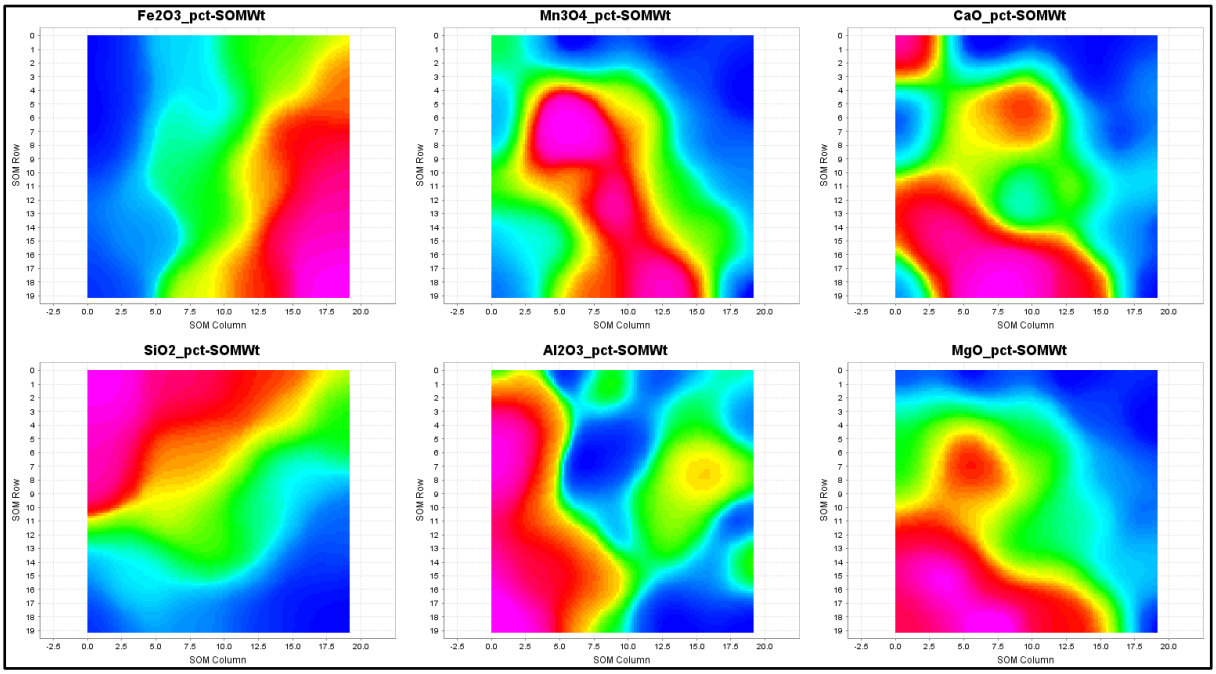

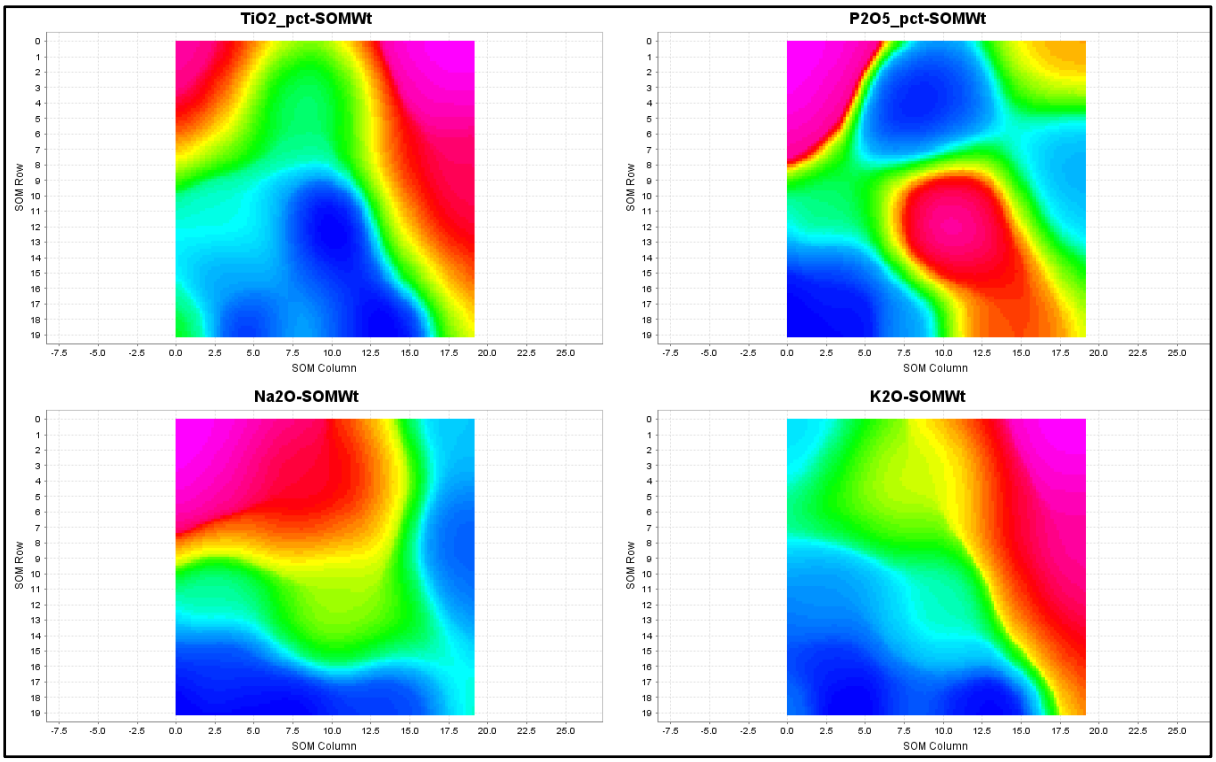

Figure 5.6: Self-organising maps for both major and minor element showing relations of different elements.

5.3 Spider plot

Certain combinations of elements reflect the petrogenetic signatures of classifiable rock suites. A common method of representing this is spider plots; the one shown here (Figure 5.6) normalises the geochemistry of the selected samples against average upper crustal for elements Al, Ca, Ti, Mn and Fe.

It becomes apparent that one of the chert breccia samples (GAST8) is quite similar to BIFs in composition. This has shown similarities to most of the BIF samples. Shale data plot just on the average line for elements except for Ca; Ca plots below upper crustal average for sedimentary rocks. BIF data plot below average for the elements Al, Ca and Ti while they plot above average for most others (see samples PK19, RUKK11, KP13, RUKK18, RUKK24, RUKK2, RUKK32 and GAST8).

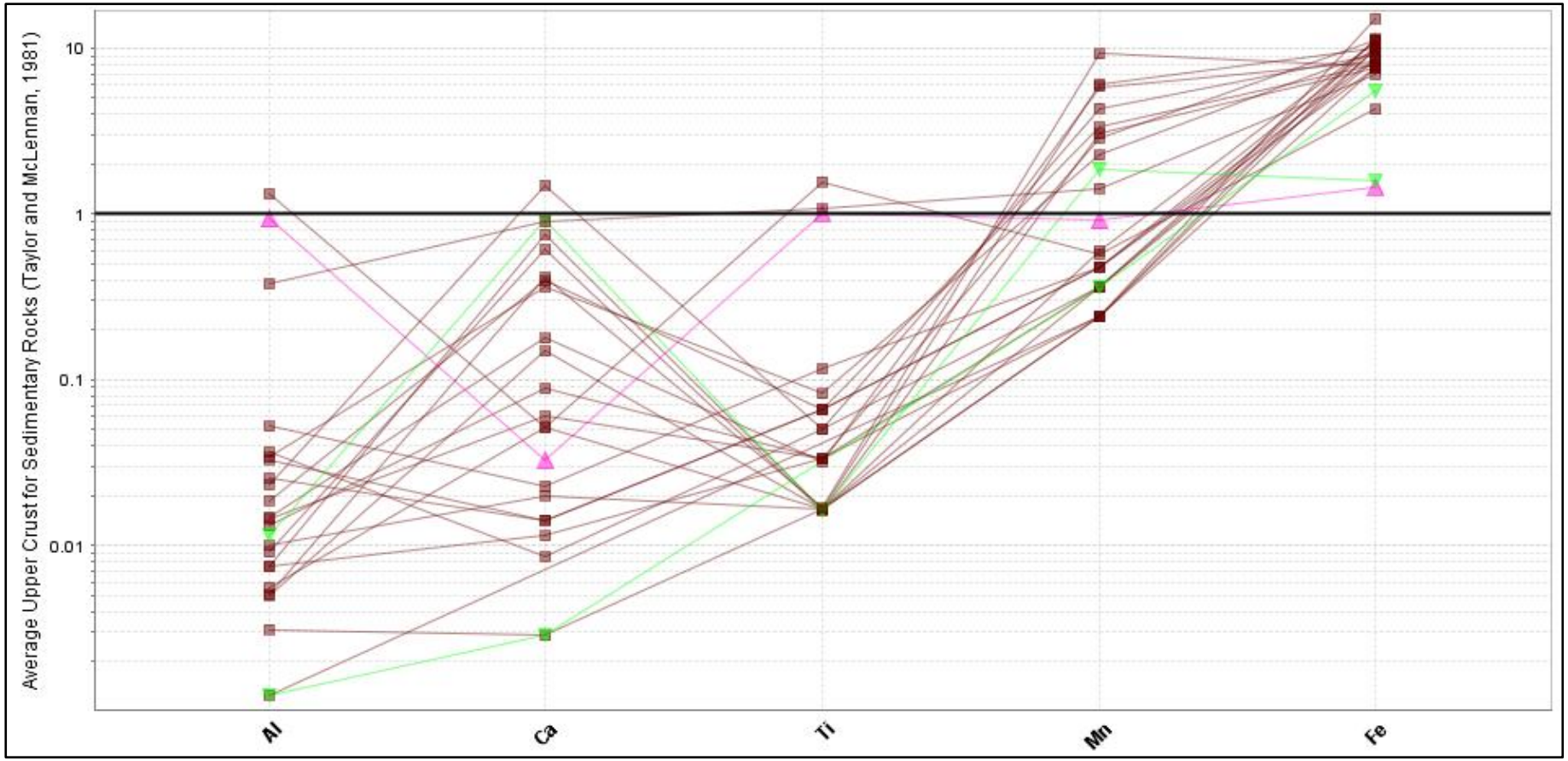

Figure 5.7: Spider diagram showing data for all selected samples normalized to average crustal abundance.

SmpleID	Y	Zr	Nb	La	Ce	Pr	Nd	Sm	Eu	Gd	Tb	Dy	Ho	Er	Tm	Lu
GAST4	6.03	1.3595	5.585	1.4165	2.305	0.435	2.09	0.7255	0.1745	0.7685	0.096	0.7315	0.159	0.4635	0.08	0.0726
GAST5	5.56	1.8445	2.33	0.638	1.1865	0.1325	0.6035	0.236	0.066	0.375	0.078	0.526	0.127	0.4795	0.06855	0.0682
GAST6	2.062	1.2765	10.065	0.7735	0.921	0.127	0.511	0.105	0.0335	0.157	0.0327	0.1465	0.0449	0.1715	0.0147	0.02555
GAST8	4.78	2.07	1.2405	2.412	5.315	0.5605	2.625	0.497	0.127	0.6065	0.0895	0.566	0.1085	0.374	0.0413	0.04235
KP13	7.205	2.885	1.191	1.8655	3.555	0.401	1.815	0.3775	0.112	0.5605	0.0753	0.638	0.16	0.562	0.07855	0.0815
KP14	8.27	5.63	10.725	3.145	5.895	0.686	2.73	0.651	0.158	0.7865	0.116	0.802	0.217	0.7465	0.082	0.121
KP19	19.685	48.075	5.185	4.46	10.365	1.4705	6.475	1.81	0.6885	2.285	0.36	2.6	0.6235	1.89	0.2755	0.245
RUKK01	3.36	6.135	1.44	1.3115	2.705	0.3585	1.695	0.529	0.172	0.635	0.0901	0.6845	0.1285	0.432	0.04125	0.04445
RUKK02	4.8	9.255	2.635	1.2965	3.155	0.444	2.355	0.925	0.279	1.0405	0.1645	0.9655	0.1685	0.4365	0.0553	0.05505
RUKK03	2.985	5.66	3.445	0.667	1.922	0.269	1.257	0.411	0.141	0.5535	0.0771	0.553	0.1105	0.309	0.03705	0.0432
RUKK08	3.37	3.95	3.295	0.942	1.864	0.263	1.1445	0.3145	0.1525	0.6075	0.07585	0.5485	0.114	0.305	0.0386	0.0402
RUKK11	3.495	5.315	3.195	1.075	2.138	0.2725	1.34	0.3935	0.146	0.512	0.06375	0.409	0.1225	0.344	0.0451	0.06035
RUKK13	2.234	1.173	2.134	0.9645	1.2785	1.4255	0.61	0.093	0.0301	0.1395	0.0259	0.2395	0.0461	0.174	0.0178	0.03235
RUKK17	3.19	3.235	10.275	0.704	1.145	0.152	0.727	0.3215	0.068	0.3515	0.03665	0.276	0.06045	0.2105	0.02945	0.036
RUKK18	2.685	4.225	7.38	0.52	0.91	0.1295	0.6135	0.215	0.0765	0.191	0.04775	0.221	0.0756	0.2425	0.0237	0.0447
RUKK22	13.595	201.13	12.945	55.765	99.05	10.295	34.585	4.94	1.241	2.95	0.3555	2.24	0.4775	1.477	0.2335	0.2275
RUKK24	9.74	5.36	1.178	1.0085	2.795	0.514	2.765	0.855	0.303	1.2055	0.182	1.15	0.247	0.717	0.07115	0.096
RUKK26	5.605	3.225	7.175	1.0055	2.2425	0.3145	1.93	0.7305	0.2345	0.829	0.127	0.6365	0.138	0.44	0.0666	0.06225
RUKK27	4.945	5.33	2.4065	1.091	2	0.2315	1.2495	0.2915	0.1135	0.507	0.0684	0.455	0.1045	0.362	0.06385	0.07855
RUKK30	3.52	5.36	3.325	1.28	2.4305	0.2645	1.177	0.275	0.0795	0.2665	0.0413	0.406	0.0773	0.305	0.04195	0.0449
RUKK32	7.51	2.9	1.334	2.156	3.615	0.441	1.72	0.3975	0.146	0.7235	0.101	0.73	0.18	0.6025	0.0892	0.1035

Table 5.2: Rare earth elements for all selected samples

5.4 Rare earth elements

The rare element geochemical plots of the selected samples have similar signature throughout the different BIFs (figure 5.9). Only three samples from the selected batch have relatively higher rare earth abundances. These samples are KP19 (altered), GAST3 (oxidised) and RUKK22 (pristine); interestingly, they represent each of the modify group plotted. Rather than this all the samples plotted very close to each other.

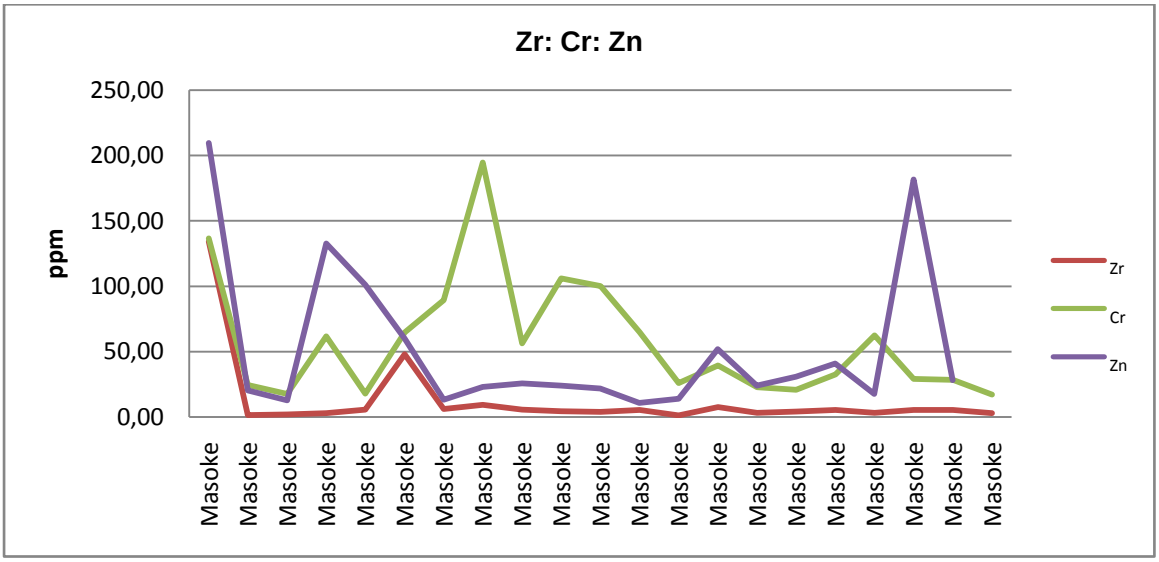

Figure 5.8 Probability plots showing the values of Zr, Cr and Zn. These values are relatively subtle through all BIF categories.

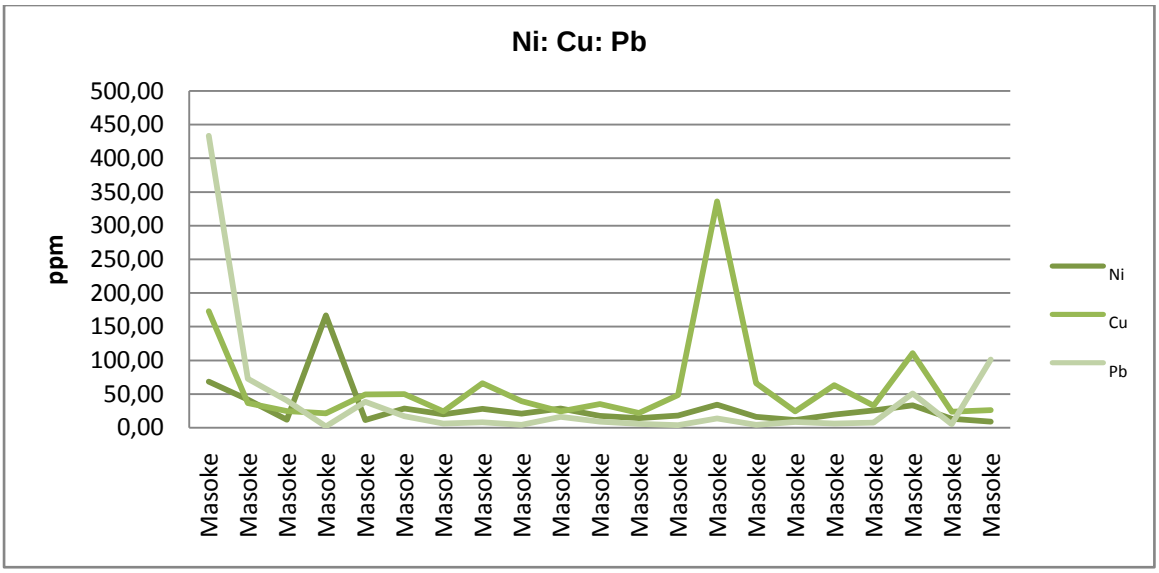

Figure 5.9 Probability plots showing values for Zr: Cr and Pb. These elements have a good positive correlation over all BIF categories.

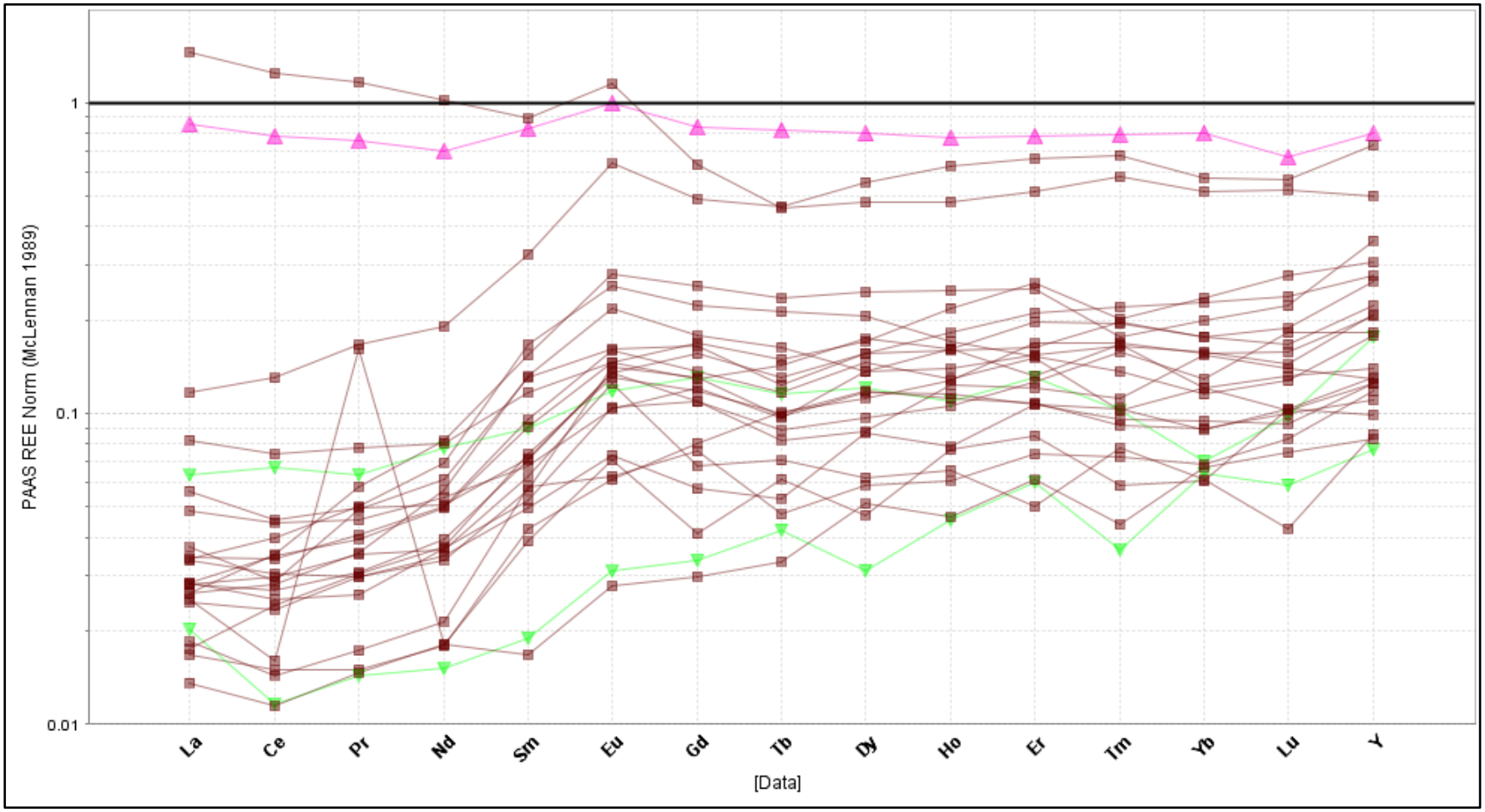

Figure 5.10: PAAS normalised BIF, shale and chert breccia histogram plot

CHAPTER VI DISCUSSION AND CONCLUSION

6.1 Introduction

BIFs contain different iron-bearing minerals, usually in intimate association with quartz. Oxide, carbonate, silicate, and sulphide facies BIF are distinguished (Beuke and Gutzmer, 2008). Rapitan-type iron formations are marked by a specifically simple mineralogy, being composed essentially of hematite intercalated with chert. Precambrian iron formations are surprisingly similar with respect to their average total iron oxide abundances which range between 35-50wt%. SiO_2 is the second major constituent, in concentration between 40 and 55 wt%. Minor constituents are usually CaO and MgO, and very seldom Al_2O_3. Average concentrations of total Mn oxide, Na_2O, K_2O, and $P_2O_5$are almost always from 0.1 to 0.5 wt%. Although the concentration of iron contained in BIFs is several orders of magnitude higher than average crust, it is usually of too low grade to be of any direct economic significance.

Table6.1: Major element geochemistry of Kuruman iron formation (Fryer, 2016).

SampleID	BIF Type	SiO2	TiO2	Al2O3	FeO	MnO	MgO	CaO	Na2O	K2O	P2O5	LOI	Total
Gas17	Kuruman	45.43	Bd	0.43	43.39	0.10	1.81	1.24	bd	0.17	0.04	6.20	99.14
Gas18	Kuruman	37.40	0.01	bd	38.04	0.60	2.84	4.07	0.02	0.03	0.21	15.40	98.88
Gas19	Kuruman	44.14	0.01	bd	40.67	0.08	2.00	1.14	bd	0.02	0.03	10.37	98.71
Gas20	Kuruman	51.12	Bd	bd	39.06	0.10	2.70	0.77	0.11	0.01	0.07	4.88	98.97
Gas21	Kuruman	49.45	0.01	bd	42.04	0.07	1.94	0.45	bd	0.04	0.08	4.68	99.00
Gas22	Kuruman	46.54	Bd	bd	43.02	0.08	1.37	1.33	0.26	0.01	0.08	5.59	98.35
Gas23	Kuruman	43.53	0.03	bd	42.27	0.71	4.65	2.76	0.02	0.19	0.20	4.71	99.52
Gas24	Kuruman	37.82	0.01	bd	51.61	0.08	2.10	0.82	0.16	0.02	0.05	5.75	98.70
Gas25	Kuruman	38.32	0.04	0.17	50.28	0.08	1.63	1.07	0.03	0.02	0.08	6.14	97.94
Gas26	Kuruman	43.74	0.03	bd	35.91	0.11	1.80	2.97	bd	0.04	0.04	14.00	98.87

Table 6.2: Penge iron formation major element geochemistry, (Weir, 2015)

SampleID	BIFType	SiO_2	TiO_2	Al_2O_3	FeO	MnO	MgO	CaO	Na_2O	K_2O	P_2O_5	LOI	Total
TBZ-4	Penge	44.32	0.01	1.25	47.60	0.12	3.25	1.19	0.00	0.02	0.10	0.01	98.05
TBZ-5	Penge	41.32	0.03	0.74	48.77	0.35	3.08	2.88	0.00	0.03	0.22	1.36	99.28
TBZ-6	Penge	56.66	0.01	0.02	36.83	0.32	2.07	2.02	0.00	0.01	0.05	0.50	98.89
TBZ-7	Penge	59.45	0.02	0.30	34.80	0.61	3.67	0.55	0.04	0.02	0.06	0.75	99.16
TBZ-9	Penge	53.13	0.05	0.92	37.67	0.92	4.28	1.66	0.08	0.09	0.08	0.34	99.02
TBZ-10	Penge	48.02	0.10	0.82	39.05	0.78	8.02	1.53	0.05	0.08	0.13	0.22	98.84
TBZ-12	Penge	54.96	0.06	1.27	34.34	0.78	5.54	2.84	0.12	0.10	0.19	0.97	99.56
TBZ-13	Penge	47.57	0.03	0.14	45.74	0.37	4.21	1.36	0.01	0.03	0.13	0.83	99.09
TBZ-14	Penge	34.72	0.02	0.20	57.49	0.12	4.78	1.46	0.00	0.01	0.20	0.85	98.53
TBZ-16	Penge	47.41	0.01	0.00	45.97	0.09	4.08	1.08	0.00	0.00	0.25	0.77	98.42
TBZ-17	Penge	48.16	0.04	1.02	40.99	1.53	7.39	1.15	0.05	0.02	0.25	0.70	100.24
TBZ-18	Penge	38.52	0.02	0.70	52.52	0.96	6.34	1.09	0.02	0.03	0.18	0.93	99.69
TBZ-19	Penge	56.11	0.03	0.45	37.25	0.94	5.40	0.46	0.01	0.01	0.13	0.91	100.17
TBZ-20	Penge	40.84	0.03	0.10	52.99	0.57	5.03	0.74	0.00	0.00	0.15	1.43	99.43
TBZ-21	Penge	43.79	0.02	0.07	48.56	0.78	5.04	0.64	0.00	0.00	0.15	1.43	98.94
TBZ-22	Penge	50.92	0.01	0.00	44.48	0.54	3.91	0.26	0.00	0.00	0.08	1.04	99.64
TBZ-23	Penge	52.79	0.01	0.03	43.11	0.13	2.44	0.42	0.00	0.00	0.05	0.32	98.78
TBZ-24	Penge	52.68	0.02	0.00	42.83	0.16	2.39	0.42	0.00	0.00	0.04	0.38	98.35
TBZ-25	Penge	37.85	0.15	1.58	51.41	0.54	6.71	0.73	0.05	0.23	0.06	1.04	98.51

6.2 Physical characteristics of the Masoke and Kuruman iron formations

The Proterophytic (Cloud, 1972) Kuruman and Griquatown Iron-formations (Beukes, 1973) constitute the Asbesheuwels Subgroup of the Ghaap Group (Beukes, 1980a) in the Griqualand West structural basin of the Transvaal Supergroup. They are correlatives of the Penge Ironformation (Beukes, 1973; Button, 1976a) of the Transvaal structural basin, unmetamorphosed and structurally little deformed. The Kuruman Iron-formation consists essentially of micro- and mesobanded autochthonous iron-formation whereas the Griquatown Iron-formation, which conformably overlies it, consists of clastic-textured iron-formations. The former is conformably underlain by dolomite and limestone of the Campbellrand Subgroup (Beukes, 1984). Hematitization and thin lamination to microbanding and occasional brecciation are the main characteristics of the Masoke Iron Formation studied here.

The Kuruman iron formation is characterised by similar features: by logging alone the two iron formations cannot be separated (refer to plate 6.1 and 6.2). The top part of both these iron formations is characterised by thickly bedded and lutitic, hematitized Griquatown iron formation.

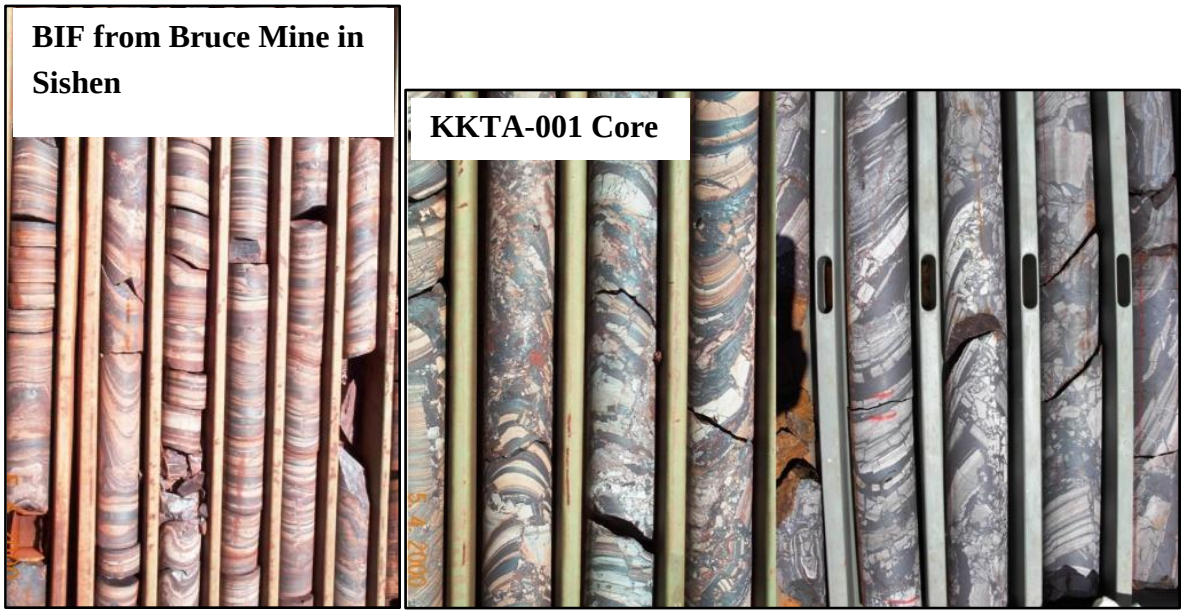

Plate 6.1: Comparison of the Kuruman iron formation from Assmang in Sishen and KKTA001 cores, both these iron formations are micro banded and brecciated.

- Kuruman (Assmang) Iron formation partly enriched and hematitized - A
- Studied Iron Formation (KKTA001) to the right - B

Plate 6.2: Comparison between Kuruman and Masoke iron formation. Kuruman iron formation is partly oxidised and enriched while Masoke iron formation is un-oxidised

Drill core GAST06 intersected a succession of the Masoke iron formation below Kalahari cover that is virtually identical to that associated with high-grade Sishen-type karst deposits on the Maremane dome. The iron formation is highly disturbed and hematite-rich Plate 6.3.C) and overlies a ferruginous chert breccia very similar in composition and appearance to the Wolhaarkop Breccia. It is overlain by hematitized iron formation displaying increasing hematite contents upwards in the succession. It is very likely that if this core had been drilled deeper it would have intersected Campbellrand dolomite below the chert breccia. The field visit supported the observations made at the core yard. Especially at Ukwi Hill the contact between the micro-banded and lutitic iron formation are well exposed as well as flat pebble conglomerate. The iron formations dip to the north and although himititization appear relatively un-deformed indicating that they are probably in normal gradational contact with the Campbellrand carbonates below.

This observation is in contrast to the highly deformed iron formation intersected towards the base of drill cores KKTA001 and KKTA006 overlying chert breccia. Similar chert breccia with large clasts of highly contorted micro-banded hematitized Kuruman iron formation outcrop in the Tshitsane Hills. These breccias most probably are located in dissolution karst structures developed in underlying Campbellrand dolomite. All in all the Ukwi-Tshitsane Hills area displays geology that is very similar to that of the Sishen area on the Maremane dome. The area could thus be considered highly prospective for discovering karst-hosted Sishen-type iron ore deposits.

In KKTA06 drill core, the iron formation is in sharp fault contact with a massive recrystallized grey dolomite (figure 3.4) that is in turn intruded by a diabase near the end of the hole. The iron formation displays crackle brecciation in proximity to the basal fault. This brecciation is similar to that observed in the lower part of core KKTA01 and it is highly probable that if that core was drilled deeper it would have intersected the fault.

6.3 Geochemical comparison of “pristine”, “oxidised” and altered iron formation

These BIF samples reflect a magnetite-hematite-quartz assemblage which shows a very similar geochemical signature throughout. There is nothing to suggest these rocks are anything other than equivalent. The BIF samples are therefore fairly straight forward. It is required to assemble a geochemical database for the BIFs, then further sampling and detailed trace element studies are suggested. Possibly a selected set of trace elements could be narrowed down to facilitate such a study.

6.3.1 Major oxides comparison

The BIFs sampled and studied belongs to the Masoke iron formation of the Taupone Group of the Kanye Basin. The BIF in these drill cores were described as “altered”, “oxidised” and “pristine”, nonetheless, their geochemical composition is similar.

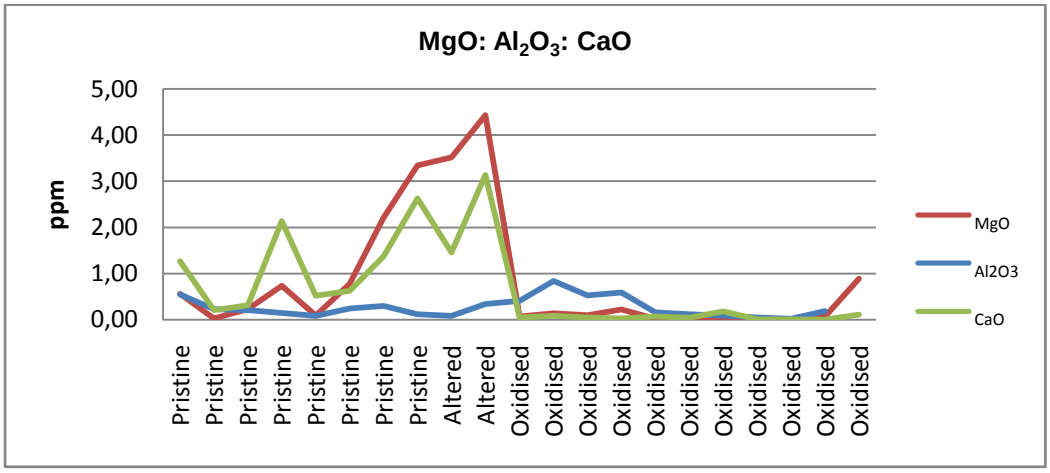

Figure 6.1 MgO, Al_2O_3 and CaO of Masoke IF types from ‘pristine’ IF, ‘altered’ and oxidised IF.

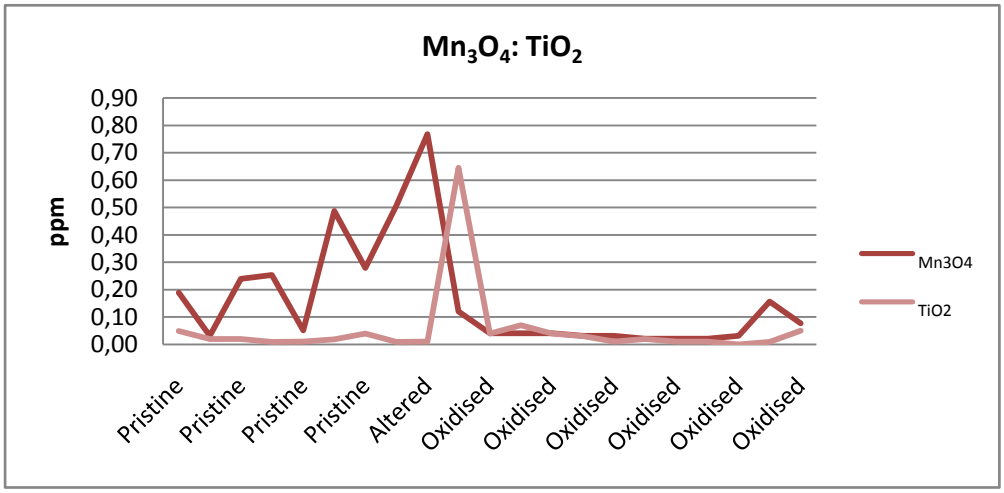

Figure 6.2 Mn_3O_4 vs. TiO_2 probability plot across 'pristine' IF, 'altered' IF and oxidised IF

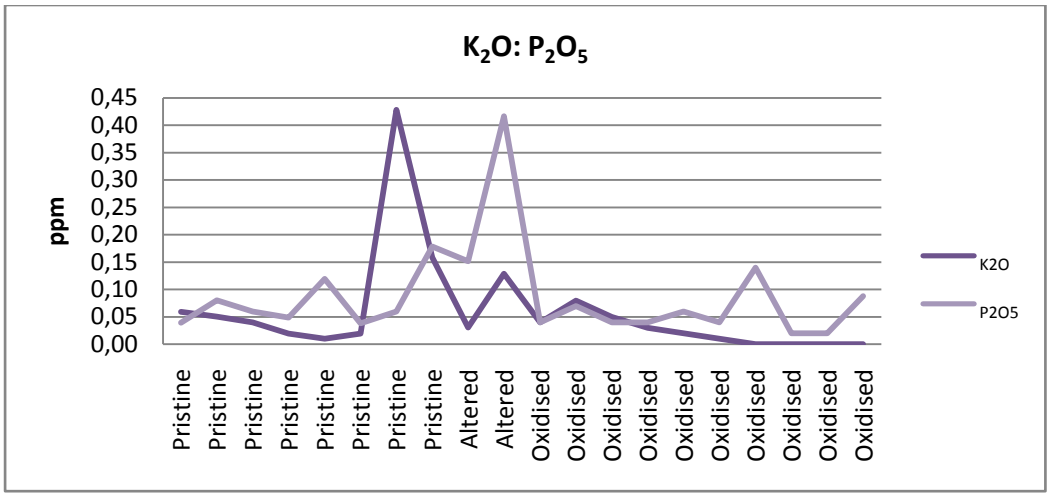

6.3 K_2O vs. P_2O_5 probability plot across the sub-types of Masoke IF ('altered IF and 'pristine' and oxidised IF.

Minor oxide correlations above shows that the sub-types of Masoke IF are inseparable, as they have similar geochemical signatures. These clusters representing 'altered', pristine and oxidised IF overlaps. The 'altered' IF of Masoke seems to have a positive kick in all the plots. This spike might be caused by the fact that these samples ('altered') were sample on the contact of the Transvaal and MFC.

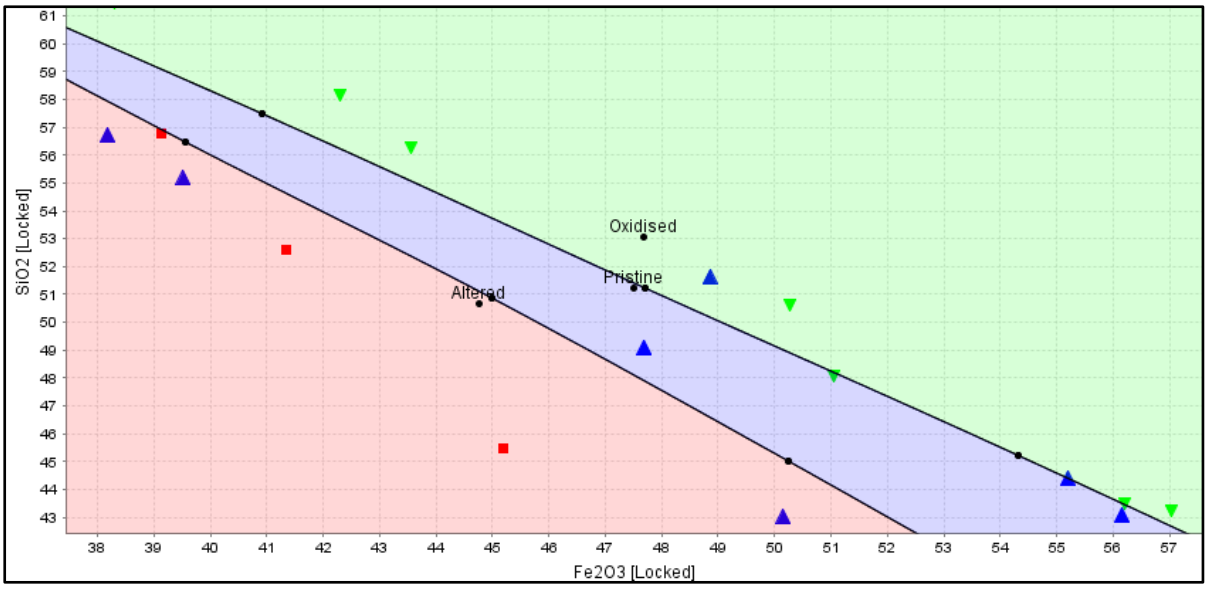

Figure 6.4: Domain classification of the three iron formation (altered, pristine and oxidised), these iron formation can not be seperated geochemically. There is an overlap between pristine and oxidised iron formations. However there seems to be clear distinction between altered and oxidised iron formation. This graph illustrate and re-emphasis that these samples are from the same iron formation.

.

6.4 Geochemical comparisoson of Masoke, Kuruman and Penge Iron Formations

This section will provide binary, probability and other types of plots which feature data for the three BIFs (Masoke, Kuruman and Penge iron formations). Generally speaking these BIFs look similar. The Penge iron formation is Mg-rich whereas the Kuruman and the Masoke are more Ca-rich (Figure 6.7 and figure 6.8). Therefore, by plotting all data on a CaO-MgO plot (for all three BIFs) illustrate that the Masoke and the Kuruman clusters overlaps whereas the Penge cluster does not.

6.4.1 Major element comparisson

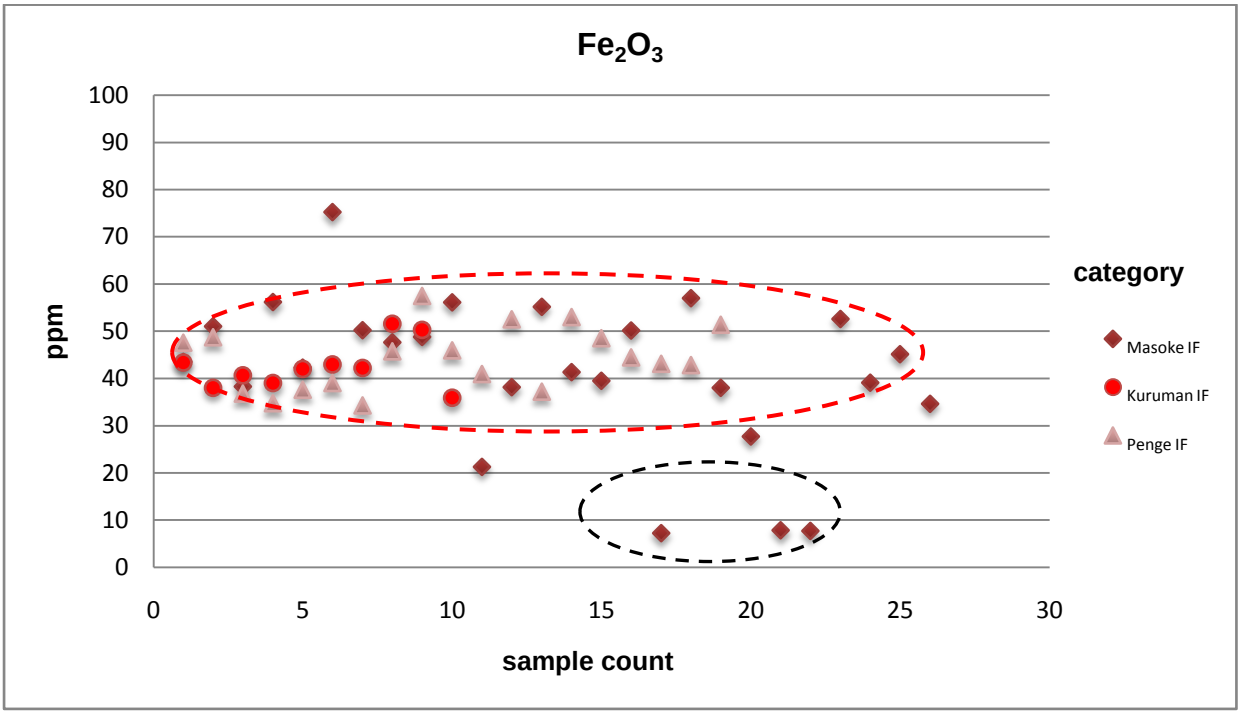

Figure 6.5 Fe_2O_3 scatter plot over the three BIF categories i.e. Masoke IF, Kuruman IF and Penge IF.

Geochemical plots for major oxides are similar through the BIF category, they have strong positive correlations. Most of the values range between 40 to 60 % as indicated by the red dotted-circle. There are few outliers, indicated by the black dotted circle; these samples plot between 5 and 10 %. The lower outliers are probably haematitized chert breccia. These simply cannot be BIF; they would rather be breccias with rich haematite matrix.

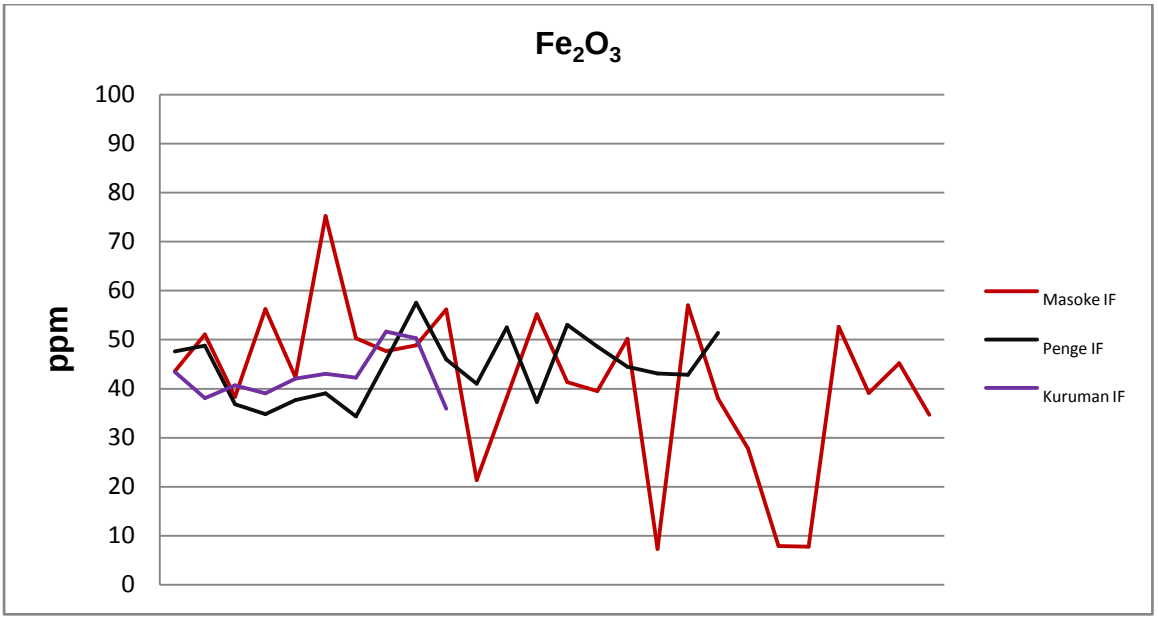

Figure 6.6 Probability plot showing Fe_2O_3 values across all BIF categories analysed. Kuruman IF and Penge IF show a very strong positive correlation. The two plots mimic each other. The sample that has higher Fe_2O_3 was sampled from the eastern side of the basin (Ukwi hill area); BIF from this part of the basin is generally oxidised.

XY plot of Fe_2O_3 against SiO_2 showing that these iron formations have similar chemical composition. They all plot in the same regions of both bi and probability plots. The major difference is that the Kuruman and penge iron formation are enriched while Masoke iron formation is not enriched. While it is evident that Masoke iron formation is oxidised and hemititized the alteration process evidently did not remove the silica. It is aparent from these plots that some of the lithologies logged as BIF could generally be haemititiesd and banded cherts, shales and/or heamititised quartzites.

Legend:

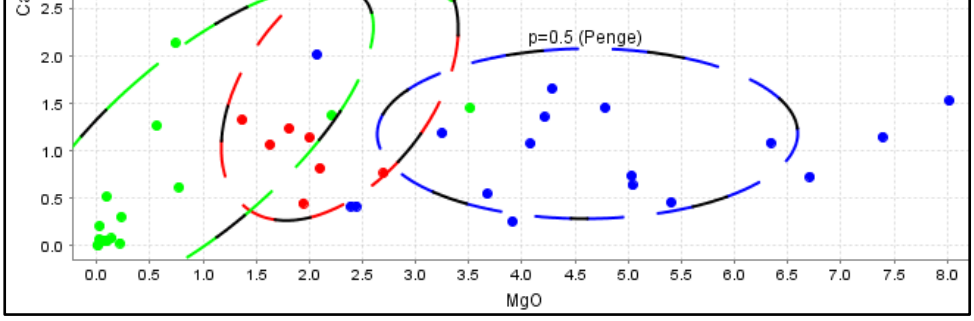

Figure 6.7: Domain classification diagram based on whole rock, CaO and MgO of the three different iron formations. This illustrates that there is a distinctive overlap between Masoke and Kuruman iron formations. Penge iron formation is slightly different from Kuruman and Masoke Iron formations in that it is enriched in MgO.

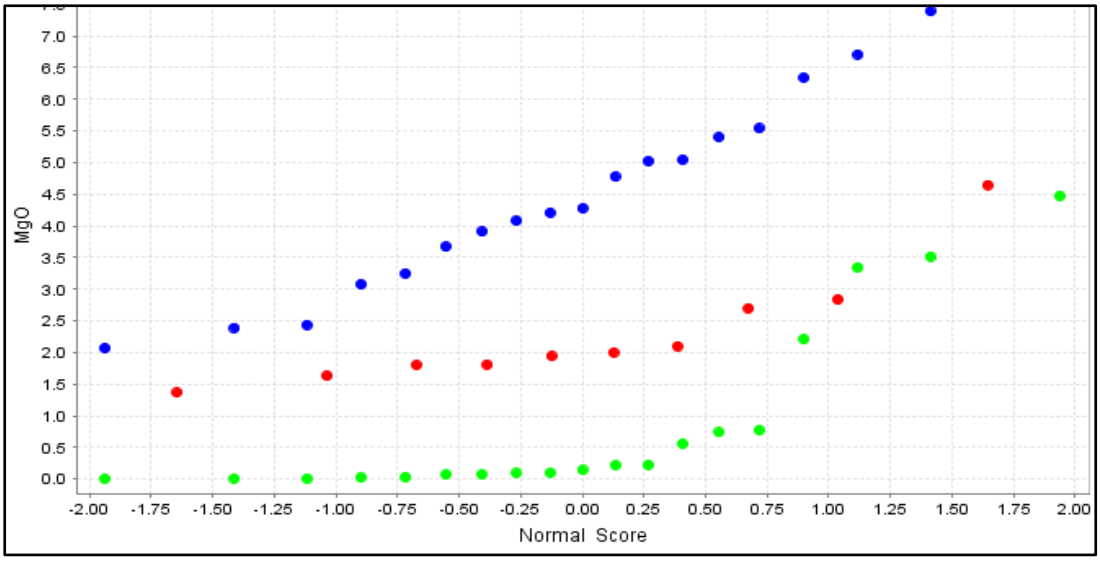

Figure 6.8: MgO probability plot of all three iron formations (Penge, Kuruman and Masoke Iron formation). Penge is Mg-rich whereas the Kuruman and the Masoke are more Ca-rich.

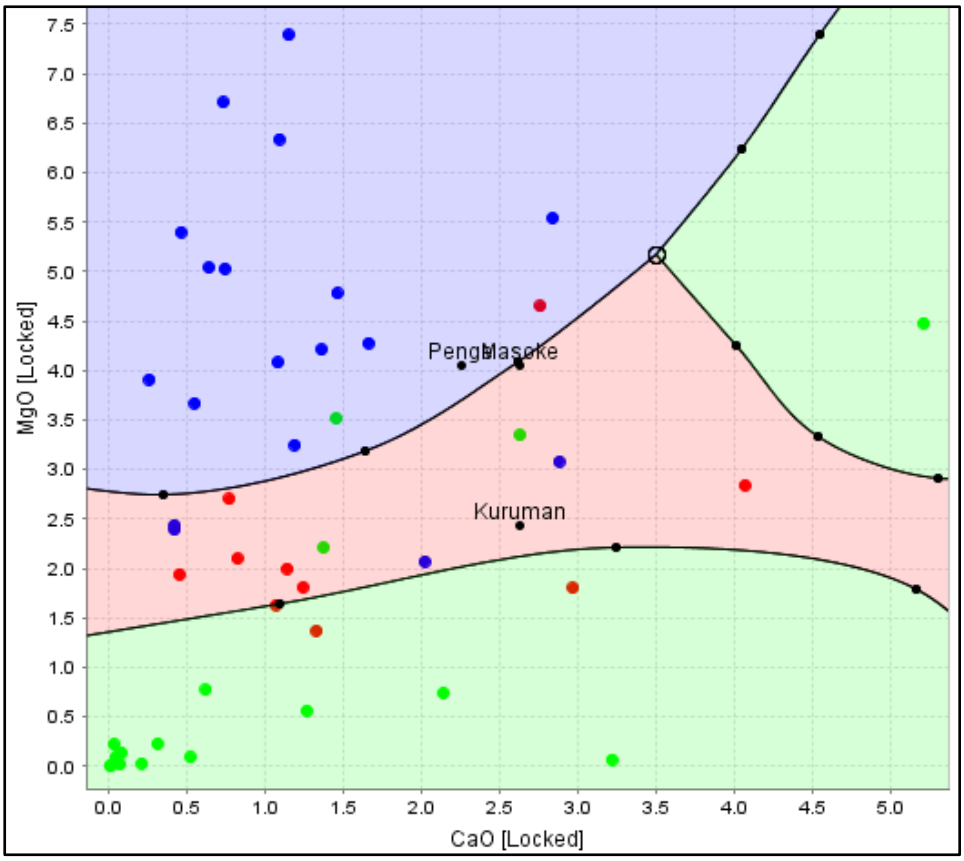

Figure 6.9: Ca and Mg domain classification diagram showing the three BIF types, Masoke and Kuruman BIFs clusters overlaps a lot and are very closely related; while Penge iron.

6.5 Minor element comparison

Only altered samples from drill core KP17 have a slight geochemical difference in that they are dominated by minerals of the pyroxene group (augite). This is likely to have been caused by metasomatic processes near the (ultra-)mafic rocks of Molopo Farms Complex. Rocks of Molopo Farms Complex have intruded the Transvaal sequence, thus drill core KP17 drilled through both Transvaal sequence and Molopo Farms Complex (MFC). Also important to note is that samples of drill core KP17 have a slightly higher concentrations of rare elements, with Zr been the most evident one, followed by Y and Nb (see ternary plot of Figure 6.4). Therefore, core samples of KP17 have similar Zr concentration to that of the Kuruman Iron Formations.

Finally it is most important to note that according to geophysical analyses of the project area, as outlined in the early chapters, KKTA001 is located alongside a major fault whereas KKTA006 and KKTA013 are distal to the fault (refer to Figure 3.5). It

would thus appear as if the hematitization of the iron formations in core KKTA001 are related to fluid movement along the fault zone. However, the process was one of only oxidation of iron minerals to hematite without leaching of silica (chert) and therefore did not result in the formation of high-grade hematite iron ore.

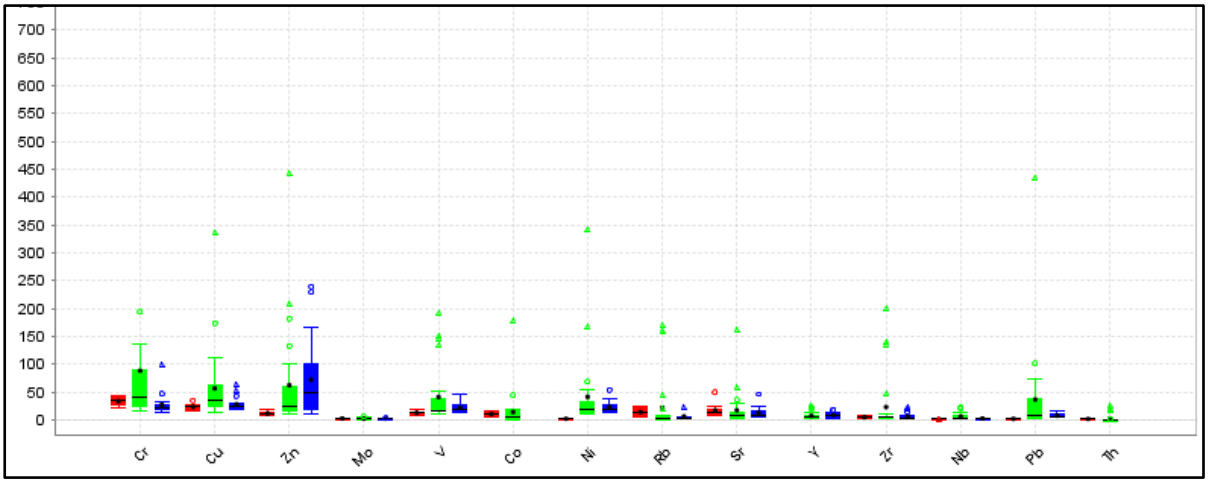

Figure 6.10: Minor element box plot for all three BIF types, most of these elements are general flat except for Cr and Zn. Masoke iron formation is slightly enriched in Cu, Cr and Zn while Penge iron formation is enriched in Zn.

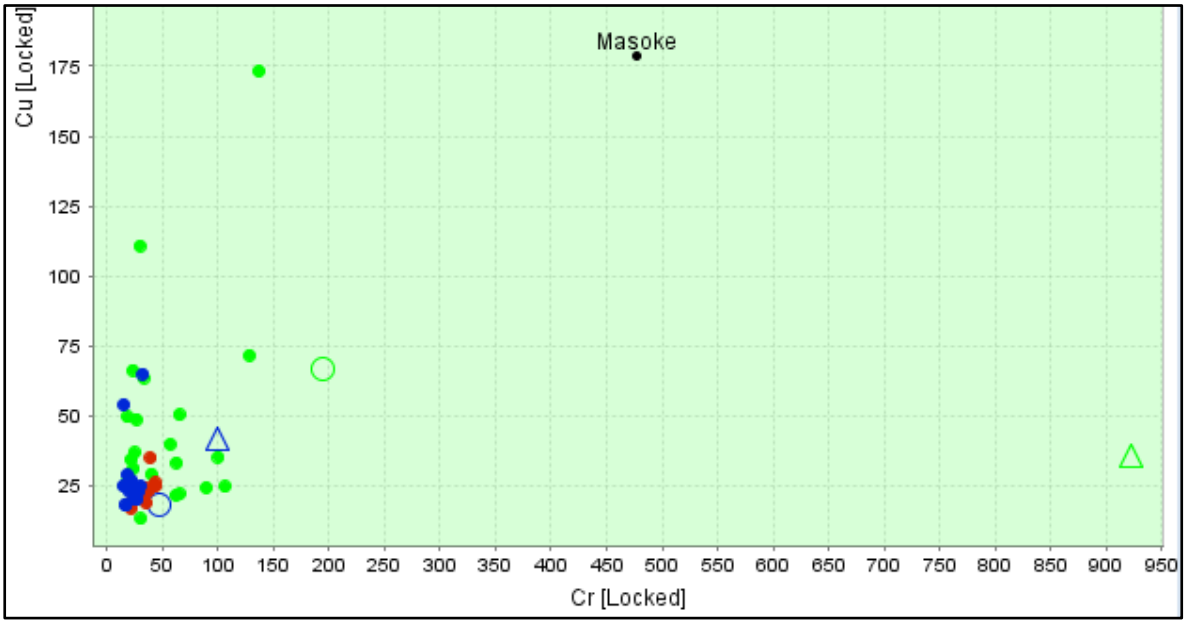

Figure 6.11: Domain classification using Cu and Cr, the three iron formations plot in the same area of the graph. Geochemical correlations of minor element chemistry. These plots show that the three iron formations are generally similar geochemically.

6.6 Conclusion

For the purpose of mineralogical investigations selected samples from five drill holes were grouped into three main groups. The selected samples were grouped based on physical and microscopic attributes such as colour, density, texture and hematite-magnetite content and/or presence of silicate minerals.

Table 6.3: Three main groups of Masoke iron formation

Group	**Colour**	**Hematite content**	**Silicate content**
Oxidised Iron Formation	Dark red	Moderate	Moderate
Pristine Iron Formation	Light grey	Low	High
Altered Iron Formation	Dark grey	High	Low

Reflected and transmitted light examination of the polished thin section indicates a bulk rock with an intricate mixture of magnetite (~40%), chert (~50%) and other minor minerals (~10%). The hematite occurs as extremely fine grains/crystals, ranging in individual size from <5µm through to rarely 50µm, with most grains > 20µm seen to be pseudomorphs after euhedral magnetite crystals. These grains are evenly dispersed throughout a matrix of equally fine-grained chert, albeit with an overall layered distribution (but only rarely as thin continuous laminae). The 5µm grains are dispersed essentially within quartz as a single population together with scattered and layered hematite pseudomorphs after magnetite of 20 to 50µm size. Moreover, another population of hematite occurs as “coarse” granular masses, irregularly layered mostly as pseudomorphs after magnetite, with grain sizes ranging from 20 to 80µm.

The quartz matrix to the hematite petrographically has a classic micro/cryptocrystalline “cherty” texture, pointing to likely siliceous chemical sediment originally. It has minor scattered hematite pseudomorphs after magnetite and veins of oxidised silicates, plus clusters of micro-platy hematite.Reflected light microscopy indicates the hematite bands to retain residuals of the very small hematite

pseudomorphs after magnetite as in other samples, but mostly converted to fine, and coarser, decussate microplaty hematite.

Hematitized iron formations specimen were studied under reflected and transmitted light. This specimen consists of homogeneous and massive ultrafine hematite in an apparently siliceous matrix of grey reddish-brown colour. Reflected and transmitted light examination of the polished thin section indicates a bulk rock with an intricate mix of hematite and chert. The hematite occurs as extremely fine crystals, ranging in individual size from <5μm through to rarely 50μm, with all crystals > 20μm seen to be pseudomorphs after euhedral-magnetite crystals.

Altered iron formation samples are dominated by augite from the mafic and ultramafic rocks of Molopo Farms Complex (MFC). They also contain silicates of calcium, sodium, magnesium, iron and aluminium and occasionally contains zinc, manganese and titanium impurities. Its chemical formula is $(Ca,Na)(Mg,Fe,Al)(Al,Si)_2O_6$ and it usually has grayish-green, greenish brown and dark brown colour as in the image below. Sulphides are also apperantly dominant, followed by the chlorite mineral clinochlore. Clinochlore is a basic iron magnesium aluminium silicate that may contain small amounts of chromium. Its chemical formula is $(Mg,Fe^{2+})_5Al_2Si_3O_{10}(OH)_8$ and has a white colour on this KP17 core.

BIFs contain different iron-bearing minerals, usually in intimate association with quartz. These BIF samples reflect a magnetite-hematite-quartz assemblage which shows a very similar geochemical signature throughout. There is nothing to suggest these rocks are anything other than equivalent. The two significant minerals in Table 6.2 are quartz and hematite. Most of these samples are dominated by hematite, while the other samples are dominated by quartz. The other minerals present are in trace levels less than 1.5 Wt %.

Table 6.4: Masoke iron formation mineralogy as identified by xrd and pretrography

Identified Minerals	Chemical Formulae
Quartz	SiO2
Chlorite	(Mg,Fe)5(Si,Al)4O10(OH)8
Muscovite	KAl2(Si3Al)O10(OH,F)2
Actinolite	Ca2(Mg,Fe)5Si8O22(OH)2
Microcline	KAlSi3O8
Sepiolite	Mg4Si6O15(OH)2•6(H2O)
Grunerite	Fe7Si8O22(OH)2
Lizardite	Mg3Si2O5(OH)4
Minnesotaite	(Fe,Mg)3Si4O10(OH)2
Hematite	Fe2O3
Magnetite	Fe3O4
Siderite	FeCO3
Calcite	CaCO3
Dolomite	CaMg(CO3)2
Plagioclase	(Na,Ca)(Si,Al)4O8
Augite	(Ca,Na)(Mg,Fe,Al)(Al,$Si)_2O_6$

In terms of bulk element geochemistry these iron formations (Masoke, Kuruman and Penge) are generally similar. The clusters overlap in most elements. However, there are few elements that can be used to draw a distinction between these iron formations. The Penge iron formation is characterised by higher Al and Mg values, these plots makes a clear distinction between Penge, Masoke and Kuruman. Moreover, Masoke and Kuruman iron formation are characterised by higher Ca.

In summary there is no evidence from the geochemical data that the Molopo Farms Complex (MFC) affects the BIF though it transacts the Transvaal in the Sekoma and Mabutsane areas. Altered BIF which is intruded by the MFC is elevated in Mn and K. In terms of mineralogical difference the altered BIF is bearing both augite and plagioclase. These two minerals may be coming from the mafic intrusions of MFC.

Based on physical characteristic, the Masoke iron formation was sub-divided into three sub-groups namely: “pristine”, “oxidised” and “altered” iron formations (table 6.1). They are characterised by slightly different geochemical signatures in terms of major and minor element geochemistry. In terms of major element geochemistry altered iron formation has higher Mn, Ca and Mg while the other two follow closely. Oxidised iron formation has Na depletion and is enriched in Al; and oxidised iron formation has slightly higher SiO2 compared to “pristine” and altered iron formation, therefore silica was not leached during oxidisation. Oxidised iron formation has higher Ti values while altered iron formation has higher K values.

There is very strong and positive geochemical association between the Masoke and Kuruman iron formations. Domain classification diagram, using major element geochemistry shows that Kuruman and Masoke iron formations are closely related and have strong overlap. Therefore Kuruman and Masoke are iron formations of the same unit; however, Masoke iron formation is not economic in that it has very high silica content. The process that could remove or leach the silica is lacking, the slight oxidation is proximal to the fault.

In conclusion, Masoke and Kuruman iron formations have similar geochemical signature. There is nothing to suggest that these iron formations are different. However, Penge is characterised by higher Mg and Al values. Masoke iron formation is partly oxidised and hemititized but not enriched; the oxidation did not lead to leaching of silica. Masoke iron formation is an extension of Kuruman iron formation; this persists under the Kalahari cover into Southern Botswana.

References

Name $ Initial	Year	Tittles	Remarks
Aldiss, D.T.	1981	Petrographic notes, CKP-8C-1. Unpublished report,	Geological Survey of Botswana
Aldiss, D.T.	1986	The chronological significance of the pre-Transvaal sequence dolorite dyke swarm in south-eastern Botswana.	Transaction Geological Society of South Africa
Aldiss, D.T., e tal,.	1989	The geology of Kanye area. Bull. Geological Survey of Botswana 33	
Altermann, W., Halbich, I.W	1990	Thrusting, folding, and stratigraphy of the Ghaap Group along the south-western margin of the Kaapvaal Craton	
Altermann, W., Halbich, I.W	1991	Structural history of the south western corner of the Kaapvaal Craton and the adjacent Namaqua Realm: new observations and reappraisal	
Alchin, D, and Botha, WJ.	2005	The Structural/stratigraphic development of the Sishen South (Welgevonden) Iron Ore Deposit, South Africa, as deduced from ground gravity data modeling.	An integrated exploration approach to the Sishen South iron ore deposit,
Barton, E.S., Altermann, W.	1994	U-Pb zircon age age for a tuff in the Campbell Group, Griqualand West Sequence, Soth Africa: implication for Early Proterozoic rock accumulation rate	
Bayley R.W and James, H.L	1973	Precambrian iron-formations of the United States, Nature, Origin, and Mineralogy	
Beukes, N.J.	1973	Precambrian iron-formations of Southern Africa	

		Die karbonaatgesteentes en ysterformasies van die Ghaap-Groep van die Transvaal Supergroep in Noord Kaapland.	
Beukes, N.J.	1978	PhD theis, Rand Afrikaans Univ., South Africa	
		Lithofacies and stratigraphy of Kuruman and Griquatown	
Beukes, N.J.	1980	Iron-Formation, Northern Cape Province, South Africa	
		Palaeoenvironmental setting of iron-formations in the depositional basin of the Transvaal Supergroup, South	
Beukes, N.J.	1983	Africa.	
		The Transvaal Sequence in Griqualand West. In:	Mineral Deposits of Southern
Beukes, N.J.	1986	Anhaeusser, C.R., Maske, S. (eds.)	African
		New evidence for thrust faulting in Griqualand West, South	
Beukes, N.J.	1987	Africa: implication for stratigraphy and the age of red beds.	
		Sedimentological and geochemical relationships between carbonate, iron formation and maganesse deposits in EarlyProterozoic Transvaal Supergroup, Griqualand West ,	
Beukes, N.J.	1989	South Africa.	
		Report on stratigraphic correlation of some drill-core intersections in the Keng Pan, Tubane and Phepheng Areas,	
Beukes, N.J.	1990	Molopo Farms Complex, 18 pp.	
Beukes, N.J. and		The Regional Geology of the Zeekoebaart high grade iron	
Dorland, H.C.	2001	ore deposit in the Boegoeberg Dam Area.	

			In: BIF-related high-grade iron ore.
Beukes, N.J. and Gutzmer, J.	2008	Origin and Paleoenvironmental Significance of Major Iron Formations at the Archean-Paleoproterozoic Boundary.	Reviews on Economic Geology, Vol.15,
Button, A.	1976	Stratigraphy and relations of the Bushveld floor in the eastern Transvaal Sequence	
Button, A.	1986	The Transvaal sub-basin of Transvaal Sequence. In: Anhaeusser, C.R., Maske, S. (eds.) Mineral Deposits of Southern Africa.	
Beukes, N.J.etal	2008	Genesis of high-grade iron ores of the Archean Iron Ore Group around Noamundi, India.	Economic Geology, Vol. 100, p. 365-386.
Carney, J.N., and Twist, D.	1986	The Waterberg basin - a reapraisal. Transactions Geological Society of South Africa	
Carney, J.N.	1987	Reports on the findings of the field excursion to greenstone-gneiss terrain in Vumba and Shashe areas. NE Botswana.	Unpublished report , Geological Survey of Botswana
Carney, J.N.	1991	Lithological information from a borehole cored through cover and basement rocks near Gweta and its bearing on the distribution of of major crustal boundries in Botswana	Botswana Journal of Earth Science
Carney, J.N.	1990b	The Archen Proterozoic boundary in the Kaapvaal Province of Southern Africa	Precambrian Research
Crockett, R.N.	1962	Note on the geology of the area northwest of Shoshong, Bamangwato Tribal Territory.	Unpublished report , Geological Survey of Botswana

Crockett, R.N.	1969	The geological signifance of the margin of the Bushveld Basin in Botswana. PhD theis, Univ. London, England	
Crockett, R.N.	1972	The Transvaal System in Botswana: its geotectonic and depositional environment and special problems	
Dalstra H.J and Rosierie C.A	2008	Structural control on high-grade iron ores hosted by banded iron formation.	A global perspective, Econ. Geol (SEG review) 15, 73-106
Dalstra H.J and Guedes S,	2008	Giant hydrothermal hematite deposit with Mg-Fe metasomatism.	A comparison of Carajas, Hamersley and other iron ores
Egune E.A	1973	Precambrian iron formation of the Soviet Union. Economic geology, 68	
Eichler, J.	1976	Origin of the Precambrian banded ironformation. Handbook of stratiform and stratabound ore deposits	Elsevier, Amsterdam, Vol. 7. 201p.
Eriksoon, K.A, Trustwell, J.F.	1974	Tidal flat associations from the lower Preterozoic carbonate sequence in South Africa	
Eriksoon, K.A e tal	1975	Limestone formation and dolomitisation in the lower Preterozoic succession from South Africa	
Eriksoon, K.A, e tal	1976	Paleoenvironmetal and geochemical models from and Early Proterozoic carbonatesuccession in South Africa. In: Walter, M.R. (ed.). Stromatolites.	
Eriksoon, K.A, e tal	1988	A hypothesis on the nature of the Pretoria Group basin. South African Journal of Geology.	

Eriksoon, P.G., Clendeenin, C.W.	1990	A review of the Transvaal Sequence, South Africa. J. Afr. Earth Sci.	
Eriksoon, P.G.,e tal	1991	A review of the sedimentology of the Early Proterozoic Pretoria Group, Transvaal Sequence, South Africa: Implication for tectonic setting.	
Eriksoon, P.G., Cheney, E.S.	1992	Evidence for the transition to an oxygen-rich atmosphere during the evolution of the red beds in the lower Proterozoic sequence of Southern Africa	
Eriksoon, P.G., e tal	1993	Transvaal sequence: an overview	
Gabaake, G.	1987a	Transvaal Dolomite Project. Geological and hydrogeological results of core borehole TDM/1 Matematema	Unpublished report , Geological Survey of Botswana
Gabaake, G.	1987b	Transvaal Dolomite Project. Geological and hydrogeological results of core borehole TDM/2, TDM/3 and TDM/4, Matematema	Unpublished report , Geological Survey of Botswana
Garrels R.M	1970	A model for deposition of the micro banded Precambrian iron formation	
French, B.M	1973	Mineral assemblages in diagenetic and low-grade metamorphic iron formations	*Econ. Geol*., **68**, 1063-1974.
Gole M.J	1981	Archean banded iron formations, Yilgarn Block, Western Australia	Econ. Geol., 76, 1954-1974
Goodwin, A.M	1956	Facies relationships in the Gunflint iron formation	Econ. Geol., 51, 565-595

Goodwin, A.M	1973	Tectonic systems and deposition of iron formations	
Gross, GA	1965	Geology of iron deposits in Canada. Vol I: General Geology and evaluation of iron deposits	*Econ. Geol. Rep*., no. **22**, p. 181.
Gross, G.A	1972	Petrography and petrology of the Precambrian banded iron formation.	
Gross, G.A.	1973	The depositional environment of, principal types of Precambrian iron formations	*UNESCO*, Proc, Kiev Symp., Earth Sciences, **9**, 15-21
Gross, G.A. and McLeod, N.A	1980	A preliminary assessment of the chemical composition of iron formation in Canada	*Can. Miner*., **181**, 223-229.
James, H.L.	1954	Sedimentary facies of iron formation.	*Econ. Geol*., **49**, 235-291.
James, H.L.	1966	Chemistry of the iron-rich sedimentary rocks	*U.S. Geol. Surv. Prof. Pap*., 440 W, 61 pp
James, H.L.	1983	Distribution of banded iron formations in space and time. Developments in Precambrian Geology, 6, 471-490	
James, H.L.	1969	Comparison between Red Sea deposits and older iron-stone and iron formations	
James, H.L. and Trendall, A.F	1982	Banded iron formation: distribution in time and palaeoenvironmental significance	
Mapeo, R.B.M	1990	Geology of the Metlobo and Mabule areas.	Bulletin: Geological Survey of Botswana, 36.
Tombale, A.R	1986a	Problems of stratigraphic nomenclature in Botswana Part I:	Unpublished report, Geological

		The Transvaal Supergroup or sequence	Survey of Botswana, ART 1/10/86,
Tombale, A.R	1986b	Geological Map of Jwaneng area (QDS2424D) (1:125000), with brief description	Geological Survey of Botswana
Trendall, A.F. and Blockley, J.G.	1970	The iron formations of the Precambrian Hamersley Group, Western	*Bull. Western Aust. Geol. Surv*., **199**, 366 pp
Trendall, A.F and De Laeter, J.A.	1972	Apparent age and origin of black porcelanite of the Joffre Member.	*Ann. Rep. Western Aust. Geol. Surv.*, **1977**, 68-74
Klein, C.	1973	Changes in mineral assemblages with metamorphism of some banded Precambrian iron-formations	Econ. Geol., 68, 1075–1088.
Klein, C.	1983	Diagenesis and metamorphism of Precambrian banded iron-fornation	*In* Trendall, A. F. and Morris, R. C. Iron formation: facts and problems. Elsevier, Amsterdam, 417-469
Klein, C.	2005	Some Precambrian banded iron-formations (BIFs) from around the world: their age, geologic setting, mineralogy, metamorphism, geochemistry, and origins	
Martin, H.	1965	The Precambrian Geology of South West Africa and Namaqualand.	The Precambrian Research Unit, University of Cape Town.
Martin, H.	1975	Mineralization in the ensialic Damara orogenic belt in Verwoerd, W.J, Mineralisatin in Metamorphic Terranes	
Master, S.	1998	New developments in understanding the origin of the Central	Abstract, Mineral Deposits Studies

		African Copperbelt.	Group Meeting, University of Greenwich, Chatham Maritime, U.K., 5-6 January 1998, 3 pp.
Master, S.	1998	A review of the world-class Katangan metallogenic province and the Central African Copperbelt: tectonic setting, fluid evolution, metal sources, and timing of mineralisation.	Québec 1998, Abstract Volume: Carrefour in Earth Sciences.
Melnik Y.P	1982	Precambrian iron formation , Volume 5, 1st Edition	
Misra, K.	1999	Understanding mineral deposits, Springer	
Miyano, T. and Beukes, N. J.	1997	Mineralogy and petrology of the contact metamorphism amphibole asbetos-bearing Penge iron formation	
Miyano, T. and Klein, C.	1983	Phase relations of orthopyroxene, olivine, and grunerite in high-grade metamorphic ironformation.	Am. Mineral., 68, 699–716.
Moore, J. M., e tal,.	2001	Deconstructing the Transvaal Supergroup, South Africa, J Afr Earth Sci, 2000, 31 (Suppl. 1A), 52–53.	
Mukhopadhyay, A	1968	Petrogenesis of the grunerite bearing rocks of Iron Ore Formation of Badampahar, Mayurbhanj, Orissa	Quar. J. Geol. Min. Met. Soc. Ind., 22, 39-42
Mukhopadhyay, D.	1988	Precambrian of the Eastern Indian Shield - Prospective of the Problems	In D Mukhopadhyay (Ed.), Precambrian of the Eastern Indian shield. Mem. Geol.
Mukhopadhyav, J. etal.	2008	Geology and genesis of the major BIF-hosted high-grade iron deposits of India. In: Hagemann, S., Rosiere, C.,	

		Gutzmer, J. and Beukes, N.J. (Eds.): BIF related high-grade iron ore, Reviews in Economic Geology, Vol.15, p. 291-315.	
Van Deventer, W. F.	2009	Textural and geochemical evidence for the supergene origin of the Palaeoproterozoic high-grade BIF-hosted iron ores of the Maremane Dome, Northern Cape Province, South Africa.	
Van Schalkwyk J.F. and Beukes N.J.	1986	The Sishen iron ore deposit, Griqualand West, 'Mineral deposits of Southern Africa, Vol. I, (ed. C. R. Anhaeusser and S. Maske), 931–956. Johannesburg, Geological Society of South Africa.	
Van Staden, A.	2002	Characterisation of the lowermost manganese ore bed of the Hotazel Formation.Gloria mine, Northern Cape Province,	unpublished M.Sc. thesis, Rand Afrikaans University, Johannesburg, 167 pp.